UNIVERSITY
OF OSLO

Master's thesis

Treatment planning comparison of IMPT and VMAT for locally advanced lung cancer

Comparing modalities in terms of the need for plan adaptation during the treatment, and additional assessement of IMPT plans using different range uncertainties

Oliwia Malinowska

Biological and Medical Physics
60 ECTS study points

Department of Physics
Faculty of Mathematics and Natural Sciences

Spring 2024

Oliwia Malinowska

Treatment planning comparison of IMPT and VMAT for locally advanced lung cancer

Comparing modalities in terms of the need for plan adaptation during the treatment, and additional assessement of IMPT plans using different range uncertainties

Supervisors:
Taran Paulsen Hellebust
Eirik Malinen

Acknowledgements

I would like to express sincere gratitude to my supervisor Taran Paulsen Hellebust for her expert guidance, insightful feedback, and unwavering patience. I appreciate immensely her continuous support, as well as the persistent attention to detail.
I would also like to acknowledge Jonas Asperud and Jørund Graadal Svestad for sacrificing their time to teach me the basics of treatment planning process. Their help was crucial in the experimental part of my research.
I am deeply grateful to my partner, Svein-Magnus Lommerud for his love, constant encouragement, and making me laugh even in the most stressful times.
Lastly, I would like to thank my family, friends and anyone else who helped me academically or emotionally throughout this journey.

Abstract

Background and purpose: Anatomical changes may occur during the course of radiotherapy, and plan adaptation may be needed. Protons are considered more sensitive to tissue inhomogeneities, compared to photons. Proton plans may therefore require adaptation more frequently. However, protons' precision in dose delivery could lower dose to organs at risk (OARs), which is beneficial for the patients. The aim of this study was to investigate how Intensity Modulated Proton Therapy (IMPT) performs when treating locally-advanced lung cancer, compared to the Volumetric Modulated Arc Therapy (VMAT). Additional objective of the research was to assess the impact of density uncertainty taken into account during robust optimization of IMPT plans.

Materials and methods: Material from the internal quality control project conducted at the Oslo University Hospital was used. In this study 67 patients were assessed in terms of need for plan adaptation by analyzing the planning CT and control CT acquired halfway through the treatment course. A group of 16 patients, with diverse tumor characteristics, were used in this thesis. For each patient one VMAT plan and one IMPT plan were prepared, both optimized on the planning CT. They were then recalculated on the control CT. The robust optimization of IMPT plans was then repeated with lower density uncertainty. Thus, for each patient, three treatment plans: VMAT, $\text{IMPT}_{4.5\%}$, and $\text{IMPT}_{3\%}$, were prepared. They were compared to each other in terms of robustness, dose delivery to the treatment volumes and OARs, as well as the overall need for adaptation.

Results: VMAT plans scored better than IMPT plans in terms of dose coverage to the ICTVu, and robustness halfway through the treatment course. Median loss of $D_{98\%}$ to the ICTVu was at 0.01% for VMAT plans, compared to 1.22% in $\text{IMPT}_{4.5\%}$ and 1.54% in $\text{IMPT}_{3\%}$ plans. Spinal cord and healthy lung tissue received lower dose with protons, compared to photons. $\text{IMPT}_{3\%}$ plans were less robust than $\text{IMPT}_{4.5\%}$ plans, but they exhibited better dose protection of the spinal cord halfway through the treatment. Two VMAT plans, five $\text{IMPT}_{4.5\%}$, and six $\text{IMPT}_{3\%}$ plans would have needed adaptation due to loss of dose coverage to ICTVu of more than 2%. Two $\text{IMPT}_{4.5\%}$ and three $\text{IMPT}_{3\%}$ plans would have needed adaptation due to global maximum dose outside of PTVu increasing with more than 3%. One of the patients would have received too high dose to one of the OARs, in both the $\text{IMPT}_{4.5\%}$ and $\text{IMPT}_{3\%}$ plan.

Conclusion: Proton plans are less robust than photon plans, and exhibit larger need for adaptation. They are, however, better in sparing OARs from radiation. Lower density uncertainty in robust optimization leads to decreased robustness, but also better dose protection of OARs.

Contents

List of Figures

List of Tables

Abbreviations

CT 1	Planning CT
CT 2	Control CT obtained three weeks into the treatment
FSU	Functional Subunit
VMAT	Volumetric Modulated Arc Therapy
IMPT	Intensity Modulated Proton Therapy
IQR	Interquartile range
LET	Linear Energy Transfer
OAR	Organ At Risk
RBE	Relative Biological Effect
RT	Radiotherapy
CI	Conformity Index
HI	Homogeneity Index

Symbols

$IMPT_{4.5\%}$	IMPT plan set optimized with 4.5% density uncertainty
$IMPT_{3\%}$	IMPT plan set optimized with 3.0% density uncertainty

Chapter 1

Introduction

According to the Cancer Registry of Norway [23], cancer of the lung accounted for 20% of the cancer mortality in 2021. Number of new cases of lung and trachea cancer in 2022 reached 1804 for men and 1730 for women [23]. This corresponds to $8,8\%$ and $9,7\%$ of all cancer cases, for men and women respectively, making lung and trachea cancer the second most common cancer type, after prostate cancer for men and breast cancer for women [23]. In addition to the high incidence, the lung cancer has a relatively low five year survival rate (2018-2022) of 26.5% for men and 33.7% for women, according to the report [23]. For comparison, the most frequent types of cancer, of prostate and breast, have much higher five year survival rate of 95.7% and 92.5%, respectively. The time of survival is strongly influenced by the stage of the cancer and unfortunately, the lung cancer patients usually receive the diagnosis at the later stages, after the cancer has spread to regional lymph nodes or distant parts of the body [23].
Radiotherapy (RT) can be used for cancer of any stage. It may also be used in combination with other treatments, for example surgery or chemotherapy. For lung cancer, radiotherapy is used in over 60% of the patients and there is a clear effect of increased radiation dose on the local tumor control [16]. However, the lung tumors can be situated in a close proximity to organs at risk (OAR), like heart, spinal canal or esophagus, and by increasing the dose to the tumor, we risk increased toxicity and damage to those organs, which can be life-threatening. In recent years, a new treatment option that deals with this problem, has emerged. Utilizing the favourable physical properties of proton interactions in tissue, proton therapy is a highly precise radiation treatment for locally advanced lung cancer [22]. Using protons, compared to high-energy photons, allows for higher dose deposition in the tumor, while at the same time, sparing the surrounding tissue and organs at risk from the damage.
The challenge with proton therapy is that the passage of protons in the tissue can be altered due to the anatomical changes that can easily occur during the fractionated course of treatment. The consequence of it may be loss of dose coverage of the tumor and increased dose to normal tissue near the tumor, including organs at risk. Radiation is often delivered in the span of several weeks, according to a CT-based treatment plan. During those weeks the anatomy of the patient may start to show changes, like decreasing size of

the tumor, displacement of tissue, or variations in atelectasis, which is a partial collapse of the lung that may be caused by a tumor. However, if the CT imaging is repeated during the course of treatment, the treatment plan can be adapted to those various changes, ensuring that the radiation will be delivered according to the original prescription. The treatment plan adaptation can be time consuming and costly, but it may also be avoided altogether with a robust treatment plan. For a plan to be considered robust throughout the entire treatment period, it must maintain satisfactory dose coverage to the treatment volumes, and keep dose to organs at risk at an acceptable level. Plan's robustness increases if the uncertainties that could affect dose delivery, are accounted for during the optimization stage of treatment planning. However, if a plan is too conservative, the advantage coming from protons' precise dose targeting characteristics is reduced. This trade-off and the plan adaptation as a possible solution are important topics to consider when discussing proton therapy.

Focus of this study is inspecting the robustness and therefore need for adaptation of two radiotherapy modalities, photons and protons, in terms of lung cancer treatment. Specifically, the treatment techniques considered here are the Volumetric Modulated Arc Therapy (VMAT) and the Intensity Modulated Proton Therapy (IMPT), both very sophisticated techniques. The initial photon and proton plans are created in the treatment planning system RayStation, using the planning CT. To evaluate the robustness of each plan, the dose is then recalculated on the control CT, to simulate that the initial plan is used halfway through treatment. The need for adaptation is assessed, and the two modalities are compared to each other. Additionally, protons' sensitivity to tissue irregularities is inspected further, for all proton plans. This is done by changing density uncertainty, an embedded setting of the Plan optimization module in the treatment planning system. This way, the advantages and disadvantages of a less conservative proton plan are examined.

Chapter 2

Background

2.1 Ionizing radiation

Ionizing radiation, compared to non-ionizing radiation, has high enough energy to remove a valence electron from an atom, which means that the irradiated matter becomes ionized by absorbing this energy. Ionizing the atoms can cause DNA damage that stops cancer cells from duplicating and effectively kills them. There are different types of radiation sources that can directly or indirectly ionize tissue. Photons and protons are two of them, and while there are significant differences in how photons and protons interact with the medium they penetrate, they are both incredibly useful modalities for cancer treatment. This section opens with a quick introduction to the process of photons and protons interacting with matter and highlighting the difference, which is crucial in understanding their advantages and limitations in radiation treatment.

2.1.1 Photon interaction

Photon radiation is an example of indirectly ionizing radiation. Photons deposit energy in the matter in two steps, first by transferring the energy to release electrons or to produce electron-positron pairs [25]. The second step is when the energy is deposited by the charged particles in the matter in the process of Coulomb interactions with the orbital electrons [25].
In radiation physics, the three most relevant types of photon interactions with matter are Compton effect, photoelectric effect and pair production [2].
Compton effect describes collision of a high-energy photon with an electron, which results in the electron gaining kinetic energy from the collision and changing its direction, while the incident photon loses some of its energy and gets scattered away from its original direction [2]. While during Compton scattering the photon doesn't give away all of its energy, it can do so when interacting with an inner-shell electron. This happens in photoelectric effect, when the absorbed energy is used to remove the electron from the atom and give it kinetic energy. The electron uses that energy to travel further into the matter, while the recoiling ionized atom gains momentum [2]. For very high-energy

photons and materials with higher atomic number, the probability of pair production increases. It is an absorption of a photon near an atomic nucleus, resulting in creation of an electron and a positron. In this process, the photon's energy is converted to mass and the electron-positron pair interacts further with the matter [2].
Probability of each of these three types of interaction happening, depends on the quantum energy of the photons and the atomic number of the medium the photons travel through. In human tissue (low atomic number), Compton effect dominates through a broad range of energies, while photoelectric effect contributes more at lower photon energies or in a medium with higher atomic number [2]. Pair production becomes relevant at energies higher than several megaelectronvolts, which makes it negligible in radiotherapy [2].

2.1.2 Proton interaction

Proton, as a charged particle, is an example of directly ionizing radiation, meaning that there is only one step in the process of depositing energy in the matter, and it is by direct Coulomb interactions with orbital electrons [25]. However, while the individual photon needs to interact with matter only few times to deposit all of its kinetic energy, charged particle, like a proton, lose only a small fraction of its incident energy in each interaction. Additionally, while a photon may also pass through tissue without ever interacting with the atoms, for charged particles, this would not happen, since they are surrounded by the Coulomb electric force field, which makes them very active in interactions with electrons or the nuclei they pass [2].
Charged particles lose their energy by interacting with orbital electrons and the nuclei of the absorber. These two types of interaction cause respectively *collision loss* and *radiation loss*.
When an incident proton is close to an atom, it interacts with the orbital electrons through a *hard* or *soft collision*, depending on the perpendicular distance between the charged particle's trajectory and the nucleus, defined as the impact parameter b, in comparison to the atomic radius a [25]. When $b \approx a$, the charged particle experiences a hard (close) collision with the electron, and when $b >> a$, they interact through a soft (distant) collision [25]. Although the energy transfer is larger in a single hard collision than in a soft collision between two particles, the energy loss of a charged particle is divided equally between those two types of collisions, since the interaction with matter consists mostly of soft collisions [25]. The interaction between a proton and orbital electron causes the proton to lose some of its kinetic energy. This results in the collision loss, since the proton slows down, while the absorber atom gets ionized in the process [25].
The radiation loss occurs when a charged particle interacts with the Coulomb field of a nucleus. This happens when the impact parameter b is much smaller than the atomic radius a [25]. The incoming particle's trajectory can change due to the interaction with a nucleus, that is either elastic or inelastic, which determines the energy loss [25]. Inelastic interaction, in addition to large energy loss, will also involve emission of x-ray photons, and is therefore called *bremsstrahlung collision*, but the probability of it happening for protons is negligible due to proton's mass [25].

2.1.3 Photons and protons traversing through matter

Dose deposition of photons in the tissue is a quite complex process. Generally, the dose deposition in depth follows the inverse-square law, which means that it is inversely proportional to the square of depth. Additionally, the dose deposition is affected by attenuation and scattering of the photon beam in tissue [25]. As illustrated in Figure 2.1 [1], the photon beam enters the tissue delivering a relatively low dose to the surface. The dose per depth unit starts to rise rapidly and quite quickly reaches a maximum. This region is called the dose *build-up region*, and is a result of how the electrons, which are the product of the photon interaction with the atoms, continue the journey and deposit their energy deeper into the patient [25]. The depth of dose maximum is controlled by the the energy and range of the secondary electrons and therefore by the energy of the incident photons, as well the type of the absorber [25]. After the build-up region, the dose deposition decreases almost exponentially, which is a result of exponential attenuation of photons governed by Compton scattering and photoelectric absorption [25].
Since individual photons deposit their energy in just a few random interactions, their travel through matter can not be mapped in the same way as charged particles densely ionizing the tissue. If we specify the energy, medium and the type of a particle, we can predict how far the individual charged particle will travel, before it loses its energy. This is described by particle's *pathlength* [2]. For heavy charged particles, like protons, the path of the particle is almost linear, and therefore, particle's *range*, which is the depth of penetration, will be approximately equal its pathlength [5].

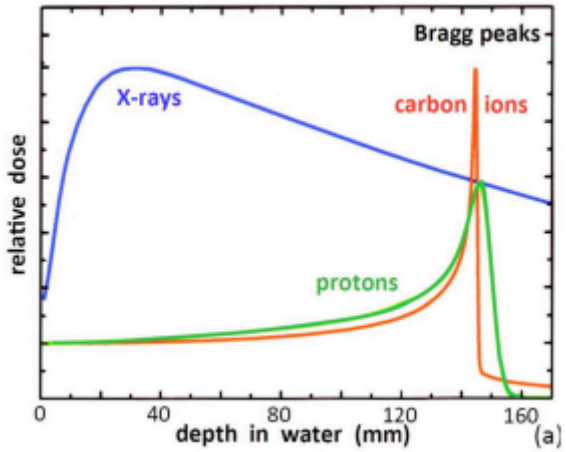

Figure 2.1: Depth dose profiles of X-rays, carbon ions and protons. Acquired from A Facility for Tumour Therapy and Biomedical Research in South-Eastern Europe [1], editor Ugo Amaldi CERN Yellow Reports: Monographs, CERN-2019-002 (CERN, Geneva, 2019), https://doi.org/10.23731/CYRM-2019-002 / Licence: Creative Commons Attribution 4.0

As illustrated in Figure 2.1 [1], for monoenergetic proton beam, the dose deposited in the tissue is relatively low as the beam enters the body, and it slowly increases with depth, since the protons slow down, increasing probability of the Coulomb interactions. Near the end of the range, the dose deposition increases dramatically, resulting in the very sharp *Bragg peak*, and then just as dramatically falls to zero. The depth at which the Bragg peak occurs depends on the initial energy of the beam, that is relatively easy to control [8]. Since the high dose deposition area directly under the Bragg peak is very narrow, in order to cover the whole tumor, the Bragg peak needs to be spread out. This is accomplished by combining multiple Bragg peaks of beams varying in range and the result is the *spread-out Bragg peak*, as illustrated in Figure 2.2 [6]. The ability to control the Bragg peak is a crucial advantage in proton therapy, allowing us to deliver high dose directly to the tumor with a substantial precision while at the same time sparing the normal tissue around the tumor [8]. However, if the tumor location in the body changes during the treatment, or other inhomogeneities appear in the way of the proton beam, this specific way of dose delivery may be a disadvantage, resulting in the Bragg peak (and therefore high dose) in the normal tissue, or low dose coverage of the tumor [8].

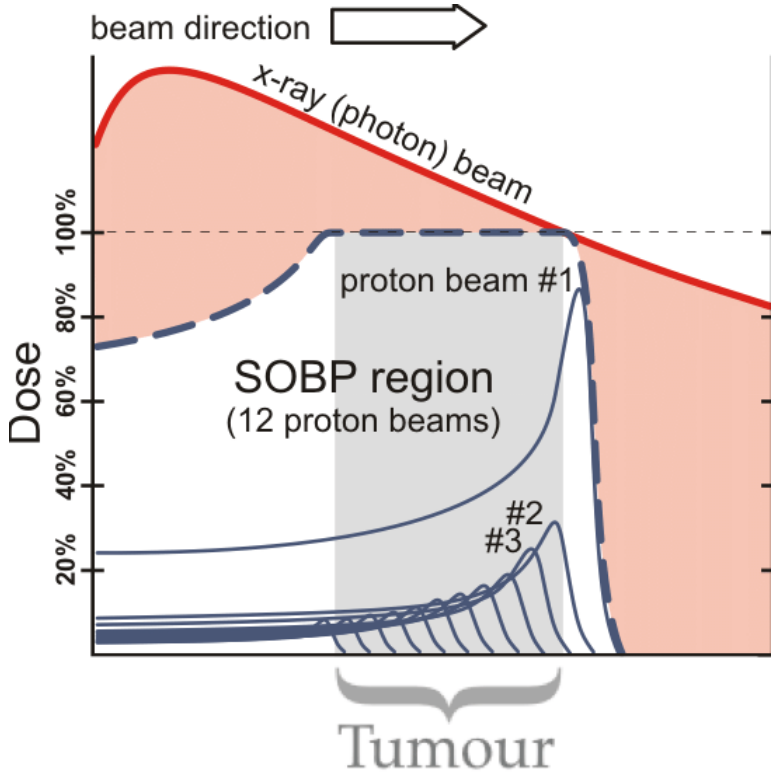

Figure 2.2: Spread-out Bragg peak. Acquired from FRED: a fast Monte Carlo code on GPU for quality control in Particle Therapy [6], M De Simoni et al, 2020, Journal of Physics: Conference Series, Ser. 1548 012020, doi:10.1088/1742-6596/1548/1/012020, Licence: Creative Commons Attribution 3.0 Unported (CC BY 3.0)

2.1.4 Linear Energy Transfer and Relative Biological Effect

Radiation particle's pattern of ionizing the tissue it traverses is described by linear energy transfer (LET). It is defined as the average energy deposited along the particle's track through matter per unit path length (the distance it travels). It is measured in units of $keV/\mu m$. Electrons, product of photon interactions with matter, participate in multiple scattering events when traversing through tissue. Their energy deposition is thinly distributed along their path, compared to that of heavy charged particles like protons. This is why electrons, and therefore incident photons, that are the source of energy for the electrons, are described as "low-LET" particles [5]. High-energy protons are also considered low-LET particles. However, as they traverse further into the tissue, their energy transfer per unit length (LET) increases, in a similar matter as the dose deposition. At depth corresponding to the Bragg peak, LET increases dramatically and beyond the Bragg peak. In this region, protons approach the end of their range, meaning they will not travel much further before they lose all of their energy. This leads to high LET.

The biological effect we want to achieve with radiation is creating enough double-strand breaks in DNA of a cancer cell, in order to kill it. Given that we deliver the same dose (energy imparted per unit mass, measured in gray-Gy [5]) of high- and low-LET radiation to a tumor, the biological effect on the cells will be different. This is described by the Relative Biological Effect (RBE):

$$RBE = \frac{dose\ of\ reference\ radiation}{dose\ of\ test\ radiation}, \tag{2.1}$$

where the reference radiation is usually 250 kVp X-rays or ^{60}Co γ-rays, and the test radiation is the radiation we are evaluating, in terms of the biological effect. Increased LET leads to higher density of the ionization pattern of the traversing particles. This leads to higher probability of damaging cell's DNA. To achieve the same biological effect (more tumor cells killed), we would have to deliver a higher dose of the low-LET radiation than of the higher-LET radiation. The RBE depends therefore on both the LET and dose level of the radiation [12]. As the LET increases near the Bragg peak, the same happens with particles' RBE.

2.2 Treatment volumes

The first step in the process of preparing and delivering radiotherapy to a patient is utilizing imaging techniques to accurately localize the tumor and delineate a target volume where we want to distribute the dose. Radiotherapy planning is based on CT images of the patient but the delineation of the treatment volumes and organs at risk is often performed using MRI in combination with CT. MRI is superior when it comes to the detail and contrast in the soft tissue imaging. This allows for better precision for delineating tumor borders and differentiating between the tumor and adjacent organs at risk. CT imaging, in addition to density information needed for dose calculations, provides a geometric framing for the organs. This helps the clinician to assess the location and size of the tumor and the healthy tissue.
The aim of treatment is to deliver a high enough dose to the visible tumor and the cancer cells around it, but at the same time spare the normal tissue around the tumor from the unnecessary dose and therefore possible side effects. The important part of treatment planning is therefore to delineate target volume and apply properly optimized margins. The aim of including extra margins is to ensure that the uncertainties linked to the treatment process are all accounted for. This includes inadequate delineation of the visible tumor, change in the position caused by internal movements, like breathing, and uncertainty associated with positioning of the patient at each treatment session.

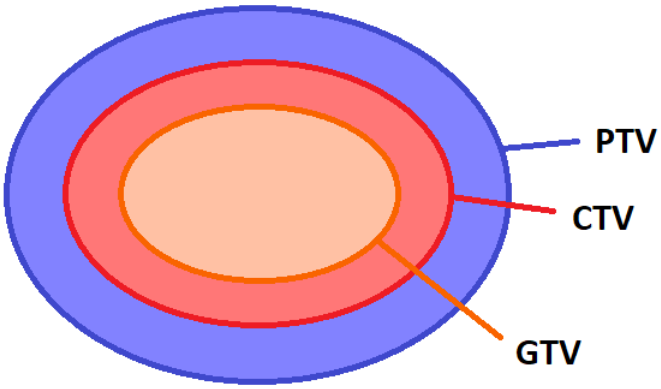

Figure 2.3: Target volumes commonly used in radiotherapy. Gross Tumor Volume (GTV) represents the visible tumor. Clinical Target Volume (CTV) represents GTV and a margin for the microscopic disease around the tumor. Planning Target Volume (PTV) includes another margin, taking account for planning and treatment uncertainties like organ motion and patient positioning.

Figure 2.3 is a simple schematic representation of the treatment volumes used in radiotherapy treatment planning, as described in ICRU 62 report (1999) [11]. The innermost volume is the Gross Tumor Volume (GTV), representing the visible tumor borders. It includes both the primary tumor, metastases and the affected lymph nodes. Tumor cells forming the visible tumor spread as the tumor grows which adds a layer of microscopic tumor cells around GTV. Clinical Target Volume (CTV) takes that into account adding an additional margin to the GTV. Due to the organ motion, uncertainties linked to patient positioning and other geometrical variations, an additional margin is needed to ensure the entire tumor receives the prescribed dose. This margin is included in the Planning Target Volume (PTV). Sometimes the organ motion is accounted for by itself in the Internal Target Volume (ITV). In those cases PTV is used to account for all others uncertainties. The organ motion can also be accounted for directly in the imaging phase, with a 4D-CT. This allows for including it already in the GTV, and therefore also in the CTV. The resulting volumes are then referred to as IGTV, ICTV and PTV [19].

2.3 Thoracic anatomy and organs at risk

A pair of lungs is divided by the mediastinum, region in the chest containing vital organs, including the heart, esophagus, trachea, main bronchi, important blood vessels, nerves,

and lymph nodes. Although it is challenging when treating lung cancer, the goal is to spare those organs from radiation, in order to protect their function. Another very important organ to spare during lung radiotherapy is the spinal cord, that can often be in close vicinity to a central lung tumor. For lung tumors close to the neck and shoulders, it becomes relevant to consider dose to the brachial plexus, which is a network of nerves connected to the arms. Additionally, parts of the lungs that are not affected by cancer, are also important to spare from exposure. The goal in treating a lung tumor is to deliver satisfactory dose to the tumor and affected lymph nodes, and at the same time spare those sensitive organs and structures. This chapter takes on the radiation effects on the organs at risk and is based on Radiotherapy in Lung Cancer by Ying (2017) [30] and Radiobiology for the Radiologist by Hall and Giaccia (2019) [8].

2.3.1 Parallel and serial organs

In radiotherapy organs are classified as parallel or serial organs, according to their functional characteristics and therefore consequences of radiation exposure. Organs are thought of as structures made up of functional subunits (FSUs), tissue parts that together maintain function of the organ they belong to. The difference between a parallel and a serial organ is the connection between the individual FSUs.
In a parallel organ, the FSUs are discrete components, like the acini, individual respiratory units of the lungs. Since the FSUs operate somewhat independently, damaging some of them, would leave the rest relatively unaffected. The surviving FSUs would then continue to sustain organ's function. This kind of functional architecture makes a parallel organ less vulnerable to radiation damage. Number of FSUs that can be injured, without it killing the whole organ, is therefore a measurement related to organ's sensitivity.
In a serial organ, the FSUs are not functionally or anatomically separated as in a parallel organ. The spinal cord is an example of a serial organ, since it can lose all of its function even if just a small part of it gets damaged. Serial organs are subsequently extremely vulnerable to radiation. It is therefore critical to not exceed the dose restrictions of a serial organ, regardless of how small part of the total volume will be exposed.

2.3.2 Organs at risk

As mentioned above, there are many organs at risk that must be taken into account during treatment planning for lung cancer. They differ in terms of dose requirements and possible side effects of radiation exposure. They are also categorized as either an early- or late-responding tissue. This is determined by how fast the tissue responds to radiation. Early-responding tissues like skin, bone marrow and intestinal epithelium consist of high turnover cells responding quickly to radiation exposure. Some organs can also exhibit both early and late response. How fast a radiation-induced damage to an organ will manifest itself depends on dose, fractionation and individual patient factors, like a pre-existing condition, age, etc. The late effects of radiation often become an irreversible chronic condition, while early effects are usually temporary. Consequently,

the risk of early and late side effects limits treatment possibilities. The early effects can in some cases lead to discontinuation of radiotherapy treatment, while the risk of late effects limits the total prescribed dose [29]. This section provides a summary of the clinical response of the organs at risk relevant for thoracic radiotherapy.

Lungs

Lungs are considered an intermediate- to late-responding tissue. At 2 to 6 months after the treatment an acute pneumonitis can occur. It is an inflammation of the lung tissue, with symptoms like fever, cough and chest pain. Months to years after the treatment a patient can develop progressive pulmonary fibrosis, tissue scarring leading to decreased lung capacity.
Although the lung is a sensitive late-responding organ, it can continue its function despite partial tissue damage. It is a parallel organ with independent functional subunits, meaning the radiation damage to some of them will not necessarily impair the whole organ. Consequently, a lung will be a dose limiting organ in a treatment plan only if substantial relative volume is exposed to radiation.

Heart

Heart is an organ exhibiting mostly late effects of radiation. The most common is pericarditis, which is an inflammation of the pericardium. It can happen early but in most cases it doesn't develop before a year after the treatment. Dose threshold for an increased probability of pericarditis is quite low if large part of the heart is irradiated. Dose tolerance increases with partial exposure and fractionation. Some years after the treatment, patient can also develop cardiomyopathy, due to the scarring. Condition comes with symptoms like chest pain, fatigue and arrhythmia (abnormal heartbeat).

Esophagus

Esophagus can display both early and late radiation-induced effects. The organ consists of layers of different types of tissue. The mucosa that lines the esophagus is an example of an early-responding tissue. Shortly after the treatment, an inflammation (esophagitis) and thickening of the esophageal wall can occur. This can cause pain and difficulty when swallowing, but the symptoms often pass relatively quickly. The muscle layer can show radiation-induced damage as necrosis and swelling in the epithelium, but this effect takes takes time to develop.

Spinal cord

Spinal cord is a classic example of a serial organ, and it is considered a late-responding organ. It has a low dose tolerance, and radiation damage to a small volume can impair the whole organ. Months to years after the treatment, patient can develop a rare but serious condition called radiation myelopathy. Symptoms include pain, burning/tingling sensation, bowel/bladder dysfunction, paralysis, etc [15]. Dose tolerance of the spinal

cord depends on the dose per fraction. In case of the probability for myelopathy, the irradiated length, as long as it's limited to maximum few centimeters, is an important factor.
Spinal cord can also display an early effect of radiation. The Lhermitte's sign can develop months after the treatment, and can happen at lower doses than the myelopathy. The condition is characterized by an abrupt sense of an electric shock going down the spine. The patient usually recovers from it after few months to a year.

Brachial Plexus

Brachial Plexus is a network of nerves connecting the neck and arms. The organ at risk is difficult to specify and delineate during treatment planning. Therefore, comparing to other thoracic organs at risk, knowledge about the dose restrictions to the brachial plexus is limited [9]. Years after the treatment patient can develop late radiation plexopathy, with symptoms like numbness, burning/tingling sensation, and in later stages even total paralysis of the arm [9].

Trachea and Bronchi

Trachea extends from the neck to the chest where it's divided into two main bronchi, right and left, leading to their respective lungs. Trachea and bronchi take crucial part in the respiratory function of lungs, and they are considered serial organs [9]. It is therefore essential to avoid delivering a high dose to those organs, even if just a small volume is irradiated.

2.4 External beam radiotherapy

External beam radiotherapy is a treatment delivered to the patient from an outside radiation source. Volumetric Modulated Arc Therapy and Intensity Modulated Proton Therapy are two very sophisticated external beam therapy techniques, utilizing photons and protons, respectively, as the outside radiation source. They are both exceptional in their precision and ability to spare the healthy tissue surrounding the target. This is an overview of how these two techniques work, based on Khan's The Physics of Radiation Therapy by Khan and Gibbons (2014) [14] and Radiation Physics for Medical Physicists by Podgoršak (2010) [25].

2.4.1 Volumetric Modulated Arc Therapy

Volumetric Modulated Arc Therapy is a radiation therapy technique that utilizes photons. Production of photons happens when high-energy electrons hit a target made of high-Z material. As an electron passes near a nucleus in the target, the Coulombic attraction deflects the electron from its initial path. In the process, some or all of the electron's energy is converted into a photon (called bremsstrahlung radiation). One electron can

experience multiple bremsstrahlung interactions in the target, before it loses all of its energy. The energy of the photon beam produced this way is a spectrum with the highest value equal the initial electron energy. The average value of the photon energy spectrum is around one third of that.

Linear accelerator

The target, where the x-ray production takes place, is situated in the head of a machine called linear accelerator (linac). Before the electrons arrive at the target, they have to be accelerated to a high energy. The beam-forming process begins with an electron gun, where the electrons are emitted from a heated cathode, focused into a beam and accelerated with the help of electrodes, and then transferred through the anode into the next component, called the accelerating waveguide. The waveguide system is connected to the radiofrequency (RF) power source that creates an RF field in the waveguide. The energy from the RF field is transferred to the electrons as they travel through the waveguide, a series of cylindrical cavities. The result is a pulsed high-energy electron beam that is transported towards the target.
The electron beam arriving in the head of the linac has a high kinetic energy and it is very narrow. As the electron beam strikes the target, the resulting x-ray beam will have a forward spatial distribution due to the high electron energy. However, due to the fact that a high-energy linac needs a longer acceleration tube, placed horizontally, the beam coming from the tube has to be bent before it reaches the target. The component used for bending the beam is a magnet system. It forces the electrons, that are charged particles, to change their path and can also change the shape and spread of the beam.
When the electron beam is incident on the target, a small fraction of the electron's kinetic energy is transformed into photons. As mentioned above, the distribution of photons leaving the target depends on the electron beam energy. With high electron energy, number of emitted photons will be highest close to the central axis of the target. Emission lobe of the photon beam leaving the target visualizes spatial distribution of photons. Because of the high electron-beam energy, the emission lobe of the photon beam has a relatively narrow and forward shape. Radiation delivered this way would have caused a pronounced peak in dose distribution in patient's tissue. Dose coverage to the treatment volume would have been uneven, with the highest dose in the center of the volume. Photon beam with an evenly distributed intensity would have produced a more manageable dose distribution in the tissue. As the beam leaves the target, its photon distribution can be modified by a flattening filter. It is a component made of high-Z material that can absorb some of the photons passing through. Its shape ensures that most photon absorption happens near the central axis, effectively making the beam intensity more uniform. Additionally, it absorbs the lower-energy photons that are not as effective in penetrating tissue. This allows for more precision when targeting a deep seated tumor and reduces dose to the patient's skin.
In order to effectively treat a tumor and simultaneously spare normal tissue from radiation, the photon beam has to be shaped according to the geometry of the treatment volume. Beam shaping process begins with a primary collimator that defines the abso-

lute borders of the field by absorbing photons that collide with it. This happens before the beam goes through a flattening filter. After that, the beam is shaped further by a secondary collimator consisting of four blocks, two upper jaws and two lower jaws, which together create a rectangular or square field. This field is further modified by the last collimator device, a multi-leaf collimator (MLC). It consists of thin and independently driven leaves that together create an irregular field.

Radiation delivery

In Volumetric Modulated Arc Therapy, linac's gantry rotates in an arc around the patient, while simultaneously delivering the radiation. It can be a full arc of 360° or a partial arc, depending on the position of the tumor and the organs at risk. As the gantry rotates, the individual leaves of the multi-leaf collimator move continuously but at a varying speed, effectively modifying the treatment field in three dimensions. The dose rate is also adjusted in real time during the treatment. This allows for dose delivery customized according to tumor's size, shape, depth in the body and vicinity to organs at risk.

2.4.2 Intensity Modulated Proton Therapy

Intensity Modulated Arc Therapy (IMPT) is another high precision radiotherapy technique, that, similarly to VMAT, accurately targets a treatment volume and simultaneously spares the normal tissue including organs at risk. IMPT utilizes protons that, as mentioned earlier, have unique characteristics of a Bragg peak dose delivery, allowing for maximizing dose to the tumor, while minimizing effect on the normal tissue. As in VMAT, the process of treatment delivery begins with a particle accelerator. In clinical applications, two types of accelerators can be used to deliver protons, a cyclotron or a synchrotron. In both machines, protons are accelerated by an electric field (synchronized with protons' direction) and maintain a circular trajectory due to a strong magnetic field. The difference between them is their structure and how they use the electric and magnetic field to accelerate the particles. This affects the energy variability of the proton beam, but also space and cost requirements. A cyclotron is more favored in clinical use due to the fact that it is more compact.

Cyclotron

A synchrotron accelerates particles in an orbit with fixed radius, through a circular vaccum chamber. To maintain particles' trajectory as they accelerate, a synchrotron applies a varying magnetic field to the chamber. The RF frequency is also increased as the particles accelerate. With a synchrotron, the energy of the beam can be controlled and adjusted to treatment requirements before the beam exits the synchrotron.
A cyclotron is a much more compact machine, than a synchrotron. It is a cylinder split into two dees with a gap between them and encased in a vacuum. The protons are injected in the center of the cylinder and follow a spiral motion outwards. As they pass from one dee to the other they accelerate due to the switch in the polarity of the

electric field. In contrast to the synchrotron, the magnetic field the dees are exposed to is constant. When the proton beam reaches the maximum energy, it exits the cyclotron. At this point the proton range is large and the beam has to be modified in order to treat a tumor at any depth and with a Spread-Out Bragg peak. The beam is usually modulated with energy degraders made of plastic materials. Using them, however, causes increased neutron contamination and calls for additional shielding measures.

Radiation delivery

The beam from a cyclotron is transported to a treatment room with the help of bending magnets. It arrives in a gantry that will bend the beam so that its direction is perpendicular to the patient laying on the treatment couch. The gantry itself is able to rotate around the patient, in order to deliver the beam from different angles. Due to different factors like tumor's irregular shape and the vicinity to the organs at risk, the IMPT treatment will usually be delivered from multiple fields. Combined together, the fields will result in a uniform target coverage and dose-sparing of the normal tissue.
The initial beam is very narrow and focused and it needs to be spread and modulated according to the size of the treatment volume and the prescribed dose distribution. There are two types of spreading techniques available: passive beam scattering and pencil beam scanning. The latter is used in the Intensity-Modulated Proton Therapy technique.
Passive beam scattering is a relatively simple technique where the beam passes through a scattering foil made of high-Z material. If a larger field is needed, a dual scattering foil is used. The first one will spread the beam, and the second one, with varying thickness, will ensure acceptable uniformity of the profile. The problem with it is that by improving the uniformity, the proton beam loses some of its range.
The scattered beam will have roughly Gaussian (bell shaped) intensity distribution. The beam will then go through a field-limiting collimator which will improve its lateral profile by trimming the edges. To take into account the nature of protons' energy deposition, with a sharp dose fall-off after the Bragg peak occurs, range compensators of low-Z materials are also used. These will ensure the dose distribution in tissue is aligned with the shape of the target volume. The same compensators are also designed to take into account irregularities in the tissue composition and surface of the patient. Simultaneously, they include a margin taking into account movement, error that comes with delineating treatment volumes and organs at risk, as well as the error in patient positioning on the treatment couch. The Spread-Out Bragg peak, necessary to cover the whole target volume with uniform dose, is created by a range modulator. It is a dynamic component placed in the beam-path before the beam goes through a scattering foil. As it rotates, filters that progress in thickness are inserted into the beam path. This creates a SOBP with a shape influenced by the thickness of each filter and how long each of them has been placed in the beam path.
The trending technique competing with passive beam scattering is the pencil beam scanning. With passive scattering, the uniformity obtained through increased thickness of the scattering foil, comes with a cost in terms of the beam range. This unfortunate trade-off and other limitations are avoided with pencil beam scanning. With this technique, the

beam is moved magnetically through the patient while the properties of the beam change, in order to deliver the prescribed dose distribution to the treatment volume. Beginning in the deepest slice of the tumor, the dose is delivered spot by spot until the whole slice is irradiated. The varying size of the tumor slices, as the depth decreases, is accounted for across the entire tumor in pencil beam scanning. In passive beam scattering, the SOBP is defined by the range modulator before the beam passes through the scattering foil and spreads laterally. The SOBP is uniform across the field size at each depth. Because of the range compensators, the shape of the tumor is accounted for, but only ranging from tumor's deepest slice to the depth of the slice with largest area. Past this point, as the dose delivery moves towards the surface of the patient, the tumor slices decrease in size. However, the field size will not continue to change according to the tumor size anymore. This means effectively that the normal tissue in front of the thinnest parts of the tumor will receive unnecessary dose. Avoiding this is an important advantage of the pencil beam technique.
A disadvantage with pencil beam scanning is the high sensitivity to organ motion during beam delivery. This is crucial when treating tumors adjacent to the organs at risk. With pencil beam scanning, the dose is delivered with a focused beam, covering the target volume with small spots. This is a precise technique, but should there be any organ movement around the treatment volume, the pencil beam can miss it and target normal tissue instead. The organ motion can also alter the density composition of the tissue in the path of the proton beam as it traverses through the patient. This will change the proton range, resulting in inaccurate Bragg peak delivery across the volume.

2.5 Dose-volume parameters

In order to describe dose distribution in the patient, including dose coverage to the treatment volumes and dose delivered to healthy tissue and organs at risk, we use dose-volume parameters. The ones that are relevant in this study are listed in Table 2.1, together with their description.
Table 2.1: Dose-volume parameters used to describe dose distribution in the irradiated volume.

Parameter	Description
$D_{X\%}$	Minimum dose received by the most irradiated X% of the volume.
D_{Xccm}	Minimum dose received by the most irradiated Xcm^3 of the volume.
D_{max}	Minimum dose delivered to the most irradiated voxel in a volume.
V_{XGy}	Part of a volume that receives at least X Gy.
Mean dose	Average dose received by a specific volume.

2.6 Statistical methods

2.6.1 Box-plots

A box-plot is used to illustrate distribution of a dataset, highlighting the spread and skewness of the data [17]. Figure 2.4 shows an example of a box-plot that consists of a box, two whiskers and one extra datapoint at the bottom. Given that the data is sorted in ascending order, the yellow box itself represents half of all datapoints in the dataset, spreading from Q_1, which is the first quartile of the dataset (25th percentile), up to Q_3, which is the third quartile (75th percentile). The box is therefore defined as the interquartile range (IQR) of the dataset. The other half of datapoints is outside of the box with first 25% below it and last 25% above it [17]. In addition to the box, the plot consists also of two whiskers labelled Q_0 and Q_4. They mark the minimum and maximum value in the dataset, as long as the values are inside the range of $1.5 * IQR$ below Q_1 and above Q_3. This means that the lower whisker can extend down to $Q_1 - 1.5 * IQR$ value, while the upper whisker can extend up to $Q_3 + 1.5 * IQR$ value, where $IQR = Q3 - Q1$.

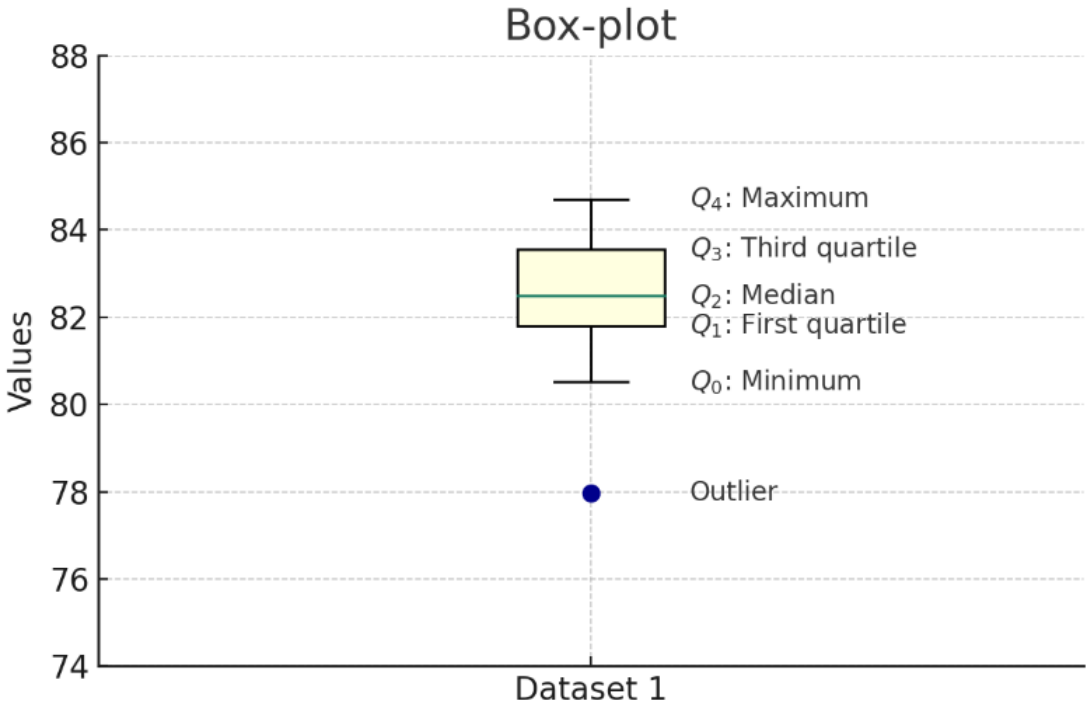

Figure 2.4: Example of a box plot used to show distribution of a dataset.

2.6.2 Wilcoxon matched-pairs test

The Wilcoxon matched-pairs test is a statistical test that compares two groups of data and determines if there is a significant difference between the median values of the two

groups [4]. For this test, data points from the first group are paired with the points from the second group. Result of the Wilcoxon test is a p-value that indicates a significant difference if it's below 0,05.
The Wilcoxon matched-pairs test is a non-parametric test, meaning it doesn't include assumptions on data distribution. For the more popular t-test, data has to be normally distributed. This requirement is hard to achieve in small samples of data or in the presence of outliers. A non-parametric test, like the Wilcoxon test, can be used in those cases.

Chapter 3

Method

3.1 Patient material

Patient material used in this thesis is a part of data coming from an internal quality control project conducted at the Oslo University Hospital. In the project, 67 patients with locally advanced lung cancer were studied for possible need of treatment plan adaptation during curative radiotherapy [3].
Each patient had a planning CT scan (here referred to as CT 1) prior to the treatment, and a control CT (CT 2) done halfway through the treatment. The planning CT was a free-breathing CT scan, which means that the patients could breathe normally during the scanning. It was used for delineation and treatment planning. The respiratory motion was then evaluated with the help of 4D-CT, a CT scan that captures images over time. The control CT was used to recalculate the initial dose distribution and evaluate the treatment plan according to anatomical changes. The control CT was co-registered with the planning CT [3].
Data utilized in the present study are the two sets of CT scans, planning CT and control CT, for 16 patients. These 16 patients are a representative collection, including cases with different grade of anatomical changes and different tumor characteristics. It is a diverse group when it comes to the size of the tumor, its proximity to organs at risk and its location in the lungs.

3.2 Treatment volumes and organs at risk

Treatment volumes IGTV, ICTV and PTV were provided for each patient from the earlier project, together with the OARs. Organ motion was accounted for with the help of 4D-CT imaging. In terms of the margins, the ICTV was created by adding a margin of 5 mm, uniform in each direction around the IGTV. This margin was also reduced, if needed, to exclude the bone tissue and large blood vessels [3]. The PTV was defined by adding a $5 - 8$ mm margin to the ICTV.
Treatment volumes vary in size and location for each patient. For half of them, in

addition to the primary tumor, some of the lymph nodes are affected by tumor cells. In the treatment planning system, the lymph nodes and the primary tumor are unified and referred to as IGTVu, ICTVu and PTVu. The overview of the patients and their treatment volumes is given in Table 3.1. Each patient was assigned a number and these numbers will be used throughout the thesis. Treatment volumes are delineated on the planning CT (CT 1) and registered on the control CT (CT 2). Although for some patients there is some tumor shrinkage from CT 1 to CT 2, the ICTVu is not necessarily reduced. This is due to the possible residual of tumor cells around the shrunken IGTVu. In those cases, where the ICTVu is reduced, it was considered necessary during the treatment in order to stay within the dose tolerance of the OARs [3]. The overview of the ICTVu size is presented in Appendix A (Table 6.1).

Table 3.1: Patient list specifying the treatment volumes.

Patient	Treatment volume
1	Primary Tumor + 5 Nodes
2	Primary Tumor
3	Primary Tumor + 2 Nodes
4	Primary Tumor
5	Primary Tumor + 1 Node
6	Primary Tumor + 5 Nodes
7	Primary Tumor
8	Primary Tumor + 1 Node
9	Primary Tumor + 1 Node
12	Primary Tumor
13	Primary Tumor
15	Primary Tumor
16	Primary Tumor
17	Primary Tumor + 1 Node
18	Primary Tumor
21	Primary Tumor
22	Primary Tumor + 1 Node

Only organs in the vicinity of the tumor were delineated. Organs delineated for all patients were lungs, esophagus, and spinal cord. For the lungs only the healthy parts are considered as an organ at risk. The region of interest used in the planning system is therefore a union of right and left lung excluding the IGTVu. The updated OAR is therefore referred to as Lungs-IGTV. All organs were delineated in the planning CT (CT

1) prior to the treatment, and adjusted on the control CT (CT 2) halfway through. In some cases, the lungs seemed to be copied from CT 1 over to CT 2 without any extra modifications. For this study, the decision was to adjust those using RayStation contouring tool called Smart brush.
The rest of the OARs, i.e. the heart, brachial plexus (right and left), trachea, and main bronchus (right and left), were not delineated for all patients. This is due to the distance from part of the chest receiving the treatment. Being far away means that there is high probability that the organs would receive negligible dose. The heart was not delineated for Patient 15 and 16, both having tumor in the upper region of their right lung. The left brachial plexus was delineated only for Patient 1, with a tumor in close vicinity to the tumor. The right brachial plexus was delineated for Patient 3, 6, 15 and 16, due to the same reason. Trachea was delineated for 11 out of 16 patients. For half of the patients, both right and left main bronchus was delineated, and for one patient (Patient 8) only the right one was delineated.

3.3 Treatment planning in RayStation

The treatment planning was performed in RayStation 12A SP1 application created by RaySearch Laboratories [27]. Process began with defining the dose prescription. Initial beam setup was chosen according to multiple factors depending on the modality. Some initial objectives were applied, in order to initiate the inverse planning. In order to track the quality and performance of the initial plan and later optimizing adjustments, a list of clinical goals was assembled. Those goals included requirements for the treatment volume coverage and restrictions for organs at risk. Dose calculations were performed using the Collapsed Cone algorithm for VMAT plans and the Monte Carlo algorithm for IMPT plan, as described in the RayStation's User Manual [27].
If the goals were not met or had potential for improvement different strategies were applied. The initial objectives and their weighting could be modified. New objectives related to already delineated volumes, and in some cases objectives for self-defined volumes, were added. At times, adjusting the beam setup was deemed necessary to improve the treatment plan. This section includes details on the entire treatment planning process.

3.3.1 Dose prescription

Treatment planning for all 16 patients was performed using dose prescription of 66 Gy, delivered in 33 $2Gy$ fractions. This was used both for VMAT- and IMPT plans. In all plans, the prescription type is median dose ($D50\%$) to the ICTVu, meaning that 50% of the ICTVu will receive the prescribed dose.

3.3.2 Clinical goals

Clinical goals are a tool used in treatment planning to assess if a plan is clinically acceptable. The list of clinical goals used in this study is acquired from the official guideline

document for the curative treatment planning for lung cancer, formulated at the Oslo University Hospital [28]. The goals include dose coverage to treatment volumes and dose restrictions to organs at risk. They are listed in Table 3.2, the way they were applied in the RayStation software.

Table 3.2: Clinical goals, used in treatment planning process, including dose restrictions to the organs at risk and the required dose coverage of the regions of interest. The goals are acquired from the official guidelines proposed by the Oslo University Hospital [28].

Goal		Priority
ICTVu $D_{98\%}$	$D_{98\%} > 95\%$ av 66 Gy	critical
PTVu $D_{98\%}$	$D_{98\%} > 95\%$ av 66 Gy $D_{98\%} > 90\%$ av 66 Gy	desired critical
Max. D_{2ccm}	$D_{2ccm} < 69,96$ Gy	critical
Max. Dose	Point max. $< 71,30$ Gy	desired
Lungs-IGTV V_{20Gy}	$V_{20Gy} < 35\%$	critical
Lungs-IGTV V_{5Gy}	$V_{5Gy} < 65\%$	desired
Mean Lung Dose	$MLD < 20$ Gy	critical
Heart V_{50Gy}	$V_{50Gy} < 20\%$	desired
Heart V_{45Gy}	$V_{45Gy} < 25\%$	desired
Heart V_{30Gy}	$V_{30Gy} < 30\%$	desired
Mean Esophagus Dose	$MED < 34$ Gy	critical
Esophagus D_{1ccm}	$D_{1ccm} < 68$ Gy	critical
Esophagus V_{60Gy}	$V_{60Gy} < 15cm^3$ $V_{60Gy} < 5cm^3$	desired desired
Spinal cord D_{1ccm}	$D_{1ccm} < 50$ Gy	critical
Spinal cord D_{max}	$D_{max} < 52$ Gy	critical
Brachial Plexus (right) D_{max} Brachial Plexus (right) D_{max}	$D_{max} < 60$ Gy $D_{max} < 66$ Gy	desired critical
Trachea D_{1ccm} Main Bronchus (right) D_{1ccm} Main Bronchus (left) D_{1ccm}	$D_{1ccm} < 68$ Gy $D_{1ccm} < 74$ Gy	desired critical

The goals have different priority in treatment planning. The goals described as critical were used as the absolute criteria in treatment planning in this study. The goals described as desired were also considered very important, but achieving each of them was not an absolute requirement to finalize the optimization process. The list of goals was used to track the optimization and as a reference to modify the objectives for the next optimization attempt. For patients with treatment volume consisting of affected lymph nodes, in addition to the primary tumor, those different volumes were listed together with the union volume (PTVu, ICTVu). This would enable discovering which part of the union is deficient in dose, an important information needed to improve the optimization process. The dose-volume parameters used in the list of clinical goals are described in

Table 2.1.

3.3.3 Objectives

As mentioned above, setting up a list of initial objectives is how the inverse treatment planning process begins. Depending on the modality, the beam setup, and tumor characteristics, the list of objectives varies for each patient. The objectives can be different RayStation functions, like a maximum dose function or a uniform dose function. How each function is applied and to which region of interest, is influenced by the clinical goals described in previous section. Each objective on the list has a specific weight assigned to it. In the initial optimization process, all objectives were weighted equally. After running the initial optimization process and checking the results in the clinical goal list, the objectives were modified accordingly. Possible improvement tools were changing the weights of the objectives, changing function specifications, or adding new objectives. In some cases, a new volume was delineated, and then used in an objective, in order to manipulate the dose distribution.
For most patients, the initial list of objectives included a uniform dose objective of 66 Gy to the ICTVu volume, maximum dose objective of $71,30$ Gy to the whole patient volume, maximum dose of 18 Gy to the spinal cord, and several other objectives for the relevant organs at risk or regions of interest. Objectives assigned to treatment volumes would also often be separately defined for the primary tumor, the affected nodes and the union volume. Distinguishing between those volumes would enable more targeted optimization. This would often be necessary to achieve dose coverage to the union volume more effectively.
The software functions used in the objective list have certain characteristics that need to be taken into consideration, when applying them to different organs. According to the RayStation documentation [26], the maximum dose function is very restrictive, since it will try to reduce the dose in each voxel of the volume to a certain value. That is beneficial when trying to spare a serial organ, like the spinal cord or to avoid hot spots (spots receiving higher than prescribed dose [13]). The restrictiveness of the maximum dose function can however cause conflicts with the other optimizing functions [26]. Therefore, for parallel organs, like lungs, a maximum DVH (Dose Volume Histogram) function was used instead. This is a function that manipulates the shape of the dose volume histogram, for instance, by forcing 60% of lung volume to receive max. 5 Gy.

3.3.4 VMAT plans

In terms of the beam setup for photon plans, the approach suggested in the guideline document [28] mentioned above, was used. Some patients received 2 half arcs treatment plan, some of the patients with a centrally situated tumor received 1-2 full arcs treatment plan, and the patients with tumor on one side of the body received a treatment plan with arcs covering only that side, in order to spare the opposite lung. The initial beam setup was in some cases modified, specifically when other optimization tools, like increasing objective weight, were not sufficient. The beam setup for all of the patients

is specified in Table 6.2 in Appendix A. The machine chosen to deliver photons in the treatment planning system is not able to cross through the point at 180 degrees (right below the patient). A half arc could therefore span from 0 degrees (right above the patient) to max. 179 degrees in the clockwise direction, or from 179 degrees to 360 degrees in counterclockwise direction. A full arc could span from 181 to 179 degrees in clockwise direction, or from 179 to 181 degrees in counterclockwise direction. Collimator setting for all patients was 15 degrees for the clockwise rotation and 345 degrees for the counterclockwise rotation, in order to achieve a complementary dose distribution. Additionally, photon energy used in all photon plans was 6 MV (due to the recommendations from the guideline document [28]), and the treatment couch was kept at 0 degrees.
To achieve acceptable dose coverage to the PTV, a minimum DVH (Dose Volume Histogram) function was used, specifying that 99% of the target volume should receive 64 Gy, as indicated in table 3.2. In some cases, this function would not be sufficient, even with a large weight or higher dose assigned to it. Then, a minimum dose function was tested as a more rigid tool, in order to achieve better outcome. Additionally, to avoid hot spots in the PTV, a maximum dose function was also used in some cases. The function would force the dose in each PTV voxel to stay below 71.3 Gy.

3.3.5 IMPT plans

The beam setup for all proton plans is described in Table 6.3. Number of beams varies from patient to patient with an average of 4 beams in each case. The angle for each beam was chosen with trial and error method, with the aim to deliver a uniform dose to the treatment volume and spare as much of the healthy tissue as possible. Due to the nature of proton's dose deposition in tissue, each angle was chosen in a way that lowers the risk of Bragg peak ending up in an organ at risk right beyond the treatment volume. Additionally, protons' sensitivity to inhomogeneities was taken into account when choosing the beam angles. The necessity of this approach was especially apparent when trying to direct the beam through the lung tissue.
As in the case of VMAT plans, the treatment couch setting was 0 degrees in all proton plans. The snout (extendable part of the nozzle, through which the proton beam is delivered) was set to 42 cm away from the isocenter and in some cases the software automatically moved the snout further away, if it was needed.
For 5 patients with a tumor situated near spinal cord, that is very sensitive to radiation, an extra tool was utilized. It specifies that the beam should avoid an OAR on its way through the tissue. The relevant OAR is specified under the *Beam computation settings* tab in RayStation. The same tool was used in one of the two beams in the case of Patient 16, with a tumor very close to the right brachial plexus. See Table 6.3 for the overview of the cases in which this tool has been utilized.

Robust optimization

The goal of optimization is balancing the trade-off of delivering sufficient dose to the target and sparing healthy tissue and organs at risk. An initially accepted plan should, if well optimized, be able to uphold the clinical standard during the entire treatment period. The treatment plan is based on the planning CT taken before the treatment course begins. During the treatment, both between the fractions and in each delivery session, deviation from the initial planning geometry will occur. Sources of deviation include error in patient setup on the treatment couch, patient movement during the delivery, changes in tissue caused by patient's condition etc. In order to create a robust plan, that will perform well during the treatment, those deviations have to be considered during the optimization stage.
In VMAT plans, the PTV was included in plan optimization in order to take into account the uncertainty tied to patient position or anatomical changes. This is considered an acceptable approach for photon modality, but in the case of protons, using PTV alone may produce a plan that is not robust enough [21]. A robust plan performs well during the whole course of the treatment because possible uncertainties that could affect treatment outcome are already considered and planned for beforehand. Protons, in comparison to photons, are more sensitive to any irregularities during treatment delivery. In IMPT, dose distribution inside and around treatment volume is created by matching doses from multiple beams coming from different directions. In case of any variations in the tissue happening during the treatment delivery, the individual doses may be misaligned, causing inhomogeneous dose coverage to treatment volumes and excessive dose deposition in normal tissue [24]. One of the effects of the misalignment could be underdosage in the target volume. Adding an extra margin could minimize this problem at the edge of the target, but it is not a sufficient solution for dose misalignment in the rest of the volume [24].
A robust optimization was therefore performed in all IMPT plans, including following parameters: density uncertainty, patient position uncertainty, and a systematic organ motion uncertainty. The position uncertainty setting of 5 mm was applied isotropically and universally for all beams. Density uncertainty was initially set to 4.5%, universally for all beams. The systematic organ motion uncertainty was based on the planning CT image set. Those optimization settings were applied directly to the ICTV objectives in RayStation, including the ICTVu and the individual parts of it. During the robust optimization process, multiple scenarios are created, to take into account all possible combinations of the errors. Additionally, LET distribution map was used to ensure no hotspots would target an OAR.
The effect of density uncertainty setting on the robustness was also explored by changing it to 3% for all patients.

3.3.6 Robust Evaluation

All plans, both the VMAT plans and the two sets of IMPT plans (optimized with 4.5% and 3% density uncertainty) were evaluated in terms of their robustness using the Robust

Evaluation module in RayStation. The proton plans were evaluated using the same scenario uncertainties as in the Plan Optimization module, while the photon plans were evaluated only in terms of the shift in patient position and systematic organ motion uncertainty. The settings used in the Plan evaluation module are listed in Table 3.3.

Table 3.3: Uncertainty settings used in the Plan evaluation module in RayStation. The three sets of treatment plans are the photon (VMAT) plan set and two proton plan sets, $IMPT_{4.5\%}$ and $IMPT_{3\%}$, optimized with 4.5% and 3% density uncertainty respectively. The settings used for proton plans are therefore the same as those used in the Plan optimization module.

Plan set	Patient position uncertainty [mm]	Density uncertainty [%]	Organ motion uncertainty
VMAT	5	0	systematic and based on CT 1
$IMPT_{4.5\%}$	5	4.5	systematic and based on CT 1
$IMPT_{3\%}$	5	3	systematic and based on CT 1

The Plan evaluation and Plan optimization modules were used together in order to achieve a robust VMAT and IMPT plan for each patient. Robust evaluation highlighted which clinical goals would be most susceptive to the uncertainties in the current plan. This worked as a guideline for further improvements in the optimization process. Flowchart in figure 3.1 summarizes the treatment planning process from start to finish.

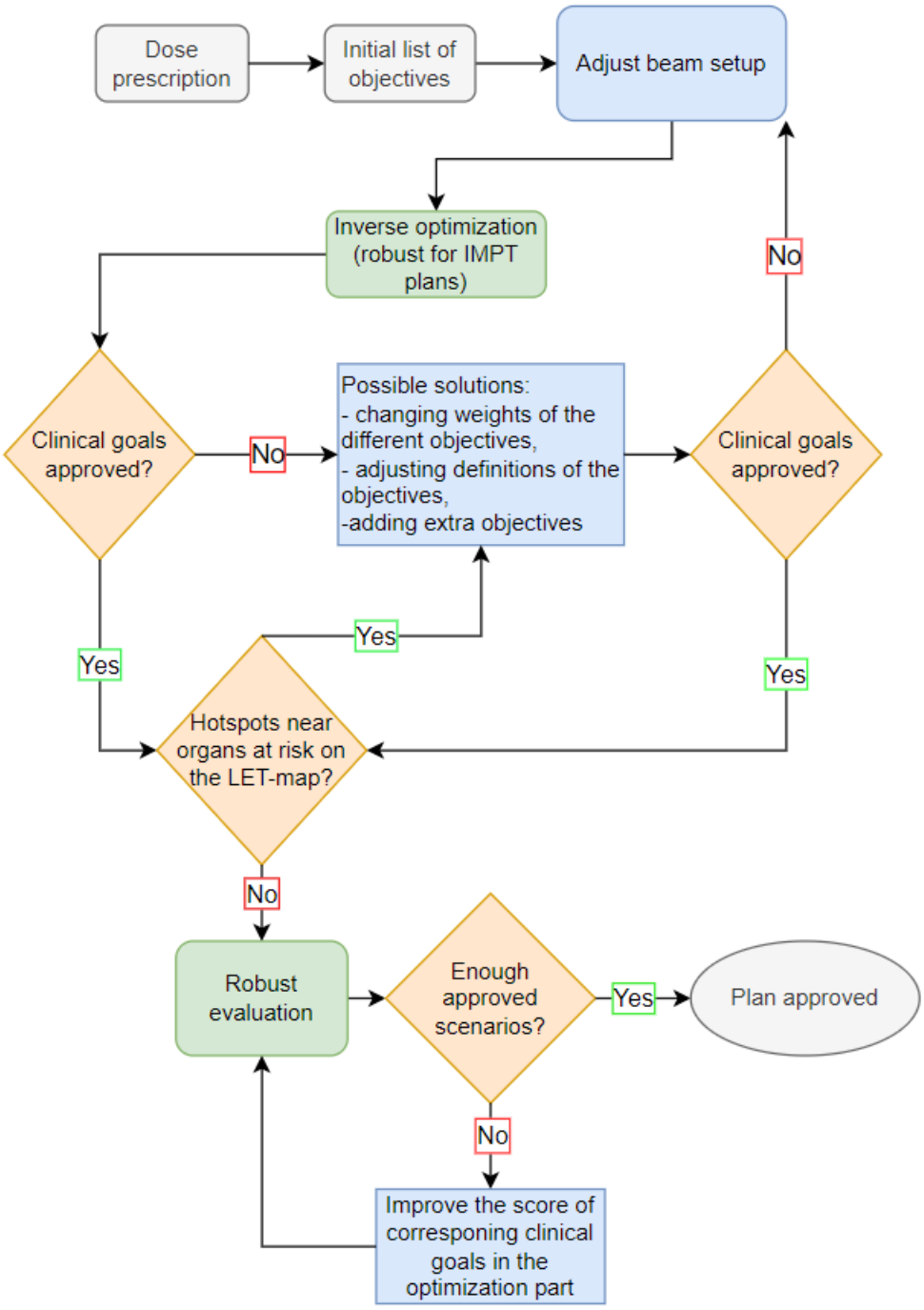

Figure 3.1: A flowchart describing the process of treatment planning, including the initial setup, the inverse optimization, and the robust evaluation.

3.4 Need for adaptation

All treatment plans were created using the planning CT (CT 1). The control CT (CT 2), taken halfway through the treatment, was used in further robustness assessment. The dose distribution, originally planned on CT 1, was recalculated on CT 2. This was performed for all VMAT-plans and both sets of IMPT-plans (optimized with different density uncertainty). The two sets of dose calculations (made on CT 1 and CT 2) were compared to each other in terms of the achievement of clinical goals and other parameters. For each modality, the difference in dose calculations from CT 1 to CT 2 was analyzed in order to determine if the original plan would have needed adaptation halfway through the treatment. Benchmarks that would cause the need for adaptation were taken from the internal quality control project [3], that the patient material is sourced from. The criteria include:

- loss of dose coverage ($D_{98\%}$) to the ICTVu of more than 2%,
- global maximum dose outside of PTVu increased with more than 3%,
- dose to an organ at risk increased above the critical threshold.

The global maximum dose outside of PTVu was found by creating a new volume in RayStation. The volume included the whole patient volume minus the PTVu, and the global maximum dose was measured as the dose delivered to 0% volume.
Dose to organs at risk, in the initial treatment plan and the recalculated one, was noted and compared to the respective clinical goals. For each treatment, if the initial dose to any of the relevant OARs increased above the critical threshold, the plan would have needed adaptation.

3.5 Additional comparison

As mentioned above, each treatment plan was assessed in terms of its need for adaptation halfway through the treatment. This was also one of the factors in the comparison between the two treatment techniques, VMAT and IMPT. The other factors included the overall dose coverage to the treatment volumes and the dose to organs at risk. Since IMPT is considered sensitive to variation in tissue, the impact of density uncertainty in the optimization stage, was also analyzed. To summarize, the dose delivery and plan robustness were examined in three categories:

- the original plan (VMAT/IMPT) optimized on CT 1 vs. recalculation on CT 2,
- VMAT plan vs. IMPT plan,
- IMPT plan optimized with 3% density uncertainty vs. IMPT plan optimized with 4.5% density uncertainty.

3.6 Plan quality

In a treatment plan of good quality, the target volume is homogeneously covered by the prescribed dose, while the healthy tissue around it receives as small amount of dose as possible. Choosing which treatment plan is the best option for a patient is difficult due to the large number variables that need to be considered. A possible solution is to give each plan an overall score that would tell us how well it handles the trade-off between high dose delivered to the target volume and minimized dose delivery to the normal tissue and organs at risk. Many different ways to measure the score have been introduced over the years, all with different sets of advantages and limitations.
To evaluate and compare all three sets of treatment plans in this study, two functions were calculated. They were both provided in the RayStation software, as the Conformity Index and the Homogeneity Index.

3.6.1 Conformity Index

The conformity index used in the RayStation software is defined as

$$\text{Conformity Index} = \frac{\text{target volume covered by the reference isodose}}{\text{total reference isodose volume}}. \tag{3.1}$$

It was used as one of the tools used to assess plan quality of each treatment plan for each patient. The reference isodose in the index was set to 66 Gy, which is the prescribed dose, and the target volume used in the measurement was the ICTVu in each case.

3.6.2 Homogeneity Index

The other function used to analyze the plan quality was the Homogeneity Index, also provided in the RayStation software. It is defined as:

$$\text{Homogeneity Index} = \frac{D(x)}{D(100-x)}, \tag{3.2}$$

where $D(x)$ is the dose at $x\%$ of the reference volume, set to 98% of the ICTVu in all cases. The result is therefore a ratio between the near minimum dose ($D_{98\%}$) and the near maximum dose ($D_{2\%}$). An index close to 1 means that the dose coverage in the volume is homogeneous, with high minimum dose and without undesired hotspots. A lower index value means either that the minimum dose delivered to most of the target is too low or that there are significant hotspots in the volume.

3.7 Statistical analysis

Tools used to statistically analyze the results where the box-plots and the Wilcoxon matched-pairs test. The box-plots were used to help visualize and assess data distribution in the results coming from all patients. The Wilcoxon matched-pairs test was used to determine if the difference in median values between two groups of data was statistically

significant. This was used to compare sets of treatment plans, as well as to assess the robustness and other characteristics of each modality. Both generating the box-plots and performing the Wilcoxon matched-pairs test was done with the help of a Python-script.

3.8 Ethical considerations

The internal quality control project [3] was approved by the local ethic committee with approval number 18/02240. After publication the data set was fully anonymized and a sub-set of these data was used for this thesis.

Chapter 4

Results

4.1 VMAT vs. IMPT

Two treatment techniques, VMAT and IMPT, are assessed in terms of dose delivery to the treatment volumes and organs at risk. Data for each modality includes results from two calculations, the initial dose distribution based on planning CT (CT 1), and the dose distribution recalculated on the control CT (CT 2). Here, the two modalities are assessed separately and compared to each other. IMPT plan set used here is the first one, optimized with 4.5% density uncertainty ($IMPT_{4.5\%}$). Results on dose delivery to the organs at risk are reduces to some representative examples while the rest is presented in Appendix A. Dose coverage results correspond to the whole tumor volume, including the primary tumor and affected lymph nodes. Results differentiating between these separate parts of the union volume, are presented in table 6.11 (Appendix A). The total volume of the ICTVu for each patient is presented in table 6.1. For two of the patients, ICTVu delineation was enlarged on CT 2. Volume changed from 555 cm^3 to 583 cm^3 for patient 2, and from 279 cm^3 to 311 cm^3 for patient 6.

4.1.1 Dose coverage of the treatment volumes

The first part of data on treatment planning relates to the dose received by the treatment volumes, including the ICTVu for both VMAT and IMPT plan sets, and additionally the PTVu for VMAT plans. The results in each plot are collected in two boxes displaying distribution of data from the initial (CT 1) plans and the recalculated (CT 2) plans. Figures 4.1 and 4.4 display dose coverage to the treatment volumes ICTVu and PTVu.

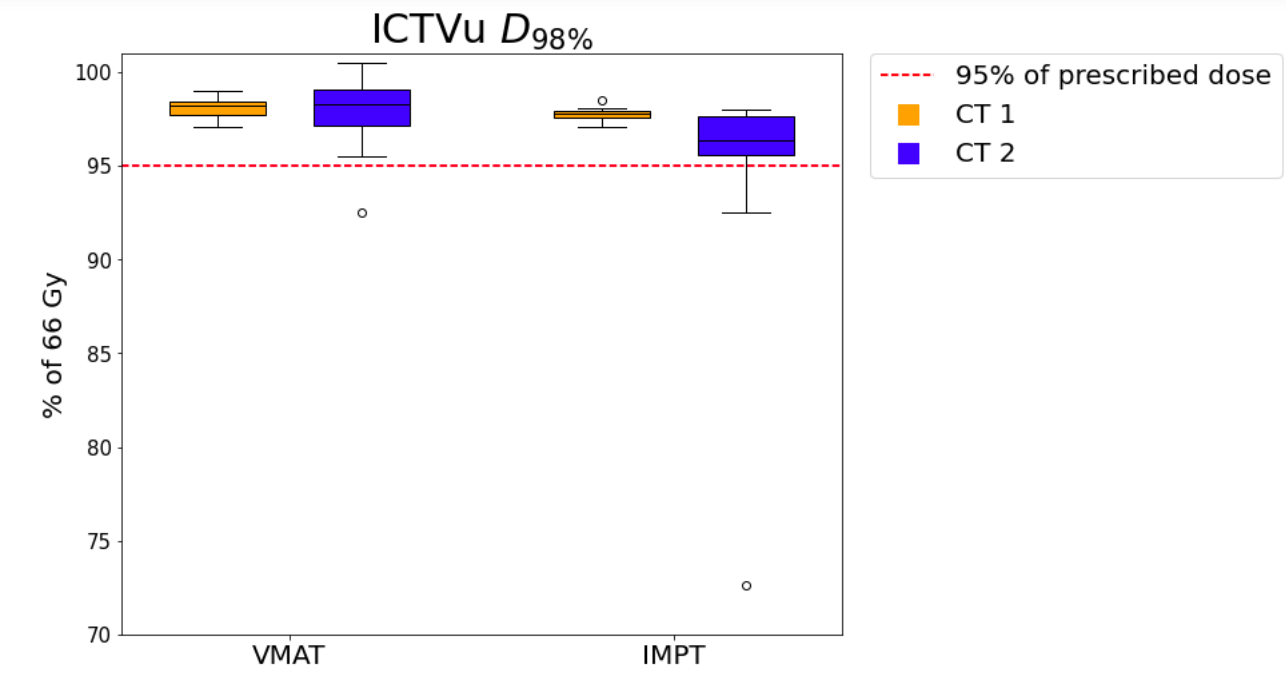

Figure 4.1: Dose coverage to ICTVu in VMAT and IMPT$_{4.5\%}$ plans, optimized on CT 1 and recalculated on CT 2. The red horizontal line shows the critical clinical goal of $D_{98\%} > 62,7$ Gy, which is the 95% of the prescribed dose (66 Gy).

For dose coverage of the ICTVu in VMAT plans (figure 4.1), CT 1 box displays dose values above the critical goal of 95% of the prescribed dose (here: 66 Gy), with the median value at around 98.2%. Dose distribution recalculated on CT 2 exhibits a larger spread of data than the original calculation (CT 1), although the median value stays approximately the same (98.3%). The one and only outlier in CT 2 box corresponds to patient 6 with a $D_{98\%} = 92.5\%$, well below the critical goal of 95%. Dose distribution for patient 6 in the VMAT plan calculated on both CT 1 and CT 2 is in figure 4.2.

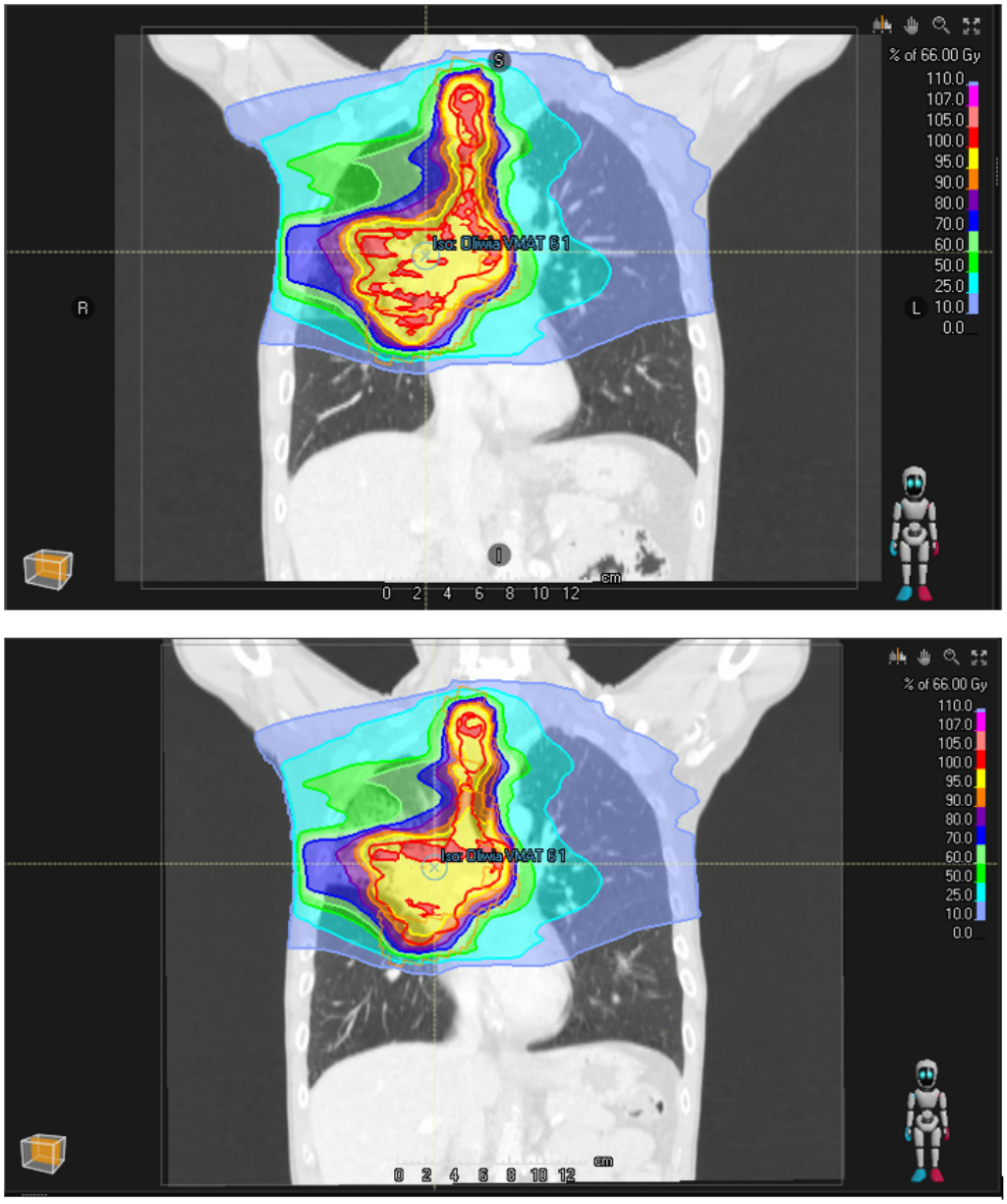

Figure 4.2: Dose distribution using VMAT technique for patient 6, based on the planning CT (above) and recalculated on the control CT (below). The red solid line shows the ICTVu.

Dose coverage of the ICTVu for IMPT plans is also displayed in figure 4.1. Coverage in the initial plan set is better than in the recalculated plan set. The median value in CT 1 box is at 97.8%, which is above the critical goal of 95% of the prescribed dose. The median decreases to 96.4% in CT 2 box. Two patients receive too low dose, patient 12 (92.5%) and patient 6 (72.6%). Both are below the red line, corresponding to the critical

goal of $D_{98\%} > 95\%$ of the prescribed dose. Dose distribution for patient 6 is in figure 4.3.

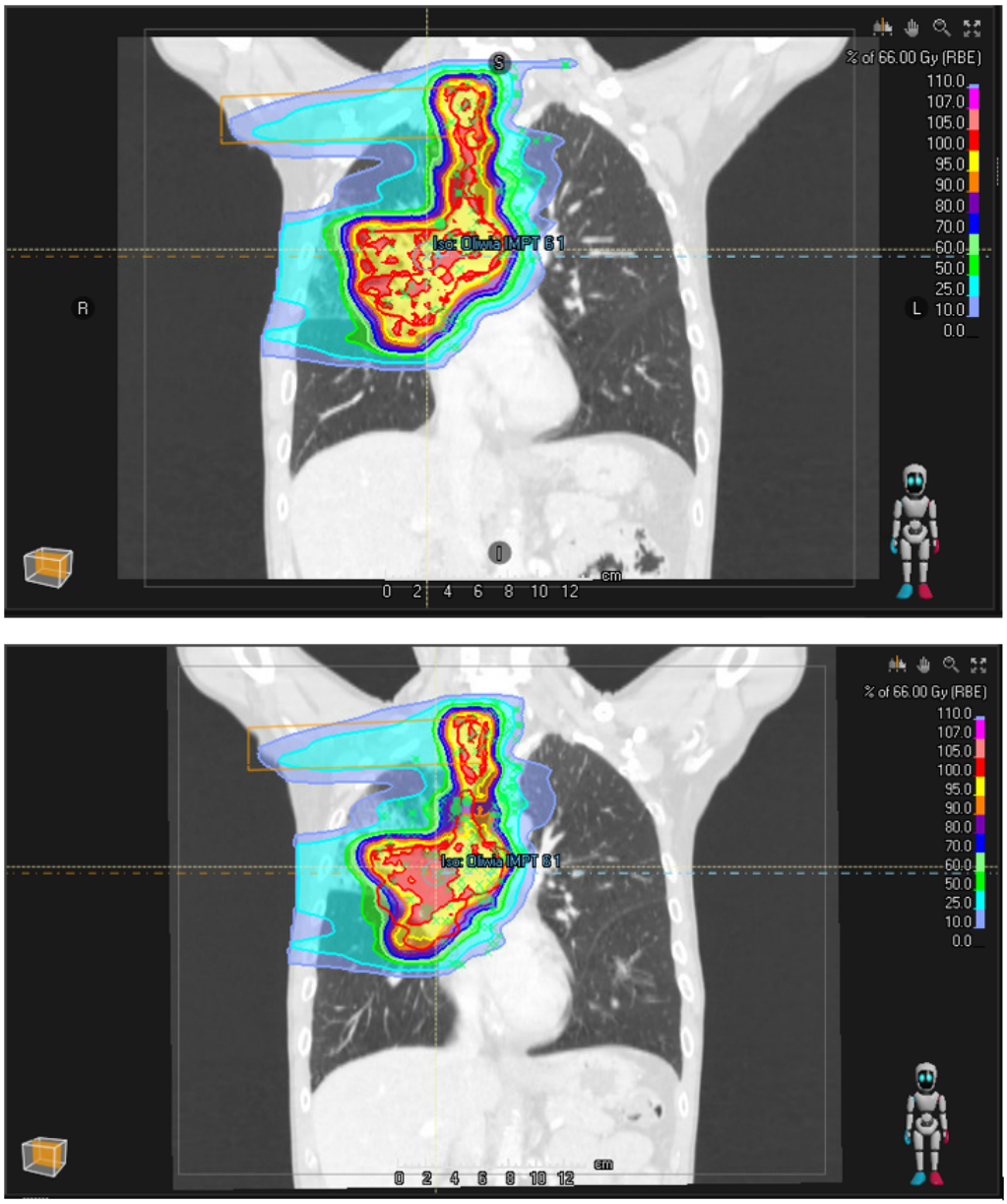

Figure 4.3: Dose distribution using IMPT technique for patient 6, based on the planning CT (above) and recalculated on the control CT (below). The red solid line shows the ICTVu.

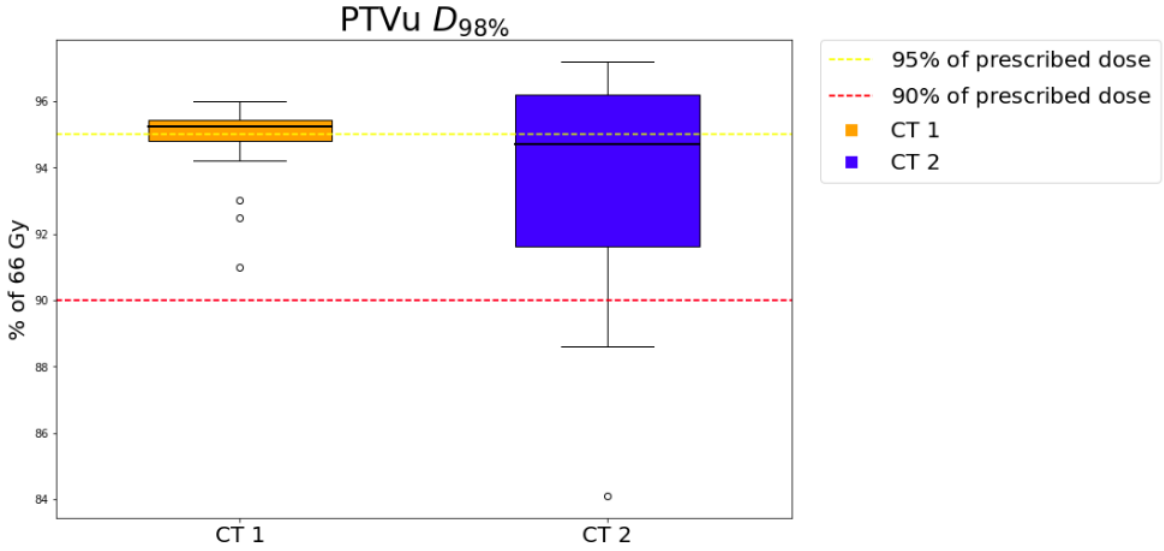

Figure 4.4: Dose coverage to PTVu using VMAT technique, optimized on CT 1 and recalculated on CT 2. The red horisontal line shows the critical clinical goal of $D_{98\%} > 59,4$ Gy, which is the 90% of the prescribed dose - 66 Gy. The orange horizontal line shows the desired clinical goal of $D_{98\%} > 62,7$ Gy, which is the 95% of the prescribed dose - 66 Gy.

Dose coverage of the PTVu in VMAT plans (figure 4.4) is lower than that of the ICTVu, with a median $D_{98\%} = 95.2\%$ in CT 1 box and a similar median $D_{98\%} = 94.7\%$ in CT 2 box. The median line in CT 1 box is therefore right above the orange line, marking the desired coverage of 95%, and right below the line in the CT 2 box.
Increased variability in dose coverage from CT 1 to CT 2 is more pronounced for PTVu than for ICTVu. For PTVu, the lower part of the CT 2 box extends below the critical threshold of 90%, and the outlier corresponding to Patient 6 has value of 84.1%.
Table 4.1 sums up the relevant p-values.

Table 4.1: Results from the Wilcoxon test, comparing dose coverage of the treatment volumes in CT 1 and CT 2 plans, for both VMAT and IMPT techniques. Difference from CT 1 to CT 2 calculations is compared between the two modalities as well. P-values below 0,05 are written in bold font.

Data	Figure/Table	p-value
ICTVu VMAT (CT 1 vs. CT 2)	Figure 4.1 Table 6.4	0,94
ICTVu IMPT (CT 1 vs. CT 2)	Figure 4.5 Table 6.6	**0,0000305**
PTVu VMAT (CT 1 vs. CT 2)	Figure 4.3 Table 6.4	0,57
ICTVu CT 2 - CT 1 (VMAT vs. IMPT)	Table 6.7	**0,003**
ICTVu CT 1 (VMAT vs. IMPT)	Table 6.7	0,058
ICTVu CT 2 (VMAT vs. IMPT)	Table 6.7	**0,003**

4.1.2 Global Maximum Dose and Organs at Risk

Complete results on global maximum dose and dose to OARs from both treatment plan sets are provided in Appendix A. The most relevant results are presented here.
Figures 4.5 and 4.6 map the results on maximum dose delivered to the irradiated patient volume, for both VMAT and $IMPT_{4.5\%}$ plans. The maximum dose is calculated in two ways. Figure 4.5 shows D_{2ccm}, the minimum dose received by the most irradiated $2cm^3$ of the patient volume. Figure 4.6 shows the global maximum dose, D_{max}, received by the most irradiated voxel in the patient volume.

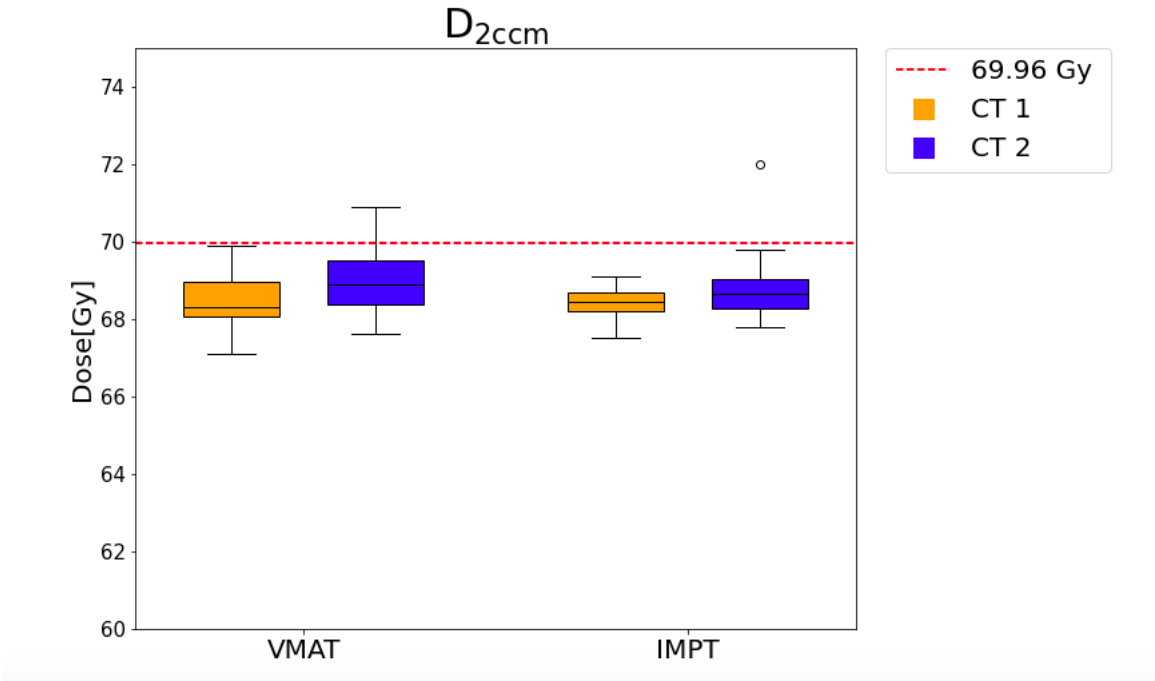

Figure 4.5: Near-maximum dose, D_{2ccm}, delivered in VMAT and IMPT$_{4.5\%}$ plans, optimized on CT 1 and recalculated on CT 2. The red horisontal line shows the critical clinical goal of $D_{2ccm} < 69.96$ Gy.

Two clinical goals were considered for the maximum dose, the critical goal of D_{2ccm} below 106% of the prescribed dose, and the desired goal of D_{max} below 108% of the prescribed dose.
The critical goal of $D_{2ccm} < 69.96$ Gy was met in all initial (CT 1) VMAT plans, where the median value was at 68.3 Gy. However, when recalculating each plan on CT 2, three of the plans exceeded the threshold, with the highest value of 70.9 Gy. The median value for VMAT plans increases from 68.3 Gy to 68.9 Gy. As it appears in figure 4.5, the overall trend in the CT 2 recalculation is an increase in D_{2ccm}, since the CT 2 boxes are shifted upwards relative to the CT 1 boxes.
In IMPT$_{4.5\%}$ plans, all D_{2ccm} values in the initial dose distribution (CT 1) are below the limit of $69,96$ Gy, with a small variability and a median value at 68.5 Gy. In the recalculated (CT 2) set, the median dose stays approximately the same (68.6 Gy). There is one data point that exceeds the critical dose limit. It corresponds to Patient 6, with a value of 72.0 Gy.

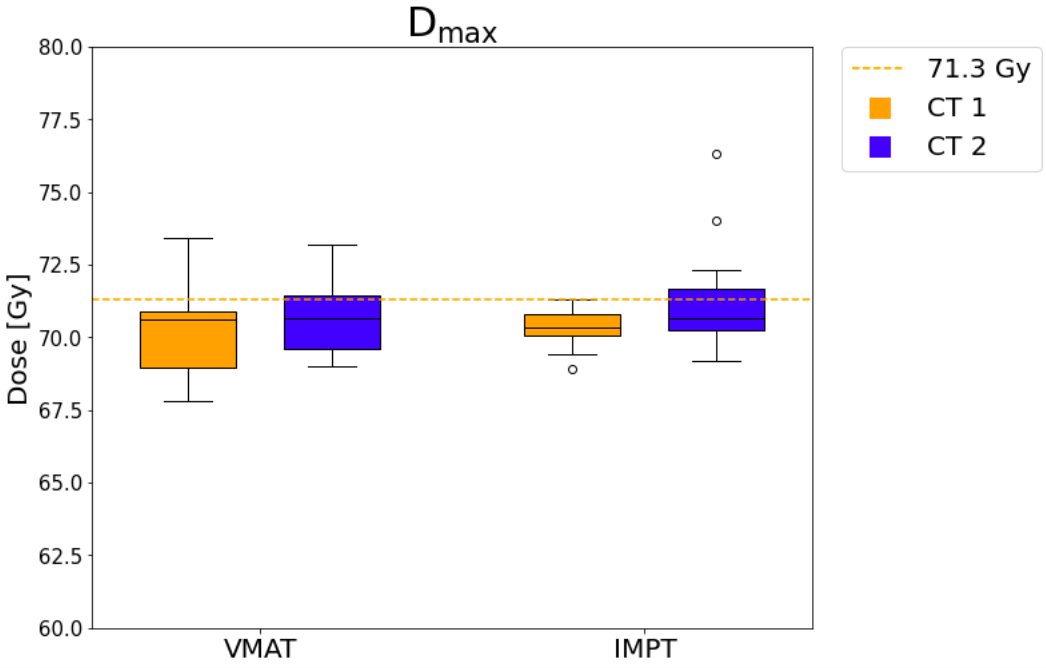

Figure 4.6: Global maximum dose, D_{max}, delivered in VMAT and IMPT$_{4.5\%}$ plans, optimized on CT 1 and recalculated on CT 2. The orange horizontal line shows the desired clinical goal of $D_{max} > 71.3$ Gy.

Figure 4.6 displays results on D_{max}, with a larger variability in data distribution than D_{2ccm}. The median D_{max} stays at around 70.6 Gy from CT 1 to CT 2, in the VMAT plans. One patient (patient 16) exceeds the desired threshold of 71.3 Gy in CT 1 box, with a value of 73.4 Gy. In CT 2 box, five exceed the threshold, with dose ranging from 71.4 Gy to 73.2 Gy.
In proton plans, median D_{max} increases from 70.3 Gy in the CT 1 box to 70.7 Gy in the CT 2 box. D_{max} recalculated on CT 2 exceeds the desired goal of 71.30 Gy for 4 out of 16 patients. This includes two outliers reaching high values of 74.0 Gy and 76.3 Gy.

Table 4.2 provides relevant p-values.

Table 4.2: Results from the Wilcoxon test for data on global maximum dose, both D_{2ccm} and D_{max}.

Data	Figure/Table	p-value
D_{2ccm} VMAT (CT 1 vs. CT 2)	Figure 4.6	**0,04**
D_{max} VMAT (CT 1 vs. CT 2)	Table 6.4	**0,04**
D_{2ccm} IMPT (CT 1 vs. CT 2)	Figure 4.7	**0,02**
D_{max} IMPT (CT 1 vs. CT 2)	Table 6.6	**0,01**
D_{2ccm} CT 2 - CT 1 (VMAT vs. IMPT)	Table 6.7	0,21
D_{max} CT 2 - CT 1 (VMAT vs. IMPT)		0,82
D_{2ccm} CT 1 (VMAT vs. IMPT)	Table 6.4 & Table 6.6	0,74
D_{2ccm} CT 2 (VMAT vs. IMPT)		0,40
D_{max} CT 1 (VMAT vs. IMPT)		0,67
D_{max} CT 2 (VMAT vs. IMPT)		0,60

Tables 6.5 and 6.7 (Appendix A) show complete results on dose delivery to organs at risk, for both modalities. Table 6.8 shows the difference between the CT 2 and CT 1 scores, indicating how robust each plan is. Due to the large amount of data on organs at risk, results presented here include only two of the OARs, the spinal cord and the healthy part of lung volume (Lungs-IGTV). Results on dose to the spinal cord are presented in figures 4.7 and 4.8, while results on the lungs are summed up in figure 4.9.

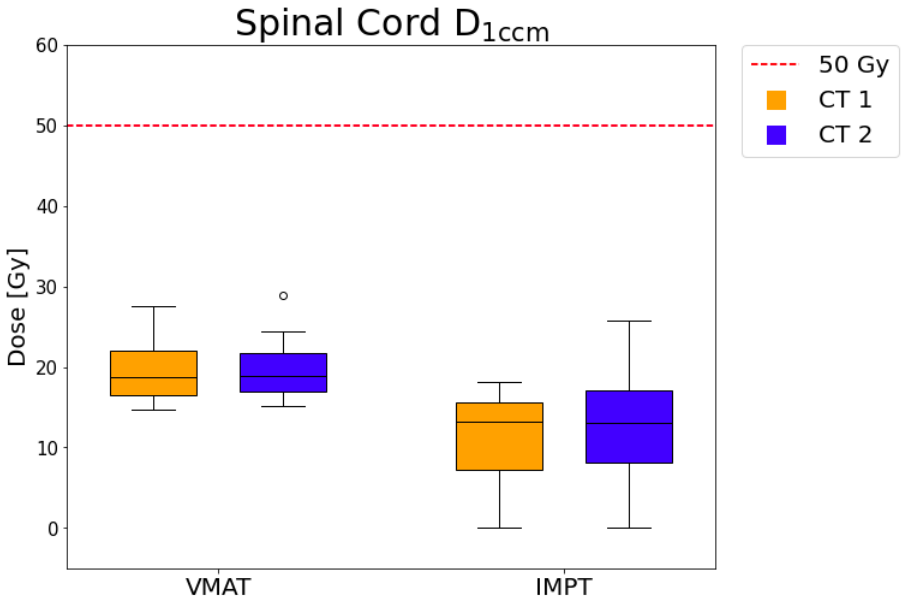

Figure 4.7: D_{1ccm} to the spinal cord in both VMAT and IMPT$_{4.5\%}$ plans, optimized on CT 1 and recalculated on CT 2. The red line corresponds to the critical clinical goal of $D_{1ccm} < 50$ Gy.

Two critical goals corresponding to the spinal cord were considered, D_{1ccm} below 50 Gy and D_{max} below 52 Gy. For VMAT-plans, all D_{1ccm} values are lower than the limit of 50 Gy, with the highest value at around 33 Gy in both CT 1 and CT 2 data sets. The two VMAT boxes in the D_{1ccm} plot are similar in size and shape, with a stable median value at around 19 Gy. For IMPT plans, D_{1ccm} values are low in both calculations (CT 1 and CT 2), with a median value at around 13 Gy in both boxes. All values in this plot are lower than the critical limit of 50 Gy. The two IMPT boxes are lower relative to the two VMAT boxes.

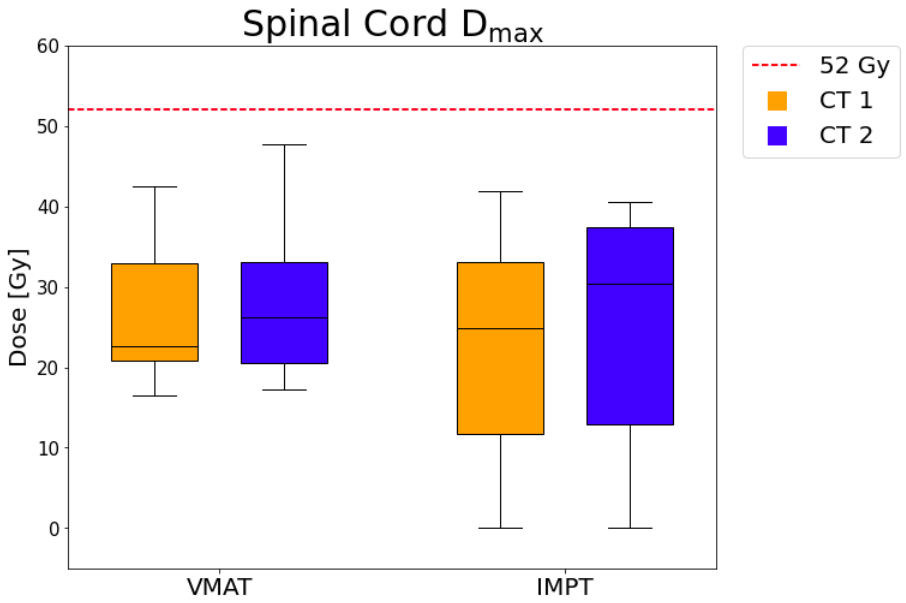

Figure 4.8: D_{max} delivered to the spinal cord in both VMAT and IMPT$_{4.5\%}$ plans, optimized on CT 1 and recalculated on CT 2. The red line corresponds to the critical clinical goal of $D_{max} < 52$ Gy.

In the D_{max} box plot (figure 4.8 the two VMAT boxes differ when it comes to the median value. It increases from 22.6 Gy in CT 1 box to 26.2 Gy in CT 2 box. Despite that, all values collected here are lower than the limit of 52 Gy. Both IMPT boxes are also below the limit, but their lower parts more extended compared to the VMAT boxes. The maximum value of D_{max} is slightly lower in CT 2 set than in CT 1 set, but the median value increases from 24.9 Gy in CT 1 box to 30.5 Gy in CT 2 box.

Relevant p-values are provided in table 4.3.

Table 4.3: Results from the Wilcoxon test on dose delivery to the spinal cord.

Data	Figure/Table	p-value
D_{1ccm} VMAT (CT 1 vs. CT 2)	Figure 4.8	0,53
D_{max} VMAT (CT 1 vs. CT 2)	Table 6.4	0,30
D_{1ccm} IMPT (CT 1 vs. CT 2)	Figure 4.9	0,13
D_{max} IMPT (CT 1 vs. CT 2)	Table 6.6	**0,02**
D_{1ccm} CT 2 - CT 1 (VMAT vs. IMPT)	Table 6.7	0,53
D_{max} CT 2 - CT 1 (VMAT vs. IMPT)		0,16
D_{1ccm} CT 1 (VMAT vs. IMPT)	Table 6.4 & Table 6.6	**0,0000305**
D_{1ccm} CT 2 (VMAT vs. IMPT)		**0,00015**
D_{max} CT 1 (VMAT vs. IMPT)		0,08
D_{max} CT 2 (VMAT vs. IMPT)		0,25

Figure 4.9 shows how VMAT and $\text{IMPT}_{4.5\%}$ plans perform when it comes to the three clinical goals for the healthy lung tissue (Lungs-IGTV). For VMAT, the first two plots show lung volume receiving respectively 20 Gy and 5 Gy. As the leftmost plot shows, all plans achieve the critical goal of $V_{20Gy} < 35\%$ both in the initial treatment planning process, and recalculated on the control CT (CT 2). The median value decreases slightly from 22.6% to 22.5%. In the V_{5Gy} plot, the median decreases from 49.7% to 49.5%, while the median Mean Lung Dose stays at around 13 Gy.

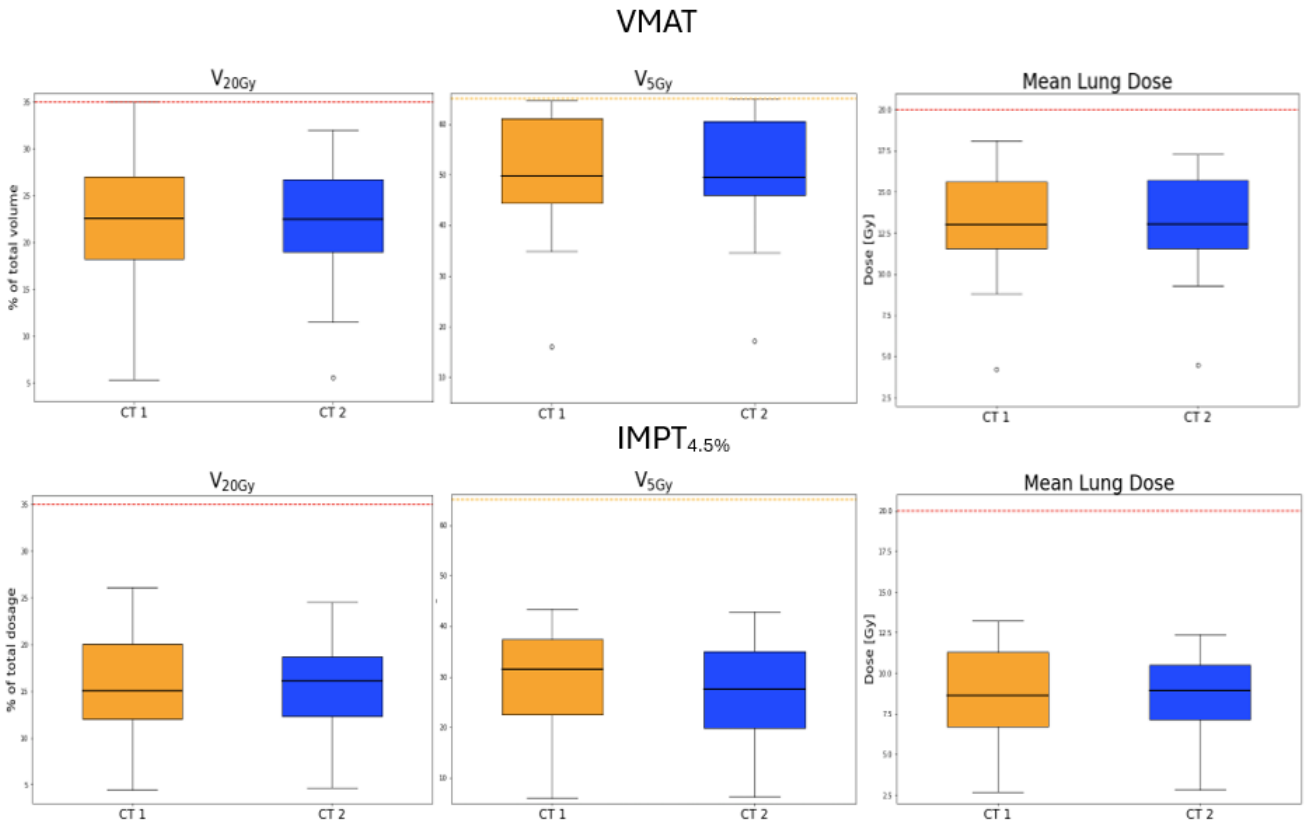

Figure 4.9: Dose delivery to the lungs minus the GTV volume in both VMAT and $\text{IMPT}_{4.5\%}$ plans, optimized on CT 1 and recalculated on CT 2. Plots on the left side and in the middle show volume of the organ that has received 20 and 5 Gy of dose, and the values are a percentage of the entire organ (lungs minus GTV) volume. Plots on the right side show the mean dose delivered to the lungs minus the GTV. The red lines correspond to the critical clinical goals of $V_{20Gy} < 35\%$ and $MLD < 20$ Gy, while the orange lines show the desired clinical goal of $V_{5Gy} < 65\%$.

The $\text{IMPT}_{4.5\%}$ boxes are all shifted downwards relative to the VMAT boxes. In case of V_{20Gy} the median value is low and goes from 15.1% in the CT 1 box to 16.1% in the CT 2 box. For V_{5Gy}, the median value decreases from 31.5% in the CT 1 box to 27.5% in the CT 2 box. Median MLD increases from 8.7 Gy in the CT 1 box to 9.0 Gy in the CT 2 box.

The relevant p-values are presented in table 4.4.

Table 4.4: Results from the Wilcoxon test on dose delivery to the Lungs-IGTV volume.

Data	Figure 4.10/Table 6.4	p-value
V_{20Gy} VMAT (CT 1 vs. CT 2)	Figure 4.11 Table 6.6	0,46
V_{5Gy} VMAT (CT 1 vs. CT 2)		0,43
MLD VMAT (CT 1 vs. CT 2)		0,86
V_{20Gy} IMPT (CT 1 vs. CT 2)	Figure 4.11 Table 6.7	0,36
V_{5Gy} IMPT (CT 1 vs. CT 2)		0,71
MLD IMPT (CT 1 vs. CT 2)		0,53
V_{20Gy} CT 2 - CT 1 (VMAT vs. IMPT)	Table 6.7	0,065
V_{5Gy} CT 2 - CT 1 (VMAT vs. IMPT)		0,175
MLD CT 2 - CT 1 (VMAT vs. IMPT)		0,074
V_{20Gy} CT 1 (VMAT vs. IMPT)	Table 6.4 & Table 6.6	**0,00015**
V_{20Gy} CT 2 (VMAT vs. IMPT)		**0,00015**
V_{5Gy} CT 1 (VMAT vs. IMPT)		**0,0000305**
V_{5Gy} CT 2 (VMAT vs. IMPT)		**0,0000305**
MLD CT 1 (VMAT vs. IMPT)		**0,0000305**
MLD CT 2 (VMAT vs. IMPT)		**0,0000305**

4.2 Density uncertainty

Complete results from both IMPT plan sets are collected in tables 6.9 and 6.10 in Appendix A. The three representative features presented here are $D_{98\%}$ to ICTVu, mean lung dose (received by lung volume minus IGTV), and the global maximum dose (D_{max}).

Table 4.5: Comparison of the two IMPT plan sets in terms of $D_{98\%}$ of the ICTVu in the initial (CT 1) plan and the recalculated one (CT 2), using 4.5% and 3% as density uncertainty in the robust optimization. The largest decrease in dose coverage for each patient is marked with yellow. Dose coverage values below the critical threshold of 95% are marked with red.

Patient	CT 1		CT 2		CT 2 - CT 1		Difference
	4.5%	3%	4.5%	3%	4.5%	3%	
1	97.5	98.1	95.6	94.5	-1.9	-3.6	-1.7
2	97.9	98.2	97.8	98.2	-0.1	0	0
3	97.4	97.8	95.6	96.5	-1.8	-1.3	0.5
4	98.5	98.0	97.9	98.0	-0.6	0	0.6
5	97.1	97.9	96.4	96.0	-0.7	-1.9	-1.2
6	97.5	97.7	72.6	72.4	-24.9	-25.3	-0.4
7	97.8	98.4	95.7	91.7	-2.1	-6.7	-4.6
8	97.9	98.4	97.6	97.3	-0.3	-1.1	-0.8
9	97.9	98.4	95.0	95.8	-2.9	-2.6	0.3
12	97.8	98.6	92.5	84.6	-5.3	-14.0	-8.7
13	98.0	97.8	95.6	94.7	-2.4	-3.1	-0.7
15	97.7	98.0	97.4	97.5	-0.3	-0.5	-0.2
16	97.4	97.9	97.5	97.5	0.1	-0.4	-0.5
17	98.1	98.2	98.0	97.9	-0.1	-0.3	-0.2
21	97.9	97.9	96.4	96.2	-1.5	-1.7	-0.2
22	97.6	97.6	96.7	96.8	-0.9	-0.8	0.1
Average	97.8	98.1	94.9	94.1	-2.9	-4.0	
Median	97.8	98.0	96.4	96.3	-1.2	-1.5	
p-value	**0.009**		0.21		**0.039**		

Table 4.5 shows dose coverage ($D_{98\%}$) of the ICTVu as % of 66 Gy, which is the prescribed dose. The two IMPT plan sets ($IMPT_{4.5\%}$ and $IMPT_{3\%}$) are compared to each other in terms of how the dose coverage changes from the initial (CT 1) plan to the recalculated (CT 2) plan. Which density uncertainty leads to the largest decrease in dose coverage for each patient is marked with yellow. Two patients received $D_{98\%}$ of the ICTVu below the critical threshold of 95%, in the recalculated (CT 2) $IMPT_{4.5\%}$ plan. The table shows that changing density uncertainty to 3% causes too low dose coverage for three additional patients.

Table 4.6: Comparison of the two IMPT plan sets in terms of the mean lung dose (delivered to lungs-GTV) in the initial (CT 1) plan and the recalculated one (CT 2), using 4.5% and 3% as density uncertainty in the robust optimization. The largest increase in MLD for each patient is marked with yellow.

Patient	CT 1		CT 2		CT 2 - CT 1		Difference
	4.5%	3%	4.5%	3%	4.5%	3%	
1	6.8	6.6	7.0	6.9	0.2	0.3	0.1
2	11.2	11.2	10.8	10.8	-0.4	-0.4	0
3	9.5	9.5	10.4	10.6	0.9	1.1	0.2
4	8.5	8.6	7.8	7.9	-0.7	-0.7	0
5	8.8	8.7	9.0	8.9	0.2	0.2	0
6	11.6	12.0	9.4	9.7	-2.2	-2.3	-0.1
7	12.7	12.3	12.0	11.3	-0.7	-1.0	-0.3
8	8.5	7.6	9.1	8.4	0.6	0.8	0.2
9	13.2	14.1	12.4	13.3	-0.8	-0.8	0
12	6.5	6.1	5.9	5.7	-0.6	-0.4	0.2
13	8.4	8.1	8.9	8.8	0.5	0.7	0.2
15	6.3	6.3	6.3	6.3	0	0	0
16	2.7	2.7	2.8	2.8	0.1	0.1	0
17	12.7	12.6	12.4	12.2	-0.3	-0.4	-0.1
21	6.4	6.3	7.2	7.1	0.8	0.8	0
22	9.0	8.9	8.7	8.5	-0.3	-0.4	-0,1
Average	8.9	8.8	8.8	8.7	-0.2	-0.2	
Median	8.7	8.6	9.0	8.6	0.1	-0.2	
p-value	0.21		0.42		0.51		

Table 4.6 shows the results on mean lung dose (in the lung-IGTV volume). In this case, yellow is used to point out which density uncertainty leads to the largest increase in dose from the initial (CT 1) treatment plan to the recalculated (CT 2) plan. The table shows that decreasing density uncertainty from 4.5% to 3% doesn't cause any significant difference.

Table 4.7: Comparison of the two IMPT plan sets in terms of the D_{max} to the spinal cord in the initial (CT 1) plan and the recalculated one (CT 2), using 4.5% and 3% as density uncertainty in the robust optimization. The largest increase in D_{max} for each patient is marked with yellow.

Patient	CT 1		CT 2		CT 2 - CT 1		Difference
	4.5%	3%	4.5%	3%	4.5%	3%	
1	17.1	15.4	18.1	15.9	1.0	0.5	-0.5
2	15.6	13.3	17.1	14.9	1.5	1.6	0.1
3	34.0	34.2	40.1	38.9	6.1	4.7	-1.4
4	0.3	0.3	0.4	0.4	0.1	0.1	0
5	34.8	32.9	34.8	33.2	0	0.3	0.3
6	23.9	27.4	37.7	38.5	13.8	11.1	-2.7
7	32.8	32.5	21.0	20.7	-11.8	-11.8	0
8	42.0	37.4	37.4	38.2	-4.6	0.8	5.4
9	29.4	24.5	29.6	26.4	0.2	1.9	1.7
12	21.7	21.3	31.3	26.8	9.6	5.5	-4.1
13	29.8	30.1	33.2	32.1	3.4	2.0	-1.4
15	0.1	0.1	0.2	0.2	0.1	0.1	0
16	35.8	36.0	38.0	39.6	2.2	2.6	0.4
17	25.9	25.1	40.6	38.7	14.7	13.6	-1.1
21	0.1	0.1	0.1	0.1	0	0	0
22	0.4	0.7	0.5	0.9	0.1	0.2	0.1
Average	21.5	20.7	23.8	22.8	2.3	2.1	
Median	24.9	24.8	30.5	26.6	0.6	1.2	
p-value	0.12		**0,03**		0.53		

The overall performance of the two IMPT plan sets in terms of the D_{max} to the spinal cord is presented in table 4.7. Which density uncertainty leads to the largest increase in D_{max} from CT 1 to CT 2 calculation is marked with yellow. Decreasing density uncertainty from 4.5% to 3% causes significant difference in the recalculated (CT 2) plans, where the median decreases from 30.5 Gy in $\text{IMPT}_{4.5\%}$ plans to 26.6 Gy in $\text{IMPT}_{3\%}$ plans.

4.3 Plan quality

All three sets of plans, the VMAT plan set and two IMPT sets ($\text{IMPT}_{4.5\%}$ and $\text{IMPT}_{3\%}$), were subjected to the additional evaluation in terms of the conformity and homogeneity of the dose distribution in the target volume ICTVu. Tools used for that were the Conformity Index and the Homogeneity Index, provided in the RayStation software and defined with equations 3.1 and 3.2, respectively. For each patient, the idices were calculated in all three sets and using both the planning CT (CT 1) and the CT acquired

halfway through the treatment (CT 2). Results from the Wilcoxon test are provided in tables 4.9 and 4.11.

4.3.1 Conformity Index

The conformity index used here is a ratio between the ICTVu covered by the prescribed dose (66 Gy), and the total volume receiving the prescribed dose. Table 4.8 sums up the index score in each plan and for each patient. The lowest score in each line is marked with yellow. Additionally, the average and median values for each set are included for the overall overview of the modalities. The initial (CT 1) VMAT plans have the highest median conformity index of 0.66 while the recalculated (CT 2) VMAT plans have the lowest median of 0.60. Table 4.9 shows the relevant p-values. Figure 4.10 shows dose distribution in patient 8 as an example on varying conformity.

Table 4.8: Conformity index for all three plan sets including the VMAT set and the two IMPT sets ($IMPT_{4.5\%}$ and $IMPT_{3\%}$). The plan with the lowest conformity index score for each patient is marked with yellow.

Patient	VMAT		IMPT (4.5%)		IMPT (3.0%)	
	CT 1	CT 2	CT 1	CT 2	CT 1	CT 2
1	0.56	0.56	0.77	0.80	0.84	0.85
2	0.86	0.79	0.63	0.59	0.60	0.58
3	0.55	0.50	0.66	0.61	0.64	0.59
4	0.66	0.74	0.35	0.37	0.34	0.32
5	0.61	0.60	0.64	0.62	0.72	0.67
6	0.77	0.84	0.75	0.74	0.73	0.73
7	0.58	0.46	0.35	0.43	0.35	0.50
8	0.40	0.38	0.50	0.52	0.57	0.60
9	0.77	0.65	0.74	0.74	0.65	0.70
12	0.66	0.61	0.47	0.48	0.45	0.54
13	0.66	0.55	0.78	0.74	0.74	0.72
15	0.52	0.50	0.63	0.62	0.61	0.62
16	0.52	0.56	0.51	0.50	0.53	0.53
17	0.65	0.72	0.54	0.55	0.55	0.56
21	0.84	0.69	0.69	0.74	0.66	0.66
22	0.67	0.60	0.77	0.72	0.77	0.72
Average	0.64	0.61	0.61	0.61	0.61	0.62
Median	0.66	0.60	0.64	0.62	0.63	0.61
p-value	0.10		0.86		0.94	

Table 4.9: P-values corresponding to conformity index results.

Data	p-value
VMAT (CT 1 vs. CT 2)	0,10
IMPT 4.5% (CT 1 vs. CT 2)	0,86
IMPT 3.0% (CT 1 vs. CT 2)	0,94
CT 2 - CT 1 (VMAT vs. IMPT 4.5%)	0,21
CT 2 - CT 1 (IMPT 4.5% vs. 3.0%)	0,33
CT 2 - CT 1 (VMAT vs. IMPT 3.0%)	0,19

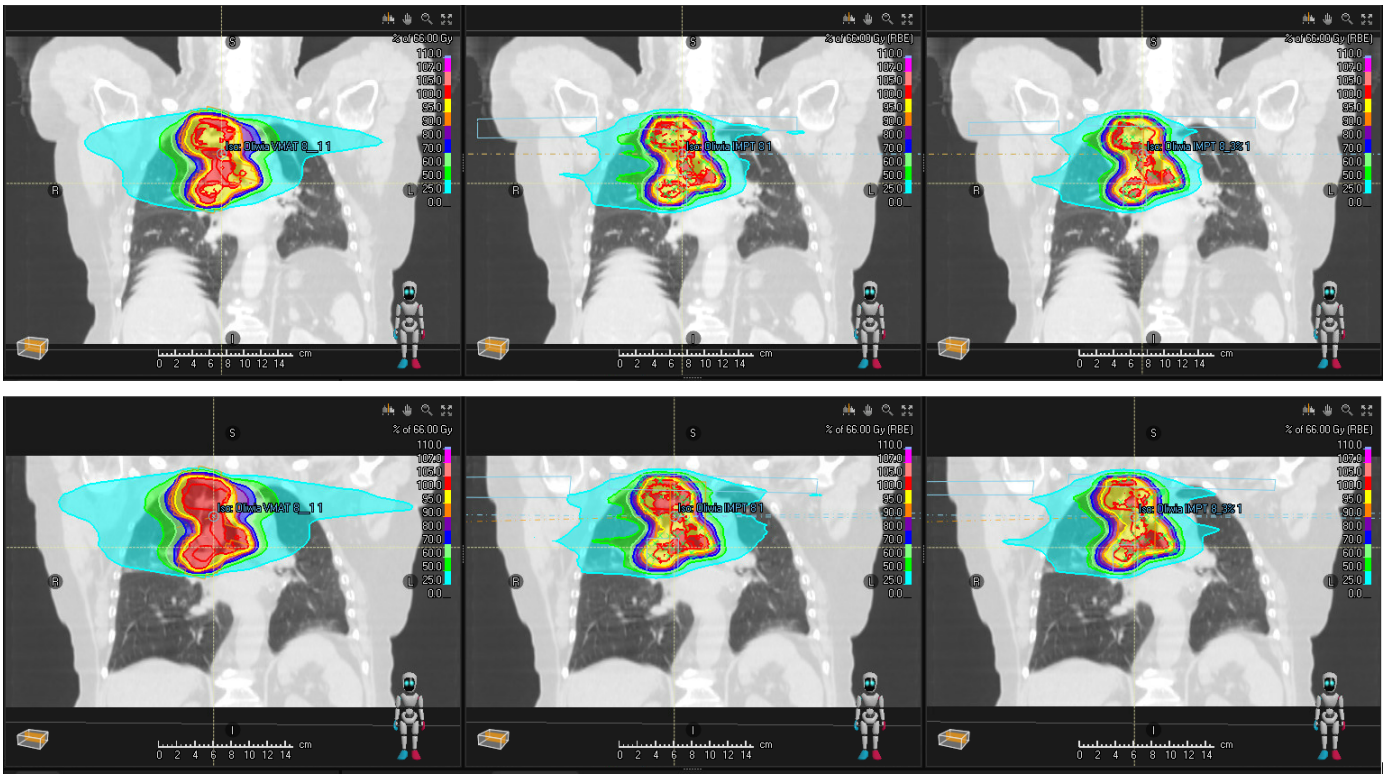

Figure 4.10: Dose distribution for patient 8 showing varying conformity. Images are from the three treatment plans, VMAT on the left side, $\text{IMPT}_{4.5\%}$ in the middle, and $\text{IMPT}_{3\%}$ on the right side. The CT 2 version of each is included below. The ICTVu is delineated in red.

4.3.2 Homogeneity Index

The homogeneity index used here is defined as the ratio between $D_{98\%}$ and $D_{2\%}$ delivered to the ICTVu. The results for all treatment plans are summed up in table 4.10. The lowest score for each patient is marked with yellow. Data distribution for all three sets

of treatment plans is presented in a box-plot in figure 4.11, where the $IMPT_{4.5\%}$ CT 2 box has the lowest median of 0.93. The average and median score in each set is provided as well. Relevant p-values are provided in table 4.11. Dose distribution for patient 6 is shown in figure 4.12 as an example on varying homogeneity.

Table 4.10: Homogeneity index for all three plan sets including the VMAT set and two IMPT sets, $IMPT_{4.5\%}$ and $IMPT_{3\%}$. The plan with the lowest homogeneity index score for each patient is marked with yellow.

Patient	VMAT		IMPT (4.5%)		IMPT (3.0%)	
	CT 1	CT 2	CT 1	CT 2	CT 1	CT 2
1	0.94	0.94	0.95	0.93	0.96	0.92
2	0.96	0.93	0.96	0.96	0.96	0.96
3	0.97	0.95	0.94	0.92	0.95	0.93
4	0.92	0.93	0.97	0.96	0.96	0.96
5	0.96	0.95	0.94	0.93	0.95	0.93
6	0.96	0.91	0.95	0.68	0.95	0.68
7	0.96	0.95	0.95	0.93	0.97	0.89
8	0.98	0.97	0.96	0.95	0.97	0.96
9	0.97	0.95	0.96	0.93	0.97	0.94
12	0.97	0.96	0.96	0.90	0.97	0.83
13	0.97	0.95	0.96	0.93	0.95	0.93
15	0.98	0.97	0.95	0.95	0.95	0.95
16	0.96	0.95	0.95	0.95	0.96	0.95
17	0.93	0.95	0.96	0.96	0.96	0.96
21	0.96	0.96	0.94	0.93	0.95	0.93
22	0.96	0.96	0.95	0.94	0.95	0.94
Average	0.96	0.95	0.95	0.92	0.96	0.92
Median	0.96	0.95	0.95	0.93	0.96	0.94
p-value	**0.02**		**0.002**		**0.002**	

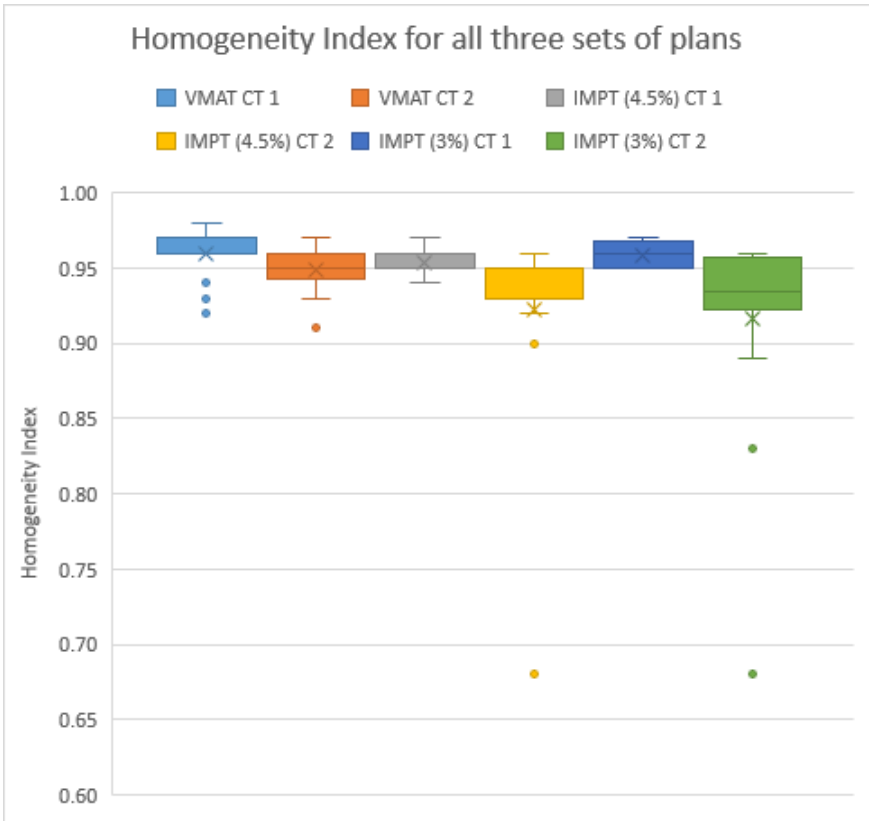

Figure 4.11: Distribution of data on homogeneity index in all three sets of treatment plans.

Table 4.11: P-values corresponding to homogeneity index results. Bold font is used to mark values below $0,05$, which indicate statistically significant difference.

Data	p-value
VMAT (CT 1 vs. CT 2)	**0,02**
IMPT 4.5% (CT 1 vs. CT 2)	**0,002**
IMPT 3.0% (CT 1 vs. CT 2)	**0,002**
CT 2 - CT 1 (VMAT vs. IMPT 4.5%)	0,08
CT 2 - CT 1 (IMPT 4.5% vs. 3.0%)	0,03
CT 2 - CT 1 (VMAT vs. IMPT 3.0%)	0,06

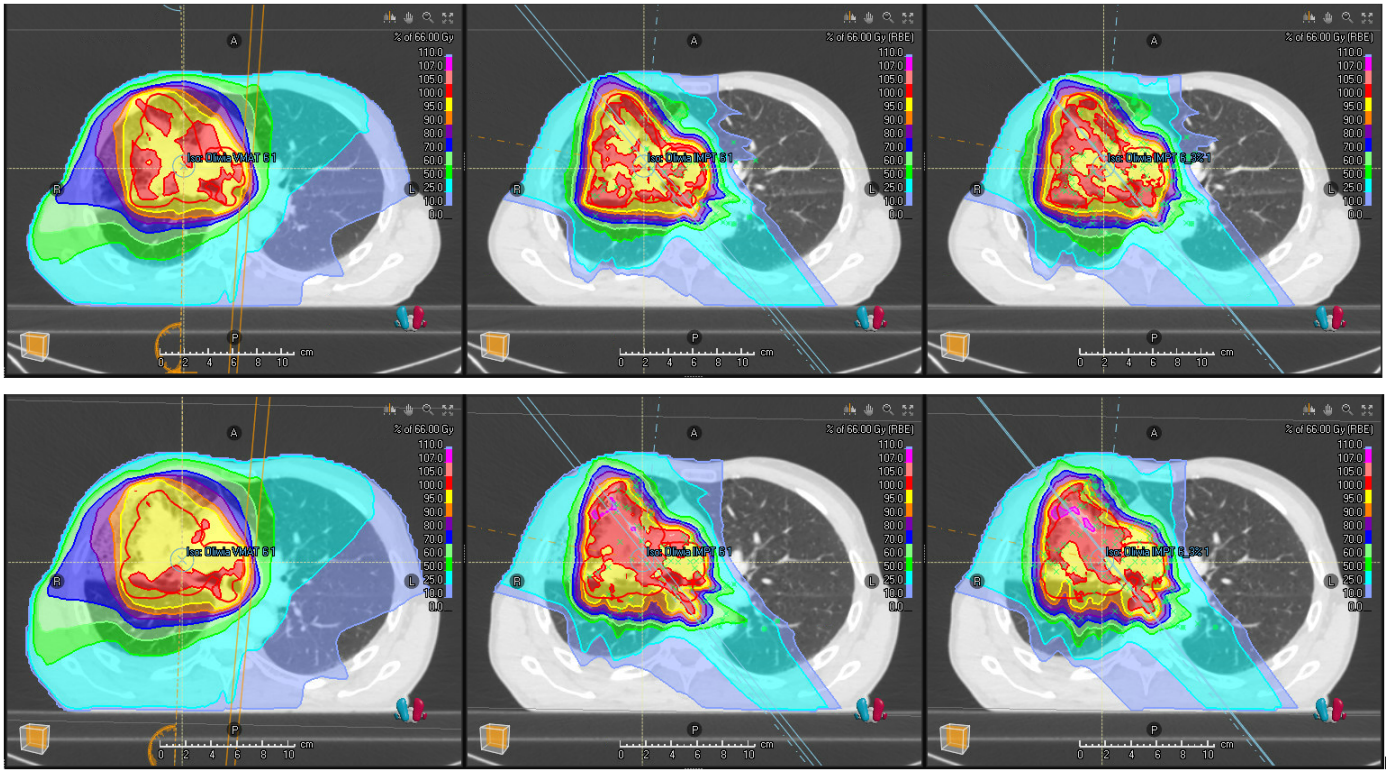

Figure 4.12: Dose distribution for patient 6 showing varying homogeneity. Images are from the three treatment plans, VMAT on the left side, $IMPT_{4.5\%}$ in the middle, and $IMPT_{3\%}$ on the right side. The CT 2 version of each is included below.

4.4 Need for adaptation

All treatment plans were assessed in terms of the need for adaptation using three criteria, taken from the internal quality control project [3] that the patient material comes from. Results from the analysis are summed up in table 4.12, with corresponding p-values in table 4.13. Numbers marked with red indicate an unacceptable result in terms of the criteria, suggesting that the corresponding plan needs adaptation halfway through the treatment. Dose to organs at risk was monitored for all relevant organs in each case, with regard to the clinical goals. The dose was below the critical limit for almost all treatment plans. The only exception is dose to the right brachial plexus in both $IMPT_{4.5\%}$ and $IMPT_{3\%}$ plans for patient 16. In the $IMPT_{4.5\%}$ plan, dose increases from 62.4 Gy to 67.7 Gy, while in the $IMPT_{3\%}$ plan, it increases from 63.0 Gy to 68.5 Gy. In this case, brachial plexus is very close and partially overlaps ICTVu and PTVu, as shown in figure 4.13. Details on dose to all organs at risk for all three plan sets can be found in tables 6.7, 6.9, 6.10 and 6.5 in Appendix A.

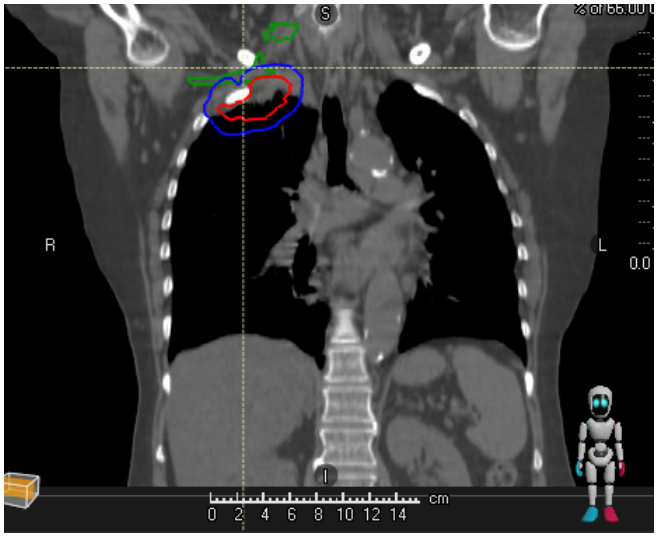

Figure 4.13: CT 1 image for patient 16 showing brachial plexus (green) in close vicinity to the ICTVu (red) and PTVu (blue).

Table 4.12: Checklist used to assess if the original treatment plan needs adaptation halfway through the treatment. Numbers are the difference between values calculated on the control CT (CT 2) and values from the initial treatment plan (based on CT 1). A negative value means a decrease from CT 1 to CT 2, and positive value means the opposite. Values exceeding the limit are marked with red, indicating the corresponding plan would need adaptation. In the last column, dose to all relevant organs at risk is analyzed and the organ receiving too high dose in the recalculated plan is specified.

Patient	Loss of dose coverage ($D_{98\%}$) to the ICTVu of more than 2%			Global maximum dose outside of PTVu increased with more than 3%			Dose to an organ at risk increased above the critical threshold		
	VMAT	IMPT 4.5%	IMPT 3%	VMAT	IMPT 4.5%	IMPT 3%	VMAT	IMPT 4.5%	IMPT 3%
1	-1,7	2,0	3,7	1,6	1,0	1,6	-	-	-
2	2,6	0,1	0	-1,0	0,3	-0,5	-	-	-
3	0	1,9	1,4	1,0	0,7	3,3	-	-	-
4	0	0,6	0	0,5	0,2	-0,3	-	-	-
5	0,3	0,8	2,0	-0,2	3,0	3,8	-	-	-
6	5,3	25,5	26,0	-2,9	7,4	6,2	-	-	-
7	1,4	2,1	6,8	0,7	0,8	-0,4	-	-	-
8	-1,5	0,3	1,1	2,2	0,3	-0,8	-	-	-
9	-1,3	3,0	2,6	3,0	1,5	-0,8	-	-	-
12	-0,1	5,5	14,2	-1,1	5,4	-0,3	-	-	-
13	-2,1	2,4	3,2	2,0	2,7	0,9	-	-	-
15	-0,2	0,3	0,6	1,1	-0,8	-0,3	-	-	-

Table 4.12 continued from previous page

16	0,1	-0,1	0,4	-0,2	-1,5	1,3	-	Brachial Plexus (right)	
17	0,4	0,1	0,3	0	1,9	-0,2	-	-	-
21	-1,5	1,6	1,7	1,4	-0,2	0,1	-	-	-
22	0,2	0,8	0,8	0	1,2	1,1	-	-	-
Average	0,1	3,0	4,0	0,5	1,5	0,9			
Median	0,01	1,22	1,54	0,57	0,94	-0,03			

Table 4.13: P-values corresponding to the criteria used to assess the need for plan adaptation.

Data	p-value
Loss of dose coverage ($D_{98\%}$) to the ICTVu	
VMAT vs. IMPT 4.5%	**0,0027**
IMPT 4.5% vs. 3.0%	**0,0408**
VMAT vs. IMPT 3.0%	**0,0034**
Increased global maximum dose outside of PTVu	
VMAT vs. IMPT 4.5%	0,71
IMPT 4.5% vs. 3.0%	0,25
VMAT vs. IMPT 3.0%	0,93

Chapter 5

Discussion

The aim of this study was to analyze the benefits and limitations of using either photons or protons in lung cancer treatment. Protons' possible advantage of more precise dose delivery was examined and weighed against their sensitivity to anatomical changes. The two modalities were evaluated in terms of their robustness and the need for plan adaptation halfway through the treatment cycle. The robust optimization of proton plans was investigated closer in terms of the impact of density uncertainty. The quality of all treatment plans was assessed with the conformity and homogeneity indices.
Patient material is very diverse in terms of target volume characteristics. Dose distribution images are therefore used here as complementary information to support the discussion of the results.

5.1 VMAT vs. IMPT

5.1.1 Dose coverage of the treatment volumes

In terms of dose coverage of the ICTVu in the initial (CT 1) treatment plans, the median value achieved in VMAT plans is around 98.2%, and 97.8% in the $IMPT_{4.5\%}$ plans. Initially, the difference between these two modalities is only 0.4%, which is statistically borderline significant ($p = 0.058$). The difference is much larger in the recalculated (CT 2) plans. For VMAT plans median $D_{98\%}$ is around 98.3%, while it is 96.4% in $IMPT_{4.5\%}$ plans. Difference of 1.9% is statistically significant ($p < 0.05$). As box-plot in figure 4.1 shows, changes happening between planning CT and control CT, have more significant influence on $IMPT_{4.5\%}$ than VMAT plans. In case of VMAT, some patients received an improved dose coverage in CT 2 calculations. In case of $IMPT_{4.5\%}$, CT 2 box extends downwards relative to the CT 1 box, as most of the patients lose dose coverage to the ICTVu. For VMAT, the median slightly increases from CT 1 to CT 2, while for $IMPT_{4.5\%}$, it decreases. Judging by the difference between the two calculations (CT 1 and CT 2) for each modality, VMAT plans are more robust than $IMPT_{4.5\%}$ plans. For the $IMPT_{4.5\%}$ plans, difference in dose coverage between CT 1 and CT 2 data is statistically significant ($p << 0.01$).

$IMPT_{4.5\%}$ plans were created with robust optimization, by including sources of uncertainties in the ICTV objectives during the inverse optimization process. Use of PTVu was the equivalent approach for VMAT plans. In case of dose coverage of PTVu, the difference between CT 1 and CT 2 data is statistically negligible. Box-plot in figure 4.4 shows that the median value doesn't shift a lot from CT 1 to CT 2 box (from 95.2% to 94.7%). For some patients (2, 3, 6, and 12), however, change in PTVu coverage is significant. For example, patient 12 initially received 95.1% dose, while in the recalculated plan, the dose dropped to 88.6%.
In research done by Hoffmann et al. (2017), 23 patients that received adaptive photon treatment were re-planned with IMPT technique, in order to evaluate the impact of anatomical changes on the protons [10]. In their research, the robust optimization was not used as it is here. Their proton plans performed poorly compared to the photon plans and 14 (61%) proton plans needed adaptation in terms of dose coverage to the CTV. None of the photon plans needed re-planning. The threshold they used was that 95% of the CTV had to receive at least 95% of 66 Gy. Here, the treatment volume is ICTVu, which includes margin for organ motion. The critical threshold used here is that 98% of the ICTVu has to receive at least 95% of 66 Gy. This means that only two out of 16 patients (patient 6 and 12) would have needed adaptation due to dose coverage, when treated with $IMPT_{4.5\%}$. One of these two (patient 6) would have also needed adaptation when treated with VMAT. Comparing results implies that using robust optimization for proton plans is very beneficial and helps create robust treatment plans.

5.1.2 Global Maximum Dose and Organs at Risk

Global Maximum Dose

Results show that global maximum dose increased significantly from CT 1 to CT 2 calculation for both modalities (4.2). This is observed both for D_{2ccm} and D_{max}. In VMAT plans, median D_{2ccm} increased slightly from 68.3 Gy to 68.9 Gy, while median D_{max} stays at approximately 70.6 Gy. In $IMPT_{4.5\%}$ plans, median D_{2ccm} increased slightly from 68.5 Gy to 68.6 Gy, while median D_{max} increased from 70.3 Gy to 70.7 Gy. Difference between CT 1 and CT 2 results is, however, more significant for the $IMPT_{4.5\%}$ plans (D_{2ccm}: $p = \mathbf{0{,}02}$, D_{max}: $p = \mathbf{0{,}01}$), than for the VMAT plans (D_{2ccm}: $p = \mathbf{0{,}04}$, D_{max}: $p = \mathbf{0{,}04}$). This suggests that the proton plans are more susceptible to tissue changes than photon plans.
In the initial (CT 1) plan set, difference between how each modality performs is not statistically significant. The same is observed in the recalculated (CT 2) plan set. It is, however, noticeable in the box-plots (4.5 and 4.6), as well as in the detailed tables in Appendix A (6.5 and 6.7), that for some patients the difference in global maximum dose in the VMAT plan vs. the $IMPT_{4.5\%}$ plan, is significant. For patient 1, D_{2ccm} is larger in the initial VMAT plan (69,4 Gy) than in the initial IMPT plan (68,6 Gy). In the recalculated (CT 2) version, dose stays at the same level for proton plan, while for VMAT plan, the dose increases to 70,9 Gy, which is above the critical goal. Similar thing happens for patients 9 and 13, who in the recalculated VMAT plan receive D_{2ccm} above

the critical goal. The opposite happens for patient 6, who in the initial (CT 1) plan receives approximately the same D_{2ccm} with both modalities, while in the recalculated (CT 2) version D_{2ccm} increases to 72.0 Gy in the $\text{IMPT}_{4.5\%}$ plan. In CT 2 VMAT plan, the dose decreases slightly, to 67.6 Gy. These are examples of significant change between the two modalities, emphasizing the diversity of this small group of patients and the need for individual assessment.

Spinal cord

For the spinal cord, important serial OAR, proton modality shows significantly larger dose protection effect than the photon modality. Both in the initial (CT 1) and the recalculated (CT 2) treatment plans, D_{1ccm} is significantly lower for $\text{IMPT}_{4.5\%}$ than for VMAT ($p << 0.01$). Difference between the median values for the the modalities is at around 6 Gy, both in CT 1 and CT 2 calculations. Reduced dose to the OAR when using protons vs. photons is as expected. For patients 4, 15, 21, and 22, both D_{1cmm} and D_{max} was reduced to approximately 0 Gy in proton plans, while in corresponding VMAT plans, the dose was at around 15 Gy.
In terms of the robustness of D_{1ccm} from CT 1 to CT 2, there is no significant change for either $\text{IMPT}_{4.5\%}$ or VMAT plans. Median D_{1ccm} increases only slightly from 18.8 Gy to 19.9 Gy for VMAT, and decreases from 13.2 Gy to 13.1 Gy for $\text{IMPT}_{4.5\%}$. The change is, however, more noticeable in case of $\text{IMPT}_{4.5\%}$ plans than VMAT plans. Very large difference between CT 1 and CT 2 happens in the $\text{IMPT}_{4.5\%}$ plan for Patient 17, where D_{1ccm} increases from $14,8$ Gy to $25,7$ Gy. Corresponding results for VMAT show increase from $22,9$ Gy to $23,4$ Gy. Dose in VMAT plan is therefore initially higher than in the proton plan, but at the same time more robust, leading to lower dose in CT 2 compared to the proton plan. Protons' sensitivity to tissue changes may have a large effect on dose to OARs halfway through the treatment. The initial dose protection in some cases comes with with heightened risk of overdosing due to tissue changes. This was also the idea behind avoiding proton beam angles that would have placed the exit-dose near an OAR.

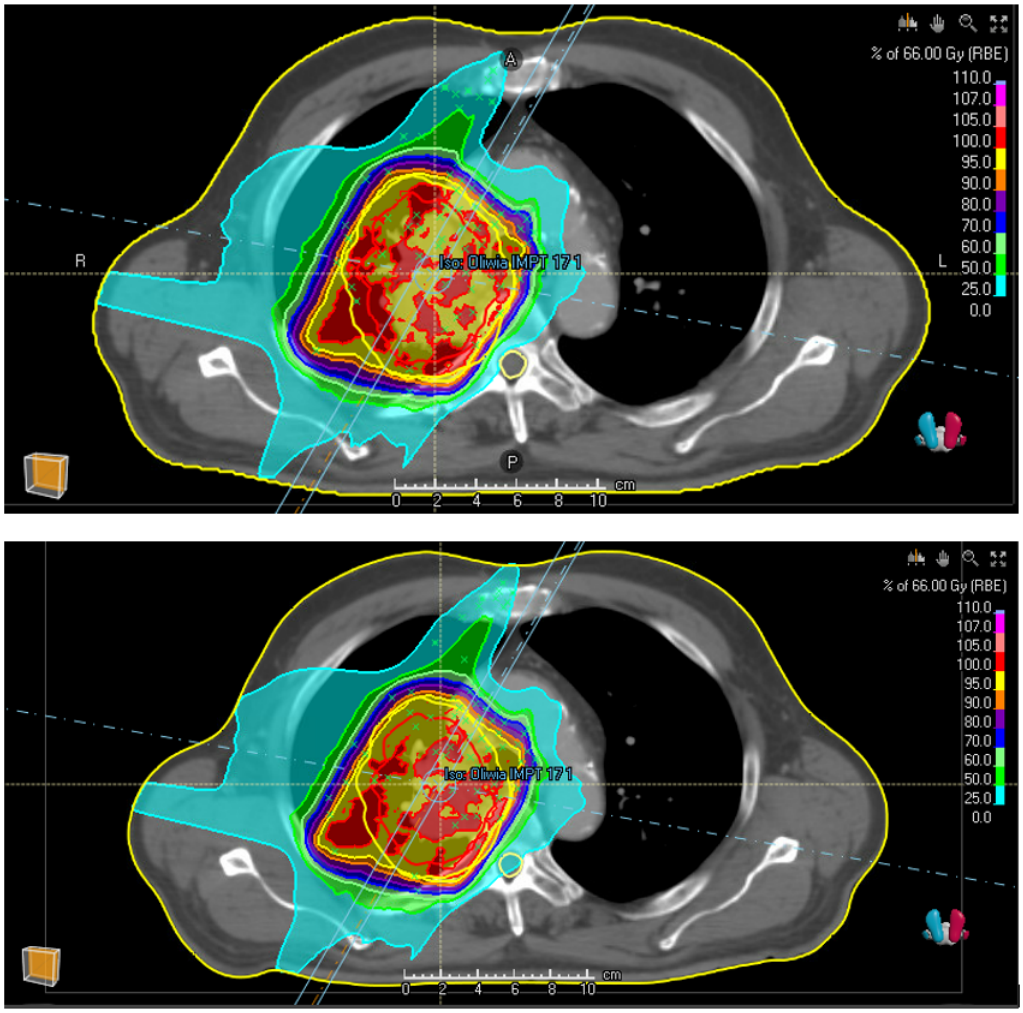

Figure 5.1: Dose distribution in a single CT slice for patient 17 using the $\text{IMPT}_{4.5\%}$ plan. The upper image shows the initial (CT 1) calculation and the image below shows dose distribution recalculated on the control CT (CT 2). Dose to spinal cord (yellow circle) changes significantly from CT 1 to CT 2.

Figure 5.1 shows how the spinal cord (yellow circle) is covered with the 16,5 Gy (25%) isodose in CT 2 compared to CT 1. As table (6.3 specifies, for patient 17 the special tool forcing the beam to avoid an OAR was used. The effect of this tool is clear in the CT 1 calculation but does not seem to translate as well to CT 2. This is a possible cause for the difference in dose delivery to spinal cord in this case. Another possible cause can be changes in tissue, like the significant tumor shrinkage shown in figure 5.2.

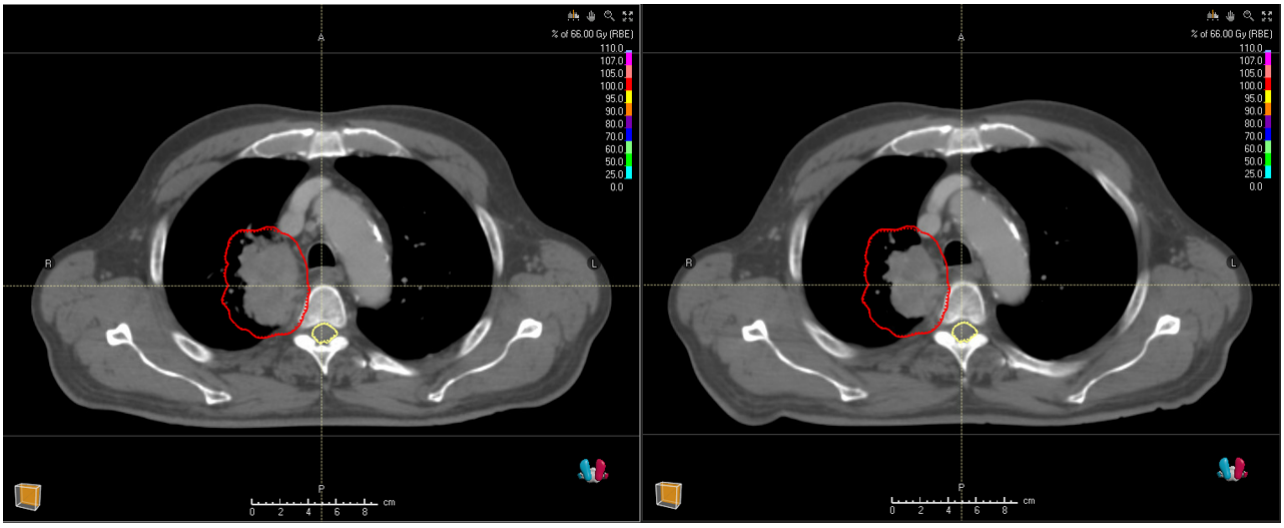

Figure 5.2: A single CT slice for patient 17 showing tumor shrinkage happening between CT 1 and CT 2 (CT 1 on the left and CT 2 on the right side).

In case of D_{max}, the difference between CT 1 and CT 2 results for IMPT$_{4.5\%}$ plans is larger than in case of D_{1ccm}. Similar difference is observed for VMAT plans. This is as expected since D_{max} represents dose in a single voxel. In IMPT$_{4.5\%}$ plans median D_{max} to spinal cord increased from 24.9 Gy to 30.5 Gy. The results are statistically significant ($p < 0.05$). In VMAT plans the median D_{max} increases from 22.6 Gy to 26.2 Gy, but the change is not statistically significant. Protons' sensitivity to tissue changes is made apparent once again.
Results for D_{1ccm} show larger dose protection in IMPT$_{4.5\%}$ plans than VMAT plans. The opposite is the case for D_{max}. The median D_{max} values are higher for proton plans than photon plans, in both CT 1 and CT 2 calculations. Using D_{1ccm} can be considered more statistically correct than using D_{max}, for the purpose of calculating maximum dose. However, in case of the spinal cord, a serial organ, avoiding hotspots is crucial. Minimizing D_{max} in a treatment plan ensures limited risk of hotspots.

Lungs

Results on dose delivery to lungs (minus IGTV) show that treatment delivered with protons is much more limited to the target volume than if photons are used. Figure 5.3 shows an example on how photons delivered to the tumor on one side of the body lead to irradiation of the healthy lung on the opposite side. With protons, the opposite lung is spared, since dose deposition is largely limited past depth of the Bragg peak.

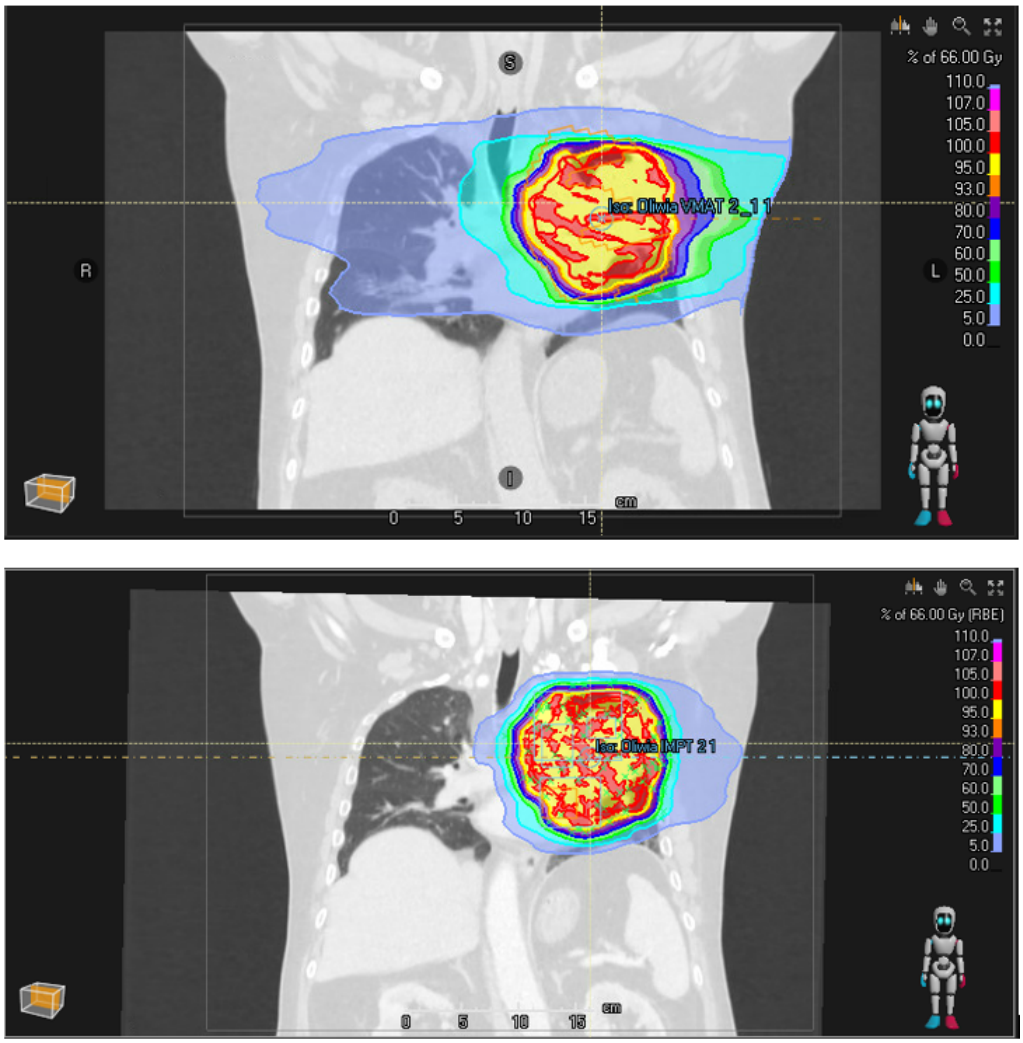

Figure 5.3: A single CT slice for patient 2, an example showing how the IMPT delivers dose more precisely than VMAT, saving dose to healthy lung tissue (VMAT above and IMPT below).

Dose received by healthy lung volume is significantly larger in VMAT plans than in IMPT-plans. The statistical significance is proved for all three dose measurements, V_{20Gy}, $V5Gy$, and MLD, in both CT 1 and CT 2 calculations ($p << 0.01$). The largest difference in median values between the two modalities is observed for V_{5Gy} (also seen in figure 4.9). In CT 1 calculation, the median value for $\text{IMPT}_{4.5\%}$ plans is $36,7\%$ lower than for VMAT plans. In CT 2 calculation, the difference in median value increases to $44,4\%$. For the two other metrics, V_{20Gy} and MLD, the median value is around 30% lower in $\text{IMPT}_{4.5\%}$ plans than in VMAT plans. Average MLD is 4.1 Gy lower in $\text{IMPT}_{4.5\%}$ plans compared to the VMAT plans ($p << 0.01$). In research done by Van der Laan et al. (2020), when comparing data for 10 patients, the mean lung dose (MLD) was on average 3,2 Gy lower

in IMPT plans than in VMAT plans [18], which is a similar result. Reduction in dose to healthy lung tissue when using protons, compared to photons, confirms the advantage of protons' precision in dose delivery.
In the previously mentioned research done by Hoffmann et al. (2017), the initial (CT 1) median MLD was at 12.3 Gy in the photon plans and 6.6 Gy for proton plans [10]. Here, median MLD is at 13.0 Gy in photon plans, and 8.7 Gy in proton plans. Higher median MLD in proton plans, compared to Hoffmanns research might be due to the robust optimization used here. For photon plans, the median MLD is very similar. For both modalities the change in dose between CT 1 and CT 2 calculations is not statistically significant. The same is confirmed with box-plots in figure 4.9.

5.2 Density uncertainty

5.2.1 Dose coverage to the ICTVu

Changing density uncertainty from 4.5% to 3.0% in the robust optimization process in IMPT plans caused significant differences in dose coverage in the initial (CT 1) treatment plans ($p < 0.05$). On average, the initial dose coverage was $0,3$ Gy higher in the $\text{IMPT}_{3\%}$ plans, compared to the $\text{IMPT}_{4.5\%}$ plans. The slight increase in dose coverage after changing to 3.0% was observed for 12 out of 16 patients. Recalculated on the control CT, both IMPT plan sets exhibit worse coverage to ICTVu, compared to the initial treatment plans. Difference in results between the two sets of plans is not statistically significant. However, lowering density uncertainty would mean that the recalculated plan delivers lower than clinically required dose coverage (below 95%) for 5 out of 16 patient. With higher density uncertainty, only two of the patients would receive too low dose coverage.
The treatment plans optimized with 3% density uncertainty show worse robustness from CT 1 to CT 2. Their average decrease in dose coverage from CT 1 to CT 2 is at $4,0\%$. For $\text{IMPT}_{4.5\%}$ plans, the average decrease is significantly lower, at around $2,9\%$ ($p < 0.05$). It is expected that taking into account larger uncertainty during the optimization process would produce a more conservative and robust treatment plan, that is less influenced by tissue changes.

5.2.2 Mean Lung Dose

Change in density uncertainty did not cause significant change in the Mean Lung Dose (MLD) either in the CT 1 or CT 2 calculations. In CT 1, the decrease in density uncertainty led to a slight decrease in median MLD from 8.7 Gy to 8.6 Gy. In CT 2, the decrease in median MLD was a little larger, from 9.0 Gy to 8.6 Gy. In $\text{IMPT}_{4.5\%}$ plans, the median increase in MLD is at 0.1 Gy, while in $\text{IMPT}_{3\%}$ plans, the MLD decreases slightly, with a median value of -0.2 Gy. The robustness of each treatment plan in terms of MLD was not significantly influences by the change in density uncertainty. The results are not surprising. The mean lung dose is measured by averaging dose delivered to the

whole Lungs-IGTV volume, which is relatively large. Small differences in small parts of the lungs are therefore difficult to catch by measuring the MLD.

5.2.3 Spinal Cord

For maximum dose (D_{max}) to the spinal cord, changing density from 4.5% to 3.0% does not cause any significant change in the initial (CT 1) treatment plans. The median D_{max} decreases very slightly from 24.9 Gy to 24.8 Gy. However, in some cases, the difference is large, like for patient 9 receiving 4.9 Gy (16.7%) lower dose with the $\text{IMPT}_{3\%}$, compared to the $\text{IMPT}_{4.5\%}$ plan. Figure 5.4 shows the difference in dose distribution between the two plans ($\text{IMPT}_{4.5\%}$ minus $\text{IMPT}_{3\%}$). The ICTVu (red line) is a large volume, that is also close to the spinal cord. The red and orange area near the spinal cord indicate that the $\text{IMPT}_{4.5\%}$ plan delivers higher dose to the spinal cord, compared to the less conservative $\text{IMPT}_{3\%}$ plan.

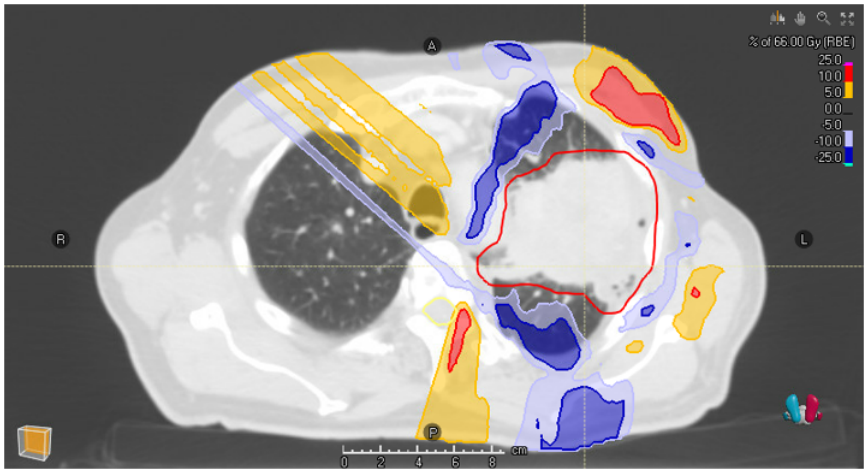

Figure 5.4: Difference in dose distribution in a single CT 1 slice for patient 9. Dose delivered with $\text{IMPT}_{3\%}$ is subtracted from dose delivered with $\text{IMPT}_{4.5\%}$. The map shows higher dose near the spinal cord (yellow circle) in the $\text{IMPT}_{4.5\%}$ plan.

Patient group used here is very diverse, for instance in terms of tumor vicinity to the OARs. Choosing density uncertainty in a treatment plan should therefore be based on individual analysis of patient's case. This would have probably increase the cost of a proton treatment. For patient 9, the corresponding VMAT plan delivers $D_{max} = 29.4$ Gy to the spinal cord (and 29.6 Gy in the recalculated (CT 2) plan). Comparing to the results from both IMPT plans, the spinal cord would not have been spared for a lot of dose if choosing the proton treatment.
In the recalculated (CT 2) treatment plans, using lower density uncertainty causes significant change ($p < 0.05$). The median value decreases with 12.6%, as the density uncertainty decreases from 4.5% to 3%. It means that for the more conservative treatment plans, maximum dose to spinal cord is larger, than for the less conservative plans.

Increased dose to healthy tissue and organs at risk is the cost of a conservative treatment plan delivering robust dose coverage to the treatment volumes. Patient 12 is an example, in which dose to the spinal cord increases more for the $IMPT_{4.5\%}$ plan than for the $IMPT_{3\%}$ plan from CT 1 to CT 2 calculation (9.6 Gy for the $IMPT_{4.5\%}$ plan and 5.5 Gy for the $IMPT_{3\%}$ plan). Difference in dose distribution is shown in figure 5.5.

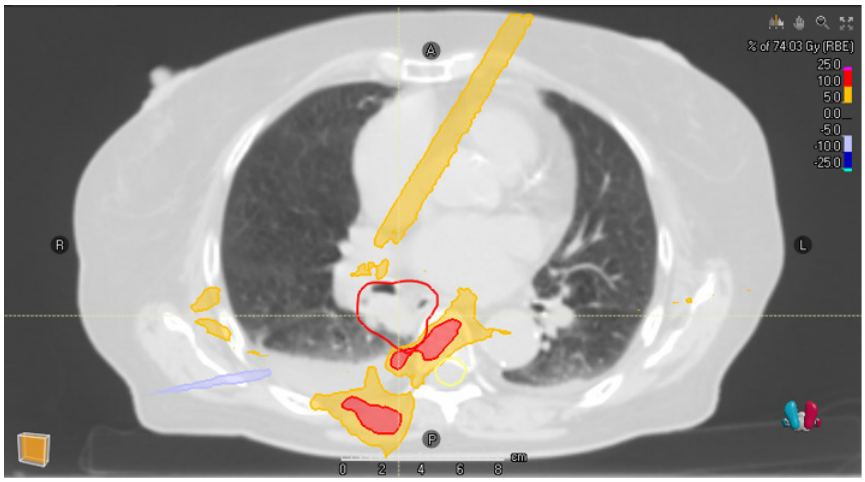

Figure 5.5: Difference in dose distribution in a single CT 1 slice for patient 12. Dose delivered with $IMPT_{3\%}$ is subtracted from dose delivered with $IMPT_{4.5\%}$. The map shows higher dose near the spinal cord (yellow circle) in a $IMPT_{4.5\%}$ plan.

In this case, the tumor volume is also close to the spinal cord, as for patient 9. There are many physical changes happening in the lung near the tumor, as shown in figure 5.6. These large changes influence dose coverage to the ICTVu, as shown in table 4.5. In both $IMPT_{4.5\%}$ and $IMPT_{3\%}$ plans, coverage drops from CT 1 to CT 2, and in both cases it leads to a value below the critical threshold of 95%. It is, however, a large difference between the two plans. For the $IMPT_{4.5\%}$ plan, the dose drops from $97,8$ Gy to $92,5$ Gy, while for the $IMPT_{3\%}$ plan, the difference is much larger, going from $98,6$ Gy to $84,6$ Gy. The $IMPT_{4.5\%}$ is therefore much better prepared for the physical changes happening during treatment. As mentioned before, the $IMPT_{4.5\%}$ plan delivers higher dose to the spinal cord in CT 2, compared to the $IMPT_{3\%}$ plan. The difference between those two in CT 2 is $4,5$ Gy. They are both, however, below the critical threshold of 52 Gy. In this case it seems beneficial to adopt the more conservative treatment plan, regardless of the larger maximum dose to the spinal cord.

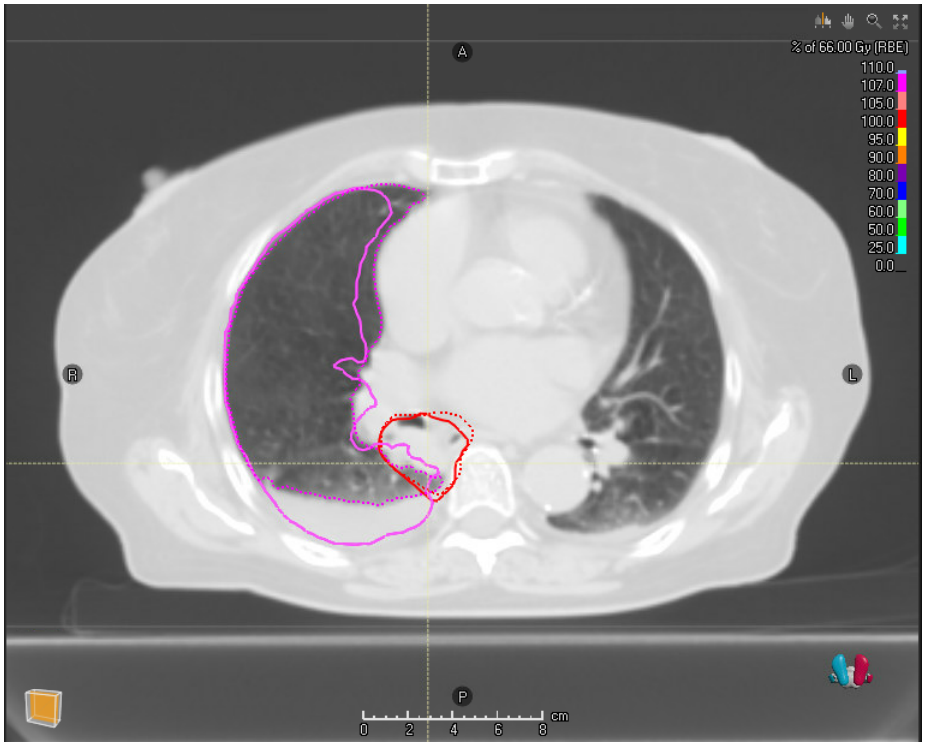

Figure 5.6: Single CT 2 slice for patient 12 showing physical changes in the lung from CT 1 to CT 2 (solid pink line shows how lung delineation in CT 1).

5.3 Plan quality

5.3.1 Conformity Index

The conformity index used in RayStation software for this study is the same as the one proposed by N.J. Lomax and S.G. Scheib (2003), called by them *Healthy Tissues Conformity Index* [20]. It indirectly measures how much of the volume covered by the reference isodose is normal tissue volume. A good score here would be as close to 1 as possible, meaning perfect protection of normal tissue. If the score is close to zero, it means that more of the normal tissue that the target volume is covered by the reference isodose. This conformity index is criticized in the review study by L. Feuvret et al. (2006) due to the difficulty with its interpretation [7]. They point out an instance in which the reference isodose is within the target volume, meaning the index would be equal 1, but that there might be some part of the target volume outside the reference isodose border, receiving lower dose. They also consider the situation in which the conformity index is equal 0.5, that could have two very different interpretations. The first one is that the target volume is within the reference isodose and equal proportion of target volume and normal tissue volume around it is irradiated with the reference dose. The other possible interpretation is that the reference isodose volume and the target volume are of similar

size and shape but the overlap between them is only a half of each volume. Those two interpretations of 0.5 score lead to very different dose coverage of the treatment volume. It is, therefore, more accurate to use this type of conformity index when assessing protection of the normal tissue, rather than efficiency of treating the tumor [7].
For a complex tumor like the one in figure 4.10, it is difficult to achieve good conformity, but in this case, the IMPT plans seem to do a better job than the VMAT plan. The tumor in this one slice of CT requires less dose in the middle of it, compared to the upper and lower part of the tumor. The VMAT plan seems to deliver high dose in the middle of the volume, whereas the two IMPT plans spare this part that is outside of the ICTVu. The 66 Gy isodose (red area) in the VMAT plan covers large parts of the tissue outside of the ICTVu (red line), which leads to low conformity index of 0.40 in CT 1 and 0.38 in CT 2. In the two IMPT plans the two areas, the 66 Gy isodose and the ICTVu seems to overlap each other better, than in the VMAT plan. The conformity index is therefore higher with protons in this case ($CI_{CT1} = 0,50$ and $CI_{CT1} = 0,52$ in the $\text{IMPT}_{4.5\%}$ plan, $CI_{CT1} = 0,57$ and $CI_{CT1} = 0,60$ in the $\text{IMPT}_{3\%}$ plan). When comparing dose coverage to the ICTVu for the same patient, the results are much better for the VMAT plan (99.0% in CT 1 and 100.5% in CT 2), compared to the two IMPT plans (ranging from 97.3% to 98.4%). The almost perfect dose coverage in the VMAT plan comes, however, with a cost to the healthy tissue around the tumor volume. That is why the conformity index used here says more about the protection of the normal tissue, instead of how well the treatment volume is covered, as Feuvret et al. (2006) have argued [7]. The results presented in table 4.8 show quite large variation in the conformity scoring for the patients. In the review study on conformity indices [7], the threshold for a good score proposed for this particular index is > 0.60. All three sets of plans (including the recalculation done on CT 2 for each of them) has the median score of equal or above 0.60, with the median for initial (CT 1) VMAT plans at 0.66 as the highest value. Recalculated (CT 2) VMAT plans have the lowest median conformity score of 0.60.

For three patients (patient 7, 8, and 16), the score did not exceed the 0.60 threshold in any calculation. For patient 7, the initial (CT 1) IMPT plans (both $\text{IMPT}_{4.5\%}$ and $\text{IMPT}_{3\%}$) had the lowest score of 0.35. Figure 5.7 shows a single CT slice with dose distribution for patient 7 in the $\text{IMPT}_{4.5\%}$ plan using both CT 1 (upper one) and CT 2 (lower one).

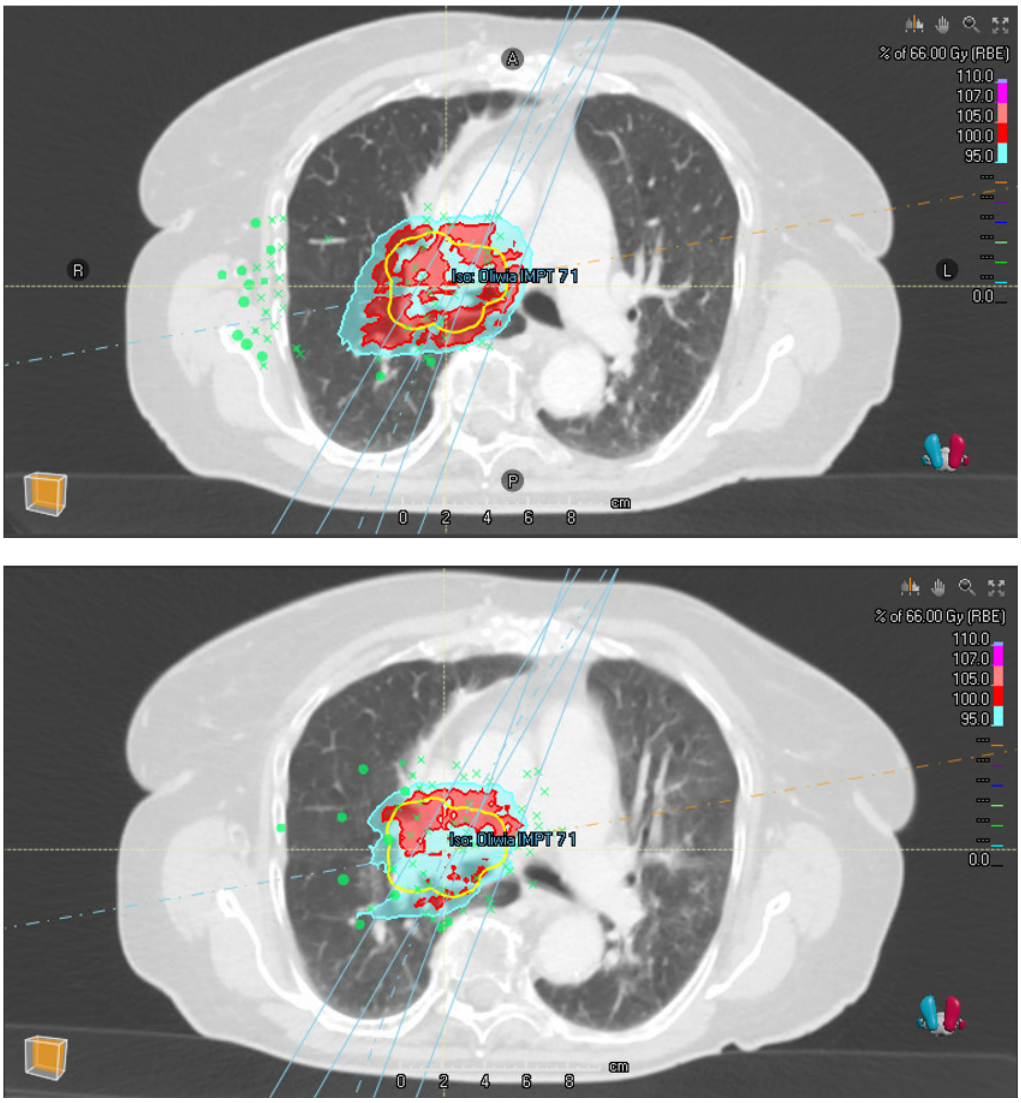

Figure 5.7: Dose distribution in a single CT slice for patient 7 using the $\text{IMPT}_{4.5\%}$ plan. The upper image shows the initial (CT 1) calculation and the image below shows dose distribution recalculated on the control CT. The upper image shows that the prescribed dose (red) is delivered to a large area outside of the ICTVu border (yellow). This can be used to explain the low conformity index. Image below it shows how the dose distribution is affected by the changes in the lung tissue. Specifically, the 80° beam (marked with the orange dash-dotted line) seems to be affected by the changes in the left lung (right side of the image).

In the initial calculation (upper image), the prescribed isodose (red color) reaches far beyond the ICTVu border (yellow line), indicating that the isodose volume is larger that the target volume, leading to poor conformity. In the image below it (CT 2), the

prescribed isodose seems to be much more confined to the target volume, which could be the reason for the higher conformity index. It seems that the 80° beam (marked with the orange dash-dotted line) is affected by the visible changes appearing in the left lung (right side of the image). This seems to cause reduced dose delivery to the region near target volume, and in this case a slight improvement in the conformity (from 0.35 to 0.43).

Table 5.1: Distribution of the best conformity index score for each patient between the treatment plan sets.

VMAT		IMPT 4.5%		IMPT 3.0%	
CT 1	CT 2	CT 1	CT 2	CT 1	CT 2
0.86 (Patient 2)	0.74 (Patient 4)	0.66 (Patient 3)		0.72 (Patient 5)	0.85 (Patient 1)
0.58 (Patient 7)	0.84 (Patient 6)	0.78 (Patient 13)		0.77 (Patient 22)	0.60 (Patient 8)
0.77 (Patient 9)	0.56 (Patient 16)	0.63 (Patient 15)			
0.66 (Patient 12)	0.72 (Patient 17)	0.77 (Patient 22)			
0.84 (Patient 21)					

For 9 out of 16 patients, the best conformity score was achieved with VMAT, either in the initial CT 1 plan (patients 2, 7, 9, 12 and 21) or in the recalculated (CT 2) version (patients 4, 6, 16 and 17). Table 5.1 shows the best conformity score for each patient and which treatment plan it is tied to. For 8 patients (patients 1, 3, 5, 8, 9, 13, 15, and 22), however, the CT 2 calculation of the VMAT plans delivered the worst conformity for each patient. The median of 0.66 in the initial (CT 1) VMAT plans is the highest median compared to the the other plan sets. It decreases, however, considerably in the recalculated (CT 2) sets, to 0.60, which is the lowest value, compared to the others. Therefore, in terms of conformity index, the VMAT technique is the least robust, compared to the two IMPT plan sets. The IMPT plans seem better at keeping the dose delivery precise and limited to the treatment volume. The VMAT technique targets the healthy tissue around the treatment volume, and in turns ensures more robust dose coverage to the tumor, despite of tissue changes affecting the beam.

5.3.2 Homogeneity Index

For most treatment plans the homogeneity index is above 0.90, with some exceptions. It means that the near-minimum dose $D_{98\%}$ is high and close to the near-maximum dose $D_{2\%}$. The dose is then distributed uniformly inside the ICTVu.
Difference in homogeneity between CT 1 and CT 2 is statistically significant for all three sets of treatment plans ($p < 0.05$).
As presented in figure 4.11, the homogeneity index is generally lower in the recalculated (CT 2) version of each treatment plan. This is true for all three sets of plans. Recalculated (CT 2) VMAT plans score the best compared to $\text{IMPT}_{4.5\%}$ and $\text{IMPT}_{3\%}$ plans. Although the change happening between CT 1 and CT 2 is significant for VMAT, the IMPT plans exhibit greater sensitivity. As marked in table 4.10, the lowest homogeneity index for most of the patients corresponds to the CT 2 calculation of either $\text{IMPT}_{4.5\%}$ plan or

$IMPT_{4.5\%}$ plan.
Patient 6 experiences the largest decrease in homogeneity, from 0.95 to 0.68 in both IMPT plans. This comes most likely from the extreme loss of $D_{98\%}$ to ICTVu, as mentioned before. This can also be seen in figure 4.3 showing dose distribution changing from CT 1 to CT 2 in the $IMPT_{4.5\%}$ plan. In figure 4.12, data distribution for patient 6 is visualized side by side for all three plan sets. In the leftmost pair of images (VMAT CT 1 and CT 2) there is less of the 66 Gy isodose covering the ICTVu in the CT 2 image, compared to the CT 1. This coincides with $D_{98\%}$ to ICTVu decreasing from 97.7% to 92.5%, which in turn could be the reason for the change in homogeneity index from 0.96 to 0.91. In the IMPT plans, there is a clear change in homogeneity from CT 1 to CT 2, with visible hotspots (pink) in the two CT 2 images. The hotspots correspond to 107% isodose. The hotspots coincide with the increased near-maximum dose, D_{2ccm}, from 68.6 Gy to 72.0 Gy in the $IMPT_{4.5\%}$ plan, and from 68.2 Gy to 71.8 Gy in the $IMPT_{3\%}$ plan.

5.4 Need for adaptation

5.4.1 Loss of dose coverage

Median values for loss of dose coverage are 0.01% for VMAT plans, 1.22% for $IMPT_{4.5\%}$ plans, and 1.54% for $IMPT_{3\%}$. This means that the IMPT plans score much worse than VMAT plans on the robustness halfway through the treatment cycle. For VMAT, two plans would have needed adaptation. In case of protons, five $IMPT_{4.5\%}$ plans and six $IMPT_{3\%}$ plans would have needed adaptation. There are significant differences in loss of dose coverage results between the VMAT plans and IMPT plans ($p < 0.05$). Difference between the two IMPT plan sets, $IMPT_{4.5\%}$ and $IMPT_{3\%}$, is smaller, but also statistically significant ($p < 0.05$).
The two VMAT plans that need adaptation correspond to patient 2 and 6. Patient 2 would have lost 2.6% of dose coverage to the ICTVu, compared to 0.1% when treated with $IMPT_{4.5\%}$ or nothing when treated with $IMPT_{3\%}$. Patient 6 would have lost 5.3% dose coverage, but the loss is significantly worse for proton plans, with 25.5% in $IMPT_{4.5\%}$ plan and 26.0% in $IMPT_{3\%}$.
The other four $IMPT_{4.5\%}$ plans that would have needed adaptation correspond to patients 7, 9, 12, and 13. For patient 7, the loss of dose coverage with $IMPT_{4.5\%}$ plan is at 2.1% which only slightly exceeds the threshold. In the $IMPT_{3\%}$ plan the loss reaches 6.8% which is much worse. For patient 9, dose coverage increases by 1.3% in the VMAT plan. In the $IMPT_{4.5\%}$ plan there is a loss of 3.0% and 2.6% for the $IMPT_{3\%}$ plan, which is slightly less. For patient 12 the $IMPT_{4.5\%}$ plan leads to 5.5% loss of coverage, while with the $IMPT_{3\%}$ plan, the loss reaches 14.2%. For patient 13 the loss of coverage is at 2.4% for the $IMPT_{4.5\%}$ and again, higher for the $IMPT_{3\%}$, reaching 3.2%. The last patient that would have needed adaptation due to loss of dose coverage is patient 1 loosing 3.7% of dose coverage with the $IMPT_{3\%}$ plan.
$IMPT_{3\%}$ plans lose more dose coverage from CT 1 to CT 2, compared to the $IMPT_{4.5\%}$ plans. This is especially apparent for patients 1, 7, and 12. $IMPT_{4.5\%}$ plans are more

robust than $IMPT_{3\%}$ plans. The best results are achieved with VMAT, indicating that it is more robust than proton modality.
There might be some limitations in using the 2% threshold for all patients. There is a nuance in each case, that could either mean that the threshold is too low or too high. For example, patient 2 whose VMAT plan needs adaptation since the loss of dose coverage is at 2.6%, would have still received satisfactory dose coverage in CT 2, 95.5% to the ICTVu and 91.4% to the PTVu. These results still exceed the critical goals (95% for ICTVu and 90% for PTVu). In this case, using the 2% threshold could be considered strict. For patient 12, the VMAT plan doesn't lose any dose coverage to the ICTVu between CT 1 and CT 2. Dose coverage to the PTVu, however, is much lower halfway through the treatment as it goes from 95.1% to 88.6%, which is below the critical goal for PTVu. In this case, using the loss of 2% in $D_{98\%}$ to the ICTVu as the only indication for robustness of dose coverage, would not be sufficient enough.
In case of proton plans, patients 7, 9, and 13, have $2.1 - 3.0\%$ loss of dose coverage. In all three cases the dose coverage is still above the critical goal of 95%, as it ranges from 95.0% to 95.7%. The 2% loss is relative to the initial dose coverage, and in cases where the initial result is very good, losing 2% could mean that the new result is still good enough. The loss of dose coverage from CT 1 to CT 2 is, however, an indication on how good the dose coverage would be through the second half of the treatment cycle. The borderline loss close to 2% could mean that during the second half the dose coverage would decrease even more. This depends on the scale of tissue changes happening for the rest of the treatment. Various changes could either accelerate or decelerate the loss of dose coverage. One could argue that for protons, that are sensitive to anatomical changes, the criteria for adaptation should be more rigid, compared to the VMAT modality.
As mentioned earlier, the article written by Hoffmann et al. (2017) states that with their criteria for dose coverage, 61% of the patients in their research would have needed adaptation when planning with protons [10]. With photons, none of their patients would have needed plan adaptation. When looking at the loss of dose coverage with threshold of more than 2%, 12.5% of VMAT plans, 31.3% of $IMPT_{4.5\%}$ plans, and 37.5% of $IMPT_{3\%}$ would have needed adaptation. Results for the VMAT plans are therefore worse, while results for the IMPT plans are better than in their case. There are multiple possible causes for that, including the treatment planning skills and the use of robust optimization in proton plans, as mentioned before.

5.4.2 Increased maximum dose

Statistically, there is no significant difference between the three plan sets in terms of the increase of global maximum dose outside of PTVu. The median increase is 0.57% in VMAT plans, 0.94% in $IMPT_{4.5\%}$ plans, and -0.03% in $IMPT_{3\%}$ plans. These results are, however, misleading due to how the median does not reflect the outliers very well.
In case of VMAT, the global maximum dose increase ranges from -2.9% to 3.0%. None of the patients would have needed adaptation in this case. Photon modality appears to be quite safe in terms of the global maximum dose to the healthy tissue. This limits the risk of hotspots as well.

For the $IMPT_{4.5\%}$ plans the increase in dose ranges from -1.5% to 7.4%. There are two patients that would have needed adaptation, patients 6 and 12. These two would have also needed adaptation due to the loss of dose coverage. The $IMPT_{3\%}$ plan for patient 6 would have needed adaptation due to the global maximum dose increasing with 6.2%. It is, however, less than in the more conservative $IMPT_{4.5\%}$, with the increase of 7.4%. The $IMPT_{4.5\%}$ plan for patient 12 would have delivered 5.4% higher maximum dose to the patient halfway through the treatment, which means that the plan would have needed adaptation. In the less conservative $IMPT_{3\%}$ plan, the global maximum dose to healthy tissue does not increase. For patient 3, the $IMPT_{3\%}$ would have needed adaptation due to the increase of 3.3% in dose. The same is true for patient 5 receiving 3.8% higher dose with the $IMPT_{3\%}$ plan, while the $IMPT_{4.5\%}$ plan would have delivered 3.0% higher dose. In summary, three $IMPT_{3\%}$ plans would have needed adaptation against two $IMPT_{4.5\%}$ plans. The median values are, however, lower for the $IMPT_{3\%}$ plans compared to the $IMPT_{4.5\%}$ plans. In general, this implies that the more conservative $IMPT_{4.5\%}$ plans have higher risk of increased dose to the healthy tissue due to the tissue changes, compared to the less conservative $IMPT_{3\%}$ plans. This is in contrast to the loss of dose coverage, where the $IMPT_{3\%}$ plans seem to have increased risk of losing dose coverage to the ICTVu, compared to the $IMPT_{4.5\%}$ plans. This supports the hypothesis that the more conservative $IMPT_{4.5\%}$ plans keep the dose coverage to treatment volumes stable, for the cost of higher dose to the healthy tissue. But, looking at the number of plans that would have needed adaptation, the $IMPT_{3\%}$ does score worse in total with 8 plans needing adaptation (due to either loss of coverage, increased maximum dose, or both), against 5 $IMPT_{4.5\%}$ plans. The photon modality scores the best with only two treatment plans in need for adaptation.

5.4.3 Organs at Risk

In case of dose to organs at risk, none of the VMAT plans would have needed adaptation. For the two IMPT plan sets, the only patient that would have need plan adaptation is patient 16. In this case, dose to the right Brachial Plexus increases above the critical threshold of 66 Gy from CT 1 to CT 2. In the $IMPT_{4.5\%}$ plan the dose goes from 62.4 Gy to $67,7$ Gy, while in the $IMPT_{3\%}$ plan it increases from 63.0 Gy to 68.5 Gy. Dose delivered with the VMAT plan increases from 64.5 Gy to 64.4 Gy, which is also very high and above the desired threshold of 60 Gy. The initial dose to the OAR is lower for the two IMPT plans compared to the VMAT plan. As the treatment progresses dose to the OAR delivered with protons surpasses dose from photons. Here, the VMAT technique is more stable than IMPT. This patient is, however, a special case, since the right Brachial Plexus is inside the ICTVu (shown in figure 4.13), meaning that it is impossible for the OAR to avoid the radiation when the tumor is treated, regardless of the modality. It could therefore, in this case, be a reason to ignore the increased dose as an indicator for plan adaptation.
Overall, the increased dose to OARs doesn't seem to be a large problem when considering plan adaptation, for either modality. It is, however, important to consider the cases of large increase of global maximum dose outside of PTVu. Possible hotspots appearing in

the healthy tissue could end up close to or inside an OAR, especially if the anatomical changes lead to a shift of OARs' position in the patient. If the adaptation could lead to significantly better dose protection of the OARs, it should be considered anyway.

5.5 Strengths and Limitations

Patient group used for this research was very diverse in terms of the tumor size, location, physical changes appearing during the treatment cycle, etc. Because of the diversity in patient data, the treatment planning process was complex, where in each case different strategies were used to achieve the best treatment plan. In each treatment plan, the same framework was utilized. This includes the list of clinical goals, that each treatment plan was assessed with, as well as the initial list of objectives used in the inverse optimization process. The diversity in patient data could mean that the results can be interpreted universally. However, the relatively small patient population could limit the universality potential.
How each treatment plan was created, personal treatment planning choices, and limited experience did influence the results. The lack of experience could mean that the treatment plans were of similar quality, regardless of the modality. It could, however, also be the case that the treatment planning was of better standard for one of the modalities, compared to the other. The density uncertainty analysis, between the $IMPT_{4.5\%}$ and $IMPT_{3\%}$ plans, was highly objective. The $IMPT_{3\%}$ plans were created in RayStation software only by changing the density uncertainty parameter and repeating the inverse optimization. The process was therefore unbiased. It was, however, difficult to find similar type of research in order to examine the results further.

5.6 Future prospects

The analysis performed here could be extended to a larger group of patients. The treatment plans could also be recreated by multiple specialists, in order to investigate the impact of personal skills and experience. This could improve the quality of the research. Artificial intelligence could also be incorporated here, in order to automate the treatment planning process, as well as to develop a prediction model for treatment outcome.

Chapter 6

Conclusion

$IMPT_{4.5\%}$ plans showcased weaker robustness in terms of dose coverage to the ICTVu, compared to the VMAT values. Proton plans exhibited, however, more effective dose protection to the spinal cord, compared to the photon plans. Although, in some cases, changes happening between CT 1 and CT 2 influenced the proton plans more than photon plans. This showcased protons' sensitivity to anatomical changes. Healthy lung tissue was substantially spared for dose in proton plans compared to the photon plans, both in CT 1 and CT 2.
Robustness of dose delivery to the ICTVu declined when $IMPT_{4.5\%}$ plans were recalculated using 3% density uncertainty. The less conservative $IMPT_{3\%}$ plans did, however, have a stronger dose protection effect on the spinal cord in the recalculated (CT 2) plans, as expected. With a less conservative plan, dose delivery to the target volume suffers halfway through the treatment cycle, while some OARs are spared for even more dose.
The initial (CT 1) VMAT plans achieved the highest median conformity index (CI) score, compared to the other treatment plans. However, halfway through the treatment cycle, VMAT plans receive the lowest median CI due to the reference isodose covering large parts of the healthy tissue, adjacent to the treatment volumes. Almost all treatment plans score well in terms of the homogeneity. The proton plans do, however, exhibit larger change from CT 1 to CT 2, compared to the photon plans.
In terms of loss of dose coverage, two VMAT plans would have needed adaptation, compared to five $IMPT_{4.5\%}$ plans, and six $IMPT_{3\%}$. None of the VMAT plans would have needed adaptation due to increased D_{max} outide of PTVu, while two $IMPT_{4.5\%}$ plans and three $IMPT_{3\%}$ plans would have needed re-planning. Dose to organs at risk did not exceed the critical threshold for any patient, except for one. In this case, the affected OAR is the right brachial plexus that overlaps the treatment volume. Both IMPT plans deliver too high dose to the organ. In summary, proton plans are less robust than photon plans, and haver larger need for adaptation halfway through the treatment cycle. They exhibit, however, better dose protection of healthy tissue.

Appendix A

6.1 Additional information on ICTVu

Table 6.1: ICTVu volume in planning CT (CT 1)

Patient	1	2	3	4	5	6	7	8	9	12	13	15	16	17	21	22
Volume cm^3	282	555	198	96	235	279	133	81	573	38	90	145	126	277	81	175

6.2 Beam setup information

Table 6.2: The VMAT beam setup for all patients.

Patient number	Beam number	Gantry start [deg]	Gantry stop [deg]	Rotation	Collimator [deg]
1	1	5	179	Clockwise	15
	2	179	5	Counterclockwise	345
2	1	10	179	Clockwise	15
	2	179	10	Counterclockwise	345
3	1	200	45	Clockwise	15
	2	45	200	Counterclockwise	345
4	1	181	5	Clockwise	15
	2	5	181	Counterclockwise	345
5	1	181	179	Clockwise	15
	2	179	181	Counterclockwise	345
6	1	181	359	Clockwise	15
	2	359	181	Counterclockwise	345

Continued on next page

Table 6.2: The VMAT beam setup for all patients. (Continued)

7	1	181	35	Clockwise	15
	2	35	181	Counterclockwise	345
8	1	181	179	Clockwise	15
	2	179	181	Counterclockwise	345
9	1	320	179	Clockwise	345
	2	179	320	Counterclockwise	15
10	1	185	170	Clockwise	15
	2	170	185	Counterclockwise	345
11	1	340	179	Clockwise	15
	2	179	340	Counterclockwise	345
12	1	185	170	Clockwise	15
	2	170	185	Counterclockwise	345
13	1	185	170	Clockwise	15
	2	170	185	Counterclockwise	345
15	1	181	359	Clockwise	15
	2	359	181	Counterclockwise	345
16	1	181	179	Clockwise	15
	2	179	181	Counterclockwise	345
17	1	181	179	Clockwise	15
	2	179	181	Counterclockwise	345
21	1	181	359	Clockwise	15
	2	0	181	Counterclockwise	345
22	1	181	179	Clockwise	15
	2	179	181	Counterclockwise	345

Table 6.3: The IMPT beam setup for all patients.

Patient number	Beam number	Gantry [deg]	Air gap [cm]		OAR range margin	
			Min	CAX	ROI	Margin [cm]
	1	350	22,42	29,82	-	-
	2	200	25,06	29,48	-	-
1						

Continued on next page

Table 6.3: The IMPT beam setup for all patients. (Continued)

	3	165	28,86	29,82	-	-
	4	5	24,73	29,88	-	-
	5	120	27,41	29,37	-	-
2	1	330	17,09	25,35	-	-
	2	30	23,75	28,6	-	-
	3	120	25,15	26,00	-	-
	4	210	16,93	25,55	-	-
	5	180	27,57	27,68	-	-
3	1	30	20,82	29,10	spinal cord	0,00
	2	210	25,72	30,23	spinal cord	0,00
	3	85	13,12	19,73	spinal cord	0,00
	4	230	22,93	26,16	spinal cord	0,00
4	1	210	28,14	30,30	-	-
	2	30	20,86	27,57	-	-
	3	80	12,96	19,88	-	-
	4	260	24,31	27,71	-	-
	5	235	26,63	28,14	-	-
5	1	60	10,46	20,19	spinal cord	0,15
	2	175	33,98	35,02	spinal cord	0,15
	3	10	19,14	22,69	spinal cord	0,15
	4	230	31,21	34,32	spinal cord	0,15
	5	200	34,3	34,6	spinal cord	0,15
6	1	280	23,78	32,90	-	-
	2	5	30,63	34,26	-	-
	3	140	20,75	27,03	-	-
7	1	200	28,86	30,95	-	-
	2	30	17,95	29,12	-	-
	3	80	13,23	21,74	-	-
	4	260	23,44	26,35	-	-
8	1	200	26,56	28,71	-	-
	2	30	15,86	27,13	-	-

Continued on next page

Table 6.3: The IMPT beam setup for all patients. (Continued)

	3	80	10,64	20,51	-	-
	4	260	15,91	21,76	-	-
9	1	350	24,17	30,65	-	-
	2	170	30,30	30,93	-	-
	3	310	8,83	25,04	-	-
	4	200	25,06	29,93	-	-
10	1	200	26,56	28,70	-	-
	2	30	15,78	27,13	-	-
	3	80	10,58	20,52	-	-
	4	260	15,83	21,80	-	-
11	1	15	26,69	32,11	-	-
	2	310	8,83	25,04	-	-
	3	210	22,27	29,09	-	-
	4	160	30,08	30,74	-	-
12	1	200	30,46	34,11	spinal cord	0,00
	2	30	22,40	24,90	spinal cord	0,00
	3	80	16,20	21,97	spinal cord	0,00
	4	260	18,77	26,96	spinal cord	0,00
13	1	200	31,13	33,46	spinal cord	0,00
	2	30	20,62	24,91	spinal cord	0,00
	3	80	13,10	15,43	spinal cord	0,00
	4	260	21,32	27,30	spinal cord	0,00
15	1	50	12,24	30,42	-	-
	2	220	27,79	29,03	-	-
16	1	200	31,97	33,46	-	-
	2	30	18,62	32,11	right brachial plexus	0,00
17	1	210	26,87	29,75	spinal cord	0,00
	2	30	21,43	27,76	spinal cord	0,00
	3	100	14,59	17,91	spinal cord	0,00
	4	280	20,61	28,31	spinal cord	0,00

Continued on next page

Table 6.3: The IMPT beam setup for all patients. (Continued)

21	1	30	22,55	35,01	-	-
	2	210	24,05	26,59	-	-
22	1	260	16,72	21,39	-	-
	2	140	27,54	28,27	-	-
	3	5	30,01	31,17	-	-

6.3 Dose delivery to treatment volumes and organs at risk

Table 6.4: Dose to the 98% of the ICTVu and PTVu, as planned using VMAT technique and the initial CT image set (CT 1), compared to the dose that the original plan would have delivered halfway through the treatment, based on the control CT (CT 2). The values are compared to the critical and desired clinical goals, where those that fall short of the desired goal for PTV are colored orange, and those that do not meet the critical goals are colored red.

Patient	ICTVu $D_{98\%}$ [Gy]		PTVu $D_{98\%}$ [Gy]	
	critical: $D_{98\%} > 62,7Gy$		desired: $D_{98\%} > 62,7Gy$	
			critical: $D_{98\%} > 59,4Gy$	
	CT1	CT2	CT1	CT2
1	64.3	65.4	63.2	63.5
2	64.7	63.0	63.0	60.3
3	65.0	65.0	63.1	59.8
4	64.1	64.0	61.4	61.3
5	64.8	64.6	63.3	63.3
6	64.5	61.1	61.1	55.5
7	65.0	64.0	62.7	61.4
8	65.4	66.3	63.0	63.8
9	65.1	66.0	63.0	64.1
12	64.9	65.0	62.8	58.5
13	64.9	66.3	62.7	63.8
15	65.2	65.3	62.9	63.5
16	64.5	64.5	60.0	60.5
17	64.4	64.2	62.1	62.1
21	64.5	65.4	62.8	62.8
22	64.8	64.7	62.9	63.1

Table 6.5: The clinical goals for the VMAT treatment plans. The values are achieved based on the initial CT image set (CT 1), compared to the values the original plan would have delivered halfway through the treatment, based on the control CT (CT 2). As in the table 6.4, the values are compared to the critical and desired clinical goals, where those that do not meet the desired goals are colored orange and the ones not satisfying the critical goals are colored red. The table includes the goals for ICTVu and PTVu from Table 6.4, but in [%] of the prescribed dose (66 Gy). Missing values mean that in the particular cases the organ at risk was not delineated on the CT, since the tumor is far away from it, and therefore monitoring dose to the OAR is not relevant.

Patient	ICTVu $D_{98\%}$ [% of 66Gy]		PTVu $D_{98\%}$ [% of 66Gy]		Max. D_{2ccm}		D_{max} [Gy]		Lungs-IGTV V_{20Gy} [%]		Lungs-IGTV V_{5Gy} [%]		Mean Lung Dose [Gy]		Heart V_{50Gy} [%]		Heart V_{45Gy} [%]		Heart V_{30Gy} [%]	
	critical: $D_{98\%} > 95\%$		desired: $D_{98\%} > 95\%$ critical: $D_{98\%} > 90\%$		critical: $D_{2ccm} < 69,96Gy$		desired: $Pointmax < 71,30Gy$		critical: $V_{20Gy} < 35\%$		desired: $V_{5Gy} < 65\%$		critical: $MLD < 20Gy$		desired: $V_{50Gy} < 20\%$		desired: $V_{45Gy} < 25\%$		desired: $V_{30Gy} < 30\%$	
	CT1	CT2	CT1	CT2	CT1	CT2	CT1	CT2	CT1	CT2	CT1	CT2	CT1	CT2	CT1	CT2	CT1	CT2	CT1	CT2
1	97.5	99.1	95.8	96.2	69.4	70.9	70.9	72.1	18.6	19.2	47.0	48.7	12.1	12.5	1.2	1.3	1.5	1.6	2.9	3.3
2	98.1	95.5	95.5	91.4	68.2	68.9	70.7	70.7	18.3	16.7	60.3	62.1	13.7	13.6	8.4	8.8	11.2	11.6	24.6	23.8
3	98.5	98.5	95.6	90.6	68.1	69.0	69.0	69.7	24.8	26.5	64.6	65.0	14.6	15.8	1.2	1.4	1.8	1.8	4.5	2.8
4	97.1	97.0	93.0	93.0	69.5	69.9	71.2	71.9	20.3	18.6	50.8	47.3	11.7	10.8	1.1	1.0	1.6	1.5	5.2	4.8
5	98.2	97.9	96.0	95.9	68.5	68.9	70.6	70.3	27.7	27.7	64.1	64.3	15.7	15.7	1.8	2.0	3.0	2.0	12.6	11.9
6	97.7	92.5	92.5	84.1	68.4	67.6	70.6	70.6	35.0	31.5	63.2	60.1	18.1	16.7	3.9	1.2	5.1	1.6	12.5	4.4
7	98.4	97.0	95.0	93.0	68.7	68.7	70.9	71.4	25.8	25.0	55.4	55.9	15.6	15.3	0.8	1.3	1.1	1.7	2.6	4.0
8	99.0	100.5	95.4	96.7	68.1	69.4	68.9	70.4	27.1	27.4	48.2	48.3	13.0	13.3	0.4	0.3	0.8	0.7	4.3	3.9
9	98.6	99.9	95.4	97.2	67.9	70.5	69.2	71.3	27.1	25.5	63.8	62.4	18.1	17.3	0.5	0.6	0.8	0.8	2.7	3.0
12	98.4	98.5	95.1	88.6	67.1	67.6	68.8	69.0	13.0	11.5	46.4	50.4	9.3	9.3	2.5	1.5	3.4	2.3	11.1	8.3
13	98.3	100.4	95.0	96.6	68.1	70.2	69.8	71.5	17.7	19.9	36.7	39.5	11.1	12.2	4.0	4.3	5.7	6.1	23.0	24.4
15	98.7	99.0	95.3	96.2	67.2	67.6	68.7	69.4	19.7	19.7	34.9	34.5	11.8	11.8	-	-	-	-	-	-
16	97.7	97.7	91.0	91.7	69.4	69.2	73.4	73.2	5.4	5.6	16.1	17.2	4.2	4.5	-	-	-	-	-	-
17	97.6	97.2	94.2	94.2	69.9	68.3	70.8	69.0	32.5	32.0	57.8	57.0	16.9	16.6	0	0	0	0	0	0
21	97.7	99.1	95.2	95.2	67.1	68.4	67.8	69.1	17.8	19.1	38.4	42.0	8.8	9.5	0	0	0	0	0	0
22	98.2	98.1	95.3	95.7	68.8	68.7	71.2	71.3	26.8	26.2	48.6	47.9	13.0	12.8	3.0	2.4	3.6	2.8	6.0	4.6

Patient	Mean Esophagus Dose [Gy]		Esophagus D_{1ccm} [Gy]		Esophagus $V_{60Gy}[cm^3]$		Spinal cord D_{1ccm} [Gy]		Spinal cord D_{max} [Gy]		Brachial Plexus (right) D_{max} [Gy]		Brachial Plexus (left) D_{max} [Gy]		Trachea D_{1ccm} [Gy]		Main Bronchus (right) D_{1ccm} [Gy]		Main Bronchus (left) D_{1ccm} [Gy]	
	critical: $MED < 34Gy$		critical: $D_{1ccm} < 68Gy$		desired: $V_{60Gy} < 15cm^3$ desired: $V_{60Gy} < 5cm^3$		critical: $D_{1ccm} < 50Gy$		critical: $D_{max} < 52Gy$		desired: $D_{max} < 60Gy$ critical: $D_{max} < 66Gy$				desired: $D_{1ccm} < 68Gy$ critical: $D_{1ccm} < 74Gy$					
	CT1	CT2	CT1	CT2	CT1	CT2	CT1	CT2	CT1	CT2	CT1	CT2	CT1	CT2	CT1	CT2	CT1	CT2	CT1	CT2
1	19.0	22.0	63.8	64.5	2.1	2.1	17.8	18.2	20.8	21.3	-	-	54.5	61.3	64.5	66.5	25.2	32.5	57.0	63.8
2	21.6	17.5	64.1	55.7	3.1	0.4	20.2	19.1	21.9	20.8	-	-	-	-	42.5	54.8	35.4	34.4	66.0	64.7
3	29.4	29.1	64.9	64.4	4.6	3.5	27.5	28.9	42.5	47.7	14.5	46.6	-	-	66.9	68.1	67.3	67.7	66.3	66.2
4	15.0	15.6	58.0	57.4	0.6	0.5	17.3	17.1	19.6	19.3	-	-	-	-	63.9	64.0	66.0	66.2	51.7	51.8
5	19.9	20.6	66.4	67.0	4.4	4.8	21.8	21.5	35.4	35.2	-	-	-	-	15.9	20.0	65.5	66.6	65.9	66.3
6	27.7	28.6	64.9	63.9	2.9	3.7	23.9	24.4	29.0	32.4	60.4	60.3	-	-	66.6	66.4	66.5	66.4	65.3	65.5
7	19.5	19.1	66.2	65.7	4.7	4.3	25.3	22.3	40.3	33.3	-	-	-	-	66.7	66.1	66.2	65.2	57.9	55.0
8	24.7	24.9	65.0	65.0	3.4	3.3	19.6	19.1	30.3	28.6	-	-	-	-	66.3	67.7	65.6	67.1	-	-
9	18.1	18.4	37.9	38.7	0	0	18.6	18.8	20.8	21.5	-	-	-	-	-	-	-	-	-	-
12	16.5	16.9	45.4	45.5	0	0	15.8	18.3	21.8	29.8	-	-	-	-	-	-	-	-	-	-
13	15.1	15.2	58.0	59.5	0.7	0.9	16.7	16.6	23.2	23.7	-	-	-	-	0.7	0.5	1.8	1.2	1.5	1.3
15	9.4	10.4	14.6	14.8	0	0	15.8	16.7	18.3	19.1	50.5	50.8	-	-	-	-	-	-	-	-
16	13.0	12.8	48.9	43.6	0	0	18.9	19.0	32.0	33.0	64.5	64.4	-	-	48.6	49.0	-	-	-	-
17	17.4	17.4	59.1	59.3	0.7	0.8	22.9	23.4	35.5	45.2	-	-	-	-	-	-	-	-	-	-
21	9.1	9.7	23.2	25.0	0	0	14.7	15.2	16.5	17.3	-	-	-	-	60.4	63.1	-	-	-	-
22	16.6	17.1	61.2	61.1	1.4	1.4	15.5	15.3	20.8	19.6	-	-	-	-	-	-	-	-	-	-

Table 6.6: Dose to the 98% of the ICTVu, as planned using IMPT technique and the initial CT image set (CT 1), compared to the dose that the original plan would have delivered halfway through the treatment, based on the control CT (CT 2). The values are compared to the critical and desired clinical goals, where those exceeding the critical goal are colored red. The values are compared to the critical clinical goal. Values that do not reach the goal are colored red.

Patient	ICTVu $D_{98\%}$ [Gy]	
	critical: $D_{98\%} > 62.7Gy$	
	CT1	CT2
1	64.4	63.1
2	64.6	64.6
3	64.3	63.1
4	65.0	64.6
5	64.1	63.6
6	64.3	47.9
7	64.5	63.2
8	64.6	64.4
9	64.6	62.7
12	64.6	61.0
13	64.7	63.1
15	64.5	64.3
16	64.5	64.5
17	64.8	64.7
21	64.6	63.6
22	64.4	63.9

Table 6.7: The clinical goals for the IMPT treatment plans. The values are achieved based on the initial CT image set (CT 1), compared to the values the original plan would have delivered halfway through the treatment, based on the control CT (CT 2). The values are compared to the critical and desired clinical goals. Values that either exceed or do not reach the desired goals are colored orange and those that do not meet the critical goals are colored red. The table includes the goals for ICTVu from Table 6.6, but in [%] of the prescribed dose (66 Gy). Missing values mean that in the particular cases the organ at risk was not delineated on the CT, since the tumor is far away from it, and therefore monitoring dose to the OAR is not relevant.

Patient	ICTVu $D_{98\%}$ [% of 66Gy]		$Max.D_{2ccm}$		D_{max} [Gy]		Lungs-IGTV V_{20Gy} [%]		Lungs-IGTV V_{5Gy} [%]		Mean Lung Dose [Gy]		Heart V_{50Gy} [%]		Heart V_{45Gy} [%]		Heart V_{30Gy} [%]		Mean Esophagus Dose [Gy]	
	critical: $D_{98\%} > 95\%$		critical: $D_{2ccm} < 69,96Gy$		desired: $Pointmax < 71,30Gy$		critical: $V_{20Gy} < 35\%$		desired: $V_{5Gy} < 65\%$		critical: $MLD < 20Gy$		desired: $V_{50Gy} < 20\%$		desired: $V_{45Gy} < 25\%$		desired: $V_{30Gy} < 30\%$		critical: $MED < 34Gy$	
	CT1	CT2	CT1	CT2	CT1	CT2	CT1	CT2	CT1	CT2	CT1	CT2	CT1	CT2	CT1	CT2	CT1	CT2	CT1	CT2
1	97.5	95.6	68.6	68.6	70.1	70.6	12.1	12.5	18.3	20.1	6.8	7.0	0.7	0.8	0.9	1.0	1.8	2.1	11.3	13.9
2	97.9	97.8	68.4	68.7	70.1	70.3	19.5	17.8	23.9	22.3	11.2	10.8	13.9	12.5	16.0	13.8	22.8	18.7	20.5	14.7
3	97.4	95.6	68.7	69.1	70.8	70.8	13.8	15.4	40.7	41.5	9.5	10.4	0.3	0.5	0.5	0.7	1.1	1.5	12.0	20.0
4	98.5	97.9	69.1	69.0	71.0	70.9	14.8	13.2	30.8	28.5	8.5	7.8	1.0	0.5	1.4	0.8	3.1	2.2	11.3	11.1
5	97.1	96.4	69.1	69.8	70.8	72.3	11.6	11.9	37.3	38.3	8.8	9.0	1.6	1.4	2.3	2.0	5.8	5.0	19.1	19.9
6	97.5	72.6	68.6	72.0	71.1	76.3	23.2	17.7	37.9	17.7	11.6	9.4	3.0	0.9	3.8	1.2	6.7	2.3	23.5	24.7
7	97.8	95.7	69.1	68.8	71.3	71.9	20.6	19.5	39.4	38.8	12.7	12.0	0.6	0.9	0.9	1.2	1.7	2.2	17.0	16.9
8	97.9	97.6	67.9	68.1	69.4	70.0	16.0	18.7	32.1	33.6	8.5	9.1	0.2	0.2	0.4	0.3	1.4	1.1	26.7	26.7
9	97.9	95.0	68.5	68.7	69.7	70.7	26.1	24.5	35.5	31.7	13.2	12.4	0.3	0.3	0.5	0.5	1.4	1.3	8.0	7.8
12	97.8	92.5	68.0	68.3	70.3	74.0	11.1	9.2	24.7	24.2	6.5	5.9	2.2	0.8	2.6	1.1	4.4	2.4	12.6	11.7
13	98.0	95.6	67.5	67.8	68.9	69.2	15.3	16.8	24.9	26.6	8.4	8.9	2.4	2.9	3.1	3.7	6.1	7.9	11.6	12.1
15	97.7	97.4	68.2	68.0	70.5	70.0	11.1	11.1	14.5	14.4	6.3	6.3	-	-	-	-	-	-	0.9	0.9
16	97.7	97.7	68.2	68.3	70.0	69.5	4.5	4.6	5.9	6.2	2.7	2.8	-	-	-	-	-	-	5.1	5.2
17	98.1	98.0	68.7	69.5	70.4	71.6	22.1	21.5	43.3	42.9	12.7	12.4	0	0	0	0	0	0	13.2	13.5
21	97.9	96.4	68.4	68.2	70.2	70.4	13.2	14.4	17.5	18.8	6.4	7.2	0	0	0	0	0	0	0.1	0.1
22	97.6	96.7	68.3	68.6	70.6	70.6	19.9	18.9	34.7	33.8	9.0	8.7	2.2	1.7	2.7	2.1	4.2	3.3	14.4	15.3

Patient	Esophagus D_{1ccm} [Gy]		Esophagus $V_{60Gy}[cm^3]$		Spinal cord D_{1ccm} [Gy]		Spinal cord D_{max} [Gy]		Brachial Plexus (right) D_{max} [Gy]		Brachial Plexus (left) D_{max} [Gy]		Trachea D_{1ccm} [Gy]		Main Bronchus (right) D_{1ccm} [Gy]		Main Bronchus (left) D_{1ccm} [Gy]	
	critical: $D_{1ccm} < 68Gy$		desired: $V_{60Gy} < 15cm^3$		critical: $D_{1ccm} < 50Gy$		critical: $D_{max} < 52Gy$		desired: $D_{max} < 60Gy$				desired: $D_{1ccm} < 68Gy$					
			desired: $V_{60Gy} < 5cm^3$						critical: $D_{max} < 66Gy$				critical: $D_{1ccm} < 74Gy$					
	CT1	CT2	CT1	CT2	CT1	CT2	CT1	CT2	CT1	CT2	CT1	CT2	CT1	CT2	CT1	CT2	CT1	CT2
1	62.0	60.5	1.5	1.2	12.8	12.8	17.1	18.1	-	-	58.7	59.4	67.3	66.7	4.3	10.6	43.8	53.5
2	65.9	65.0	5.1	2.2	13.6	14.0	15.6	17.1	-	-	-	-	46.2	56.6	31.0	24.9	66.2	66.5
3	65.2	65.1	2.3	2.4	15.4	16.8	34.0	40.1	4.3	23.3	-	-	67.1	67.4	67.0	66.9	66.8	66.5
4	48.7	44.6	0.3	0.2	0.2	0.2	0.3	0.4	-	-	-	-	66.1	66.2	66.6	66.7	47.4	44.4
5	66.5	67.2	4.9	5.4	16.2	16.2	34.8	34.8	-	-	-	-	27.2	32.4	66.2	65.9	66.8	66.5
6	64.9	64.9	2.3	2.9	18.1	18.5	23.9	37.7	61.0	60.3	-	-	66.9	66.7	66.6	66.8	65.9	66.0
7	67.0	66.7	4.9	4.8	14.1	11.0	32.8	21.0	-	-	-	-	67.5	67.4	67.1	66.5	59.3	53.0
8	65.0	64.4	3.3	2.8	18.2	18.4	42.0	37.4	-	-	-	-	66.9	66.9	66.2	66.4	-	-
9	22.4	22.4	0	0	17.8	17.7	29.4	29.6	-	-	-	-	-	-	-	-	-	-
12	37.6	36.9	0	0	9.5	12.3	21.7	31.3	-	-	-	-	-	-	-	-	-	-
13	53.1	53.8	0.1	0.1	11.3	10.8	29.8	33.2	-	-	-	-	0.1	0	0.3	0.1	0.2	0.2
15	1.2	1.3	0	0	0.1	0.1	0.1	0.2	53.3	53.5	-	-	-	-	-	-	-	-
16	32.8	32.5	0	0	12.5	13.4	37.3	40.2	65.7	66.8	-	-	41.7	36.8	-	-	-	-
17	53.8	55.1	0	0.1	14.8	25.7	25.9	40.6	-	-	-	-	-	-	-	-	-	-
21	0.5	0.6	0	0	0	0	0.1	0.1	-	-	-	-	53.6	56.9	-	-	-	-
22	58.9	60.0	0.9	1.0	0.3	0.3	0.4	0.5	-	-	-	-	-	-	-	-	-	-

Table 6.8: Calculated difference between CT 2 and CT 1 results for two sets of treatment plans, the VMAT set and the first IMPT set (optimized with 4.5% density uncertainty). Cells filled with green indicate a positive change from CT 1 to CT 2. It means either increased dose coverage or a decrease in maximum dose/dose to OARs. Cells filled with red indicate a negative change and grey indicates no significant change.

Patient	ICTVu $D_{98\%}$ [Gy]		Max. D_{2ccm}		Max. Dose [Gy]		Lungs-IGTV V_{20Gy} [%]		Lungs-IGTV V_{5Gy} [%]		Mean Lung Dose [Gy]		Heart V_{50Gy} [%]		Heart V_{45Gy} [%]		Heart V_{30Gy} [%]	
	VMAT	IMPT	VMAT	IMPT	VMAT	IMPT	VMAT	IMPT	VMAT	IMPT	VMAT	IMPT	VMAT	IMPT	VMAT	IMPT	VMAT	IMPT
1	1.7	-1.9	1.6	0.0	1.2	0.5	0.6	0.3	1.7	1.9	0.4	0.3	0.1	0.0	0.1	0.1	0.4	0.3
2	-2.5	-0.1	0.7	0.3	-0.1	0.2	-1.6	-1.7	1.8	-1.6	-0.1	-0.4	0.4	-1.5	0.4	-2.1	-0.8	-4.1
3	0.0	-1.8	0.8	0.4	0.7	0.0	1.7	1.6	0.5	0.9	1.2	1.0	0.2	0.2	0.0	0.3	-1.7	0.4
4	0.0	-0.6	0.5	-0.1	0.7	-0.1	-1.8	-1.6	-3.5	-2.3	-0.9	-0.7	-0.1	-0.4	-0.1	-0.6	-0.4	-1.0
5	-0.3	-0.8	0.3	0.7	-0.3	1.5	0.1	0.3	0.2	1.1	0.0	0.2	0.1	-0.2	-1.0	-0.3	-0.7	-0.8
6	-5.2	-24.9	-0.8	3.4	0.0	5.2	-3.5	-5.5	-3.2	-20.2	-1.4	-2.2	-2.7	-2.1	-3.6	-2.6	-8.1	-4.4
7	-1.4	-2.1	0.0	-0.3	0.5	0.6	-0.8	-1.1	0.5	-0.5	-0.2	-0.7	0.5	0.3	0.6	0.4	1.4	0.5
8	1.5	-0.3	1.4	0.2	1.5	0.6	0.3	2.7	0.1	1.5	0.3	0.7	-0.1	0.0	-0.1	0.0	-0.5	-0.2
9	1.3	-2.9	2.6	0.2	2.1	1.1	-1.6	-1.6	-1.4	-3.8	-0.8	-0.9	0.1	0.0	0.0	0.0	0.3	-0.1
12	0.1	-5.4	0.5	0.4	0.1	3.8	-1.5	-1.9	4.0	-0.5	0.0	-0.6	-1.0	-1.4	-1.2	-1.5	-2.8	-2.0
13	2.1	-2.4	2.1	0.4	1.8	0.3	2.2	1.5	2.8	1.7	1.0	0.6	0.3	0.6	0.4	0.7	1.5	1.8
15	0.2	-0.3	0.4	-0.2	0.7	-0.5	0.0	0.0	-0.3	-0.1	0.0	0.0	-	-	-	-	-	-
16	-0.1	0.0	-0.2	0.2	-0.2	-0.4	0.2	0.2	1.1	0.2	0.4	0.1	-	-	-	-	-	-
17	-0.4	-0.1	-1.7	0.8	-1.8	1.3	-0.4	-0.6	-0.8	-0.5	-0.3	-0.3	0.0	0.0	0.0	0.0	0.0	0.0
21	1.4	-1.6	1.3	-0.2	1.3	0.1	1.3	1.2	3.6	1.3	0.7	0.8	0.0	0.0	0.0	0.0	0.0	0.0
22	-0.2	-0.8	0.0	0.4	0.1	0.0	-0.5	-0.9	-0.7	-0.9	-0.2	-0.3	-0.6	-0.4	-0.7	-0.6	-1.4	-0.9

Patient	Mean Esophagus Dose [Gy]		Esophagus D_{1ccm} [Gy]		Esophagus V_{60Gy} Gy [cm^3]		Spinal canal D_{1ccm} [Gy]		Spinal canal D_{max} [Gy]		Brachial Plexus (right) D_{max} [Gy]		Brachial Plexus (left) D_{max} [Gy]		Trachea D_{1ccm} [Gy]		Main Bronchus (right) D_{1ccm} [Gy]		Main Bronchus (left) D_{1ccm} [Gy]	
	VMAT	IMPT	VMAT	IMPT	VMAT	IMPT	VMAT	IMPT	VMAT	IMPT	VMAT	IMPT	VMAT	IMPT	VMAT	IMPT	VMAT	IMPT	VMAT	IMPT
1	3.0	2.6	0.6	-1.5	0.0	-0.4	0.3	0.0	0.4	1.1	-	-	6.8	0.7	2.0	-0.6	7.4	6.4	6.7	9.7
2	-4.2	-5.8	-8.5	-1.0	-2.7	-2.9	-1.2	0.4	-1.2	1.5	-	-	-	-	12.4	10.4	-1.0	-6.1	-1.4	0.3
3	-0.4	0.1	-0.4	-0.2	-1.1	0.1	1.5	1.4	5.2	6.2	32.1	19.1	-	-	1.2	0.3	0.4	-0.1	-0.1	-0.2
4	0.6	-0.2	-0.5	-4.1	-0.1	-0.1	-0.1	0.0	-0.3	0.0	-	-	-	-	0.1	0.0	0.2	0.1	0.0	-3.0
5	0.6	0.8	0.6	0.7	0.5	0.6	-0.3	0.0	-0.2	0.0	-	-	-	-	4.2	5.3	1.1	-0.4	0.5	-0.3
6	1.0	1.2	-1.0	0.0	0.7	0.7	0.5	0.4	3.4	13.8	-0.2	-0.7	-	-	-0.3	-0.2	-0.2	0.2	0.3	0.1
7	-0.4	-0.1	-0.5	-0.3	-0.4	-0.2	-3.1	-3.1	-7.0	-11.8	-	-	-	-	-0.6	-0.1	-1.1	-0.6	-2.9	-6.3
8	0.1	0.0	0.0	-0.6	-0.2	-0.5	-0.5	0.2	-1.7	-4.6	-	-	-	-	1.4	-0.1	1.5	0.2	-	-
9	0.3	-0.2	0.8	0.1	0.0	0.0	0.2	-0.1	0.8	0.2	-	-	-	-	-	-	-	-	-	-
12	0.4	-0.9	0.1	-0.7	0.0	0.0	2.5	2.8	8.0	9.7	-	-	-	-	-	-	-	-	-	-
13	0.1	0.5	1.5	0.8	0.2	0.0	-0.2	-0.5	0.6	3.5	-	-	-	-	-0.3	0.0	-0.6	-0.2	-0.1	0.0
15	0.9	-0.1	0.2	0.1	0.0	0.0	0.9	0.1	0.8	0.1	0.4	0.2	-	-	-	-	-	-	-	-
16	-0.1	0.2	-5.3	-0.3	0.0	0.0	0.1	1.0	1.0	3.0	-0.2	1.1	-	-	0.4	-4.9	-	-	-	-
17	0.1	0.3	0.2	1.3	0.1	0.1	0.4	10.9	9.7	14.7	-	-	-	-	-	-	-	-	-	-
21	0.6	0.0	1.7	0.1	0.0	0.0	0.5	0.0	0.8	0.0	-	-	-	-	-	-	-	-	-	-
22	0.4	0.9	-0.1	1.1	0.0	0.1	-0.2	0.0	-1.1	0.1	-	-	-	-	-	-	-	-	-	-

Table 6.9: The clinical goals for the IMPT treatment plans optimized using 4.5% and 3% density uncertainty. The values are achieved based on the initial CT image set (CT 1), compared to the values the original plan would have delivered halfway through the treatment, based on the control CT (CT 2). The values are compared to the critical and desired clinical goals. Values that either exceed or do not reach the desired goals are colored orange and those that do not meet the critical goals are colored red. Missing values mean that in the particular cases the particular organ at risk was not delineated on the CT, since the tumor is far away from it, and therefore monitoring dose to the OAR is not relevant.

Patient	Density uncertainty [%]	ICTVu $D_{98\%}$ [Gy]		ICTVu $D_{98\%}$ [% of 66Gy]		$Max.D_{2ccm}$		D_{max} [Gy]		Lungs-IGTV V_{20Gy} [%]		Lungs-IGTV V_{5Gy} [%]		Mean Lung Dose [Gy]		Heart V_{50Gy} [%]		Heart V_{45Gy} [%]		Heart V_{30Gy} [%]	
		critical: $D_{98\%} > 62.7Gy$		critical: $D_{98\%} > 95\%$		critical: $D_{2ccm} < 69,96Gy$		desired: $Pointmax < 71,30Gy$		critical: $V_{20Gy} < 35\%$		desired: $V_{5Gy} < 65\%$		critical: $MLD < 20Gy$		desired: $V_{50Gy} < 20\%$		desired: $V_{45Gy} < 25\%$		desired: $V_{30Gy} < 30\%$	
		CT1	CT2	CT1	CT2	CT1	CT2	CT1	CT2	CT1	CT2	CT1	CT2	CT1	CT2	CT1	CT2	CT1	CT2	CT1	CT2
1	4.50	64.4	63.1	97.5	95.6	68.6	68.6	70.1	70.6	12.1	12.5	18.3	20.1	6.8	7.0	0.7	0.8	0.9	1.0	1.8	2.1
	3.00	64.8	62.4	98.1	94.5	67.8	68.3	70.1	70.1	11.9	12.3	17.5	19.4	6.6	6.9	0.6	0.7	0.8	0.9	1.6	1.9
2	4.50	64.6	64.6	97.9	97.8	68.4	68.7	70.1	70.3	19.5	17.8	23.9	22.3	11.2	10.8	13.9	12.5	16.0	13.8	22.8	18.7
	3.00	64.8	64.8	98.2	98.2	68.4	68.5	70.2	69.9	19.5	17.8	23.8	22.2	11.2	10.8	13.0	11.2	14.7	12.4	20.6	16.8
3	4.50	64.3	63.1	97.4	95.6	68.7	69.1	70.8	70.8	13.8	15.4	40.7	41.5	9.5	10.4	0.3	0.5	0.5	0.7	1.1	1.5
	3.00	64.5	63.7	97.8	96.5	68.4	69.4	70.0	72.3	13.3	15.0	41.4	42.5	9.5	10.6	0.3	0.6	0.5	0.8	1.2	1.5
4	4.50	65.0	64.6	98.5	97.9	69.1	69.0	71.0	70.9	14.8	13.2	30.8	28.5	8.5	7.8	1.0	0.5	1.4	0.8	3.1	2.2
	3.00	64.7	64.7	98.0	98.0	69.0	68.9	71.2	71.0	14.8	13.1	30.8	28.5	8.6	7.9	1.1	0.6	1.5	0.9	3.3	2.3
5	4.50	64.1	63.6	97.1	96.4	69.1	69.8	70.8	72.3	11.6	11.9	37.3	38.3	8.8	9.0	1.6	1.4	2.3	2.0	5.8	5.0
	3.00	64.6	63.3	97.9	96.0	68.3	69.4	69.9	71.9	11.5	11.8	37.1	38.2	8.7	8.9	1.4	1.2	2.0	1.8	5.2	4.5
6	4.50	64.3	47.9	97.5	72.6	68.6	72.0	71.1	76.3	23.2	17.7	37.9	17.7	11.6	9.4	3.0	0.9	3.8	1.2	6.7	2.3
	3.00	64.5	47.8	97.7	72.4	68.2	71.8	69.7	75.7	23.2	17.8	38.2	33.0	12.0	9.7	3.3	1.0	4.1	1.3	6.7	2.5
7	4.50	64.5	63.2	97.8	95.7	69.1	68.8	71.3	71.9	20.6	19.5	39.4	38.8	12.7	12.0	0.6	0.9	0.9	1.2	1.7	2.2
	3.00	64.9	60.5	98.4	91.7	69.0	68.7	70.4	70.1	20.0	18.6	38.7	38.1	12.3	11.3	0.6	0.8	0.8	1.1	1.6	2.0
8	4.50	64.6	64.4	97.9	97.6	67.9	68.1	69.4	70.0	16.0	18.7	32.1	33.6	8.5	9.1	0.2	0.2	0.4	0.3	1.4	1.1
	3.00	64.9	64.2	98.4	97.3	67.3	67.3	68.7	68.6	12.4	15.7	31.0	32.6	7.6	8.4	0.1	0	0.2	0.2	0.9	0.8
9	4.50	64.6	62.7	97.9	95.0	68.5	68.7	69.7	70.7	26.1	24.5	35.5	31.7	13.2	12.4	0.3	0.3	0.5	0.5	1.4	1.3
	3.00	64.9	63.3	98.4	95.8	68.1	68.1	69.8	69.2	24.7	23.0	34.0	32.1	14.1	13.3	0.3	0.2	0.4	0.4	1.2	1.1
12	4.50	64.6	61.0	97.8	92.5	68.0	68.3	70.3	74.0	11.1	9.2	24.7	24.2	6.5	5.9	2.2	0.8	2.6	1.1	4.4	2.4
	3.00	65.1	55.9	98.6	84.6	67.3	67.0	68.8	68.4	9.9	8.8	23.5	23.5	6.1	5.7	2.0	0.6	2.4	0.9	4.1	2.2
13	4.50	64.7	63.1	98.0	95.6	67.5	67.8	68.9	69.2	15.3	16.8	24.9	26.6	8.4	8.9	2.4	2.9	3.1	3.7	6.1	7.9
	3.00	64.6	62.5	97.8	94.7	68.1	67.6	69.6	69.0	14.9	16.8	24.3	26.3	8.1	8.8	2.3	2.8	2.9	3.6	5.7	7.4
15	4.50	64.5	64.3	97.7	97.4	68.2	68.0	70.5	70.0	11.1	11.1	14.5	14.4	6.3	6.3	-	-	-	-	-	-
	3.00	64.7	64.3	98.0	97.5	68.5	68.3	71.0	69.7	11.1	11.1	14.4	14.4	6.3	6.3	-	-	-	-	-	-
16	4.50	64.3	64.4	97.4	97.5	68.2	68.5	71.1	70.8	4.5	4.6	5.9	6.2	2.7	2.8	-	-	-	-	-	-
	3.00	64.6	64.4	97.9	97.5	67.8	68.0	68.8	71.3	4.5	4.7	5.9	6.2	2.7	2.8	-	-	-	-	-	-
17	4.50	64.8	64.7	98.1	98.0	68.7	69.5	70.4	71.6	22.1	21.5	43.3	42.9	12.7	12.4	0	0	0	0	0	0
	3.00	64.8	64.6	98.2	97.9	68.8	69.3	70.6	70.9	21.7	20.9	43.2	42.7	12.6	12.2	0	0	0	0	0	0
21	4.50	64.6	63.6	97.9	96.4	68.4	68.2	70.2	70.4	13.2	14.4	17.5	18.8	6.4	7.2	0	0	0	0	0	0
	3.00	64.6	63.5	97.9	96.2	68.3	68.4	70.4	70.9	13.1	14.3	17.4	18.8	6.3	7.1	0	0	0	0	0	0
22	4.50	64.4	63.9	97.6	96.7	68.3	68.6	70.6	70.6	19.9	18.9	34.7	33.8	9.0	8.7	2.2	1.7	2.7	2.1	4.2	3.3
	3.00	64.4	63.9	97.6	96.8	68.4	68.8	71.0	70.5	16.6	15.5	34.7	33.8	8.9	8.5	2.3	1.8	2.7	2.2	4.2	3.3

Table 6.10: Part two of the table 6.9

Patient	Density uncertainty [%]	Mean Esophagus Dose [Gy]		Esophagus D_{1ccm} [Gy]		Esophagus $V_{60Gy}[cm^3]$		Spinal cord D_{1ccm} [Gy]		Spinal cord D_{max} [Gy]		Brachial Plexus (right) D_{max} [Gy]		Brachial Plexus (left) D_{max} [Gy]		Trachea D_{1ccm} [Gy]		Main Bronchus (right) D_{1ccm} [Gy]		Main Bronchus (left) D_{1ccm} [Gy]	
		critical: $MED < 34Gy$		critical: $D_{1ccm} < 68Gy$		desired: $V_{60Gy} < 15cm^3$		critical: $D_{1ccm} < 50Gy$		critical: $D_{max} < 52Gy$		desired: $D_{max} < 60Gy$				desired: $D_{1ccm} < 68Gy$					
						desired: $V_{60Gy} < 5cm^3$						critical: $D_{max} < 66Gy$				critical: $D_{1ccm} < 74Gy$					
		CT1	CT2	CT1	CT2	CT1	CT2	CT1	CT2	CT1	CT2	CT1	CT2	CT1	CT2	CT1	CT2	CT1	CT2	CT1	CT2
1	4.50	11.3	13.9	62.0	60.5	1.5	1.2	12.8	12.8	17.1	18.1	-	-	58.7	59.4	67.3	66.7	4.3	10.6	43.8	53.5
	3.00	11.0	13.7	61.5	61.1	1.4	1.2	12.6	12.6	15.4	15.9	-	-	59.2	59.9	66.7	65.5	3.5	11.1	42.8	52.7
2	4.50	20.5	14.7	65.9	65.0	5.1	2.2	13.6	14.0	15.6	17.1	-	-	-	-	46.2	56.6	31.0	24.9	66.2	66.5
	3.00	19.1	13.5	65.5	63.3	4.7	1.7	12.3	12.7	13.3	14.9	-	-	-	-	43.6	57.2	28.4	20.9	65.8	66.6
3	4.50	20.0	20.0	65.2	65.1	2.3	2.4	15.4	16.8	34.0	40.1	4.3	23.3	-	-	67.1	67.4	67.0	66.9	66.8	66.5
	3.00	20.0	20.0	64.3	64.4	2.0	2.1	15.2	16.1	34.2	38.9	3.4	23.7	-	-	67.4	69.1	66.8	66.7	66.5	66.5
4	4.50	11.3	11.1	48.7	44.6	0.3	0.2	0.2	0.2	0.3	0.4	-	-	-	-	66.1	66.2	66.6	66.7	47.4	44.4
	3.00	11.2	10.9	48.6	43.7	0.2	0.1	0.2	0.2	0.3	0.4	-	-	-	-	66.3	66.3	66.5	66.6	45.0	42.1
5	4.50	19.1	19.9	66.5	67.2	4.9	5.4	16.2	16.2	34.8	34.8	-	-	-	-	27.2	32.4	66.2	65.9	66.8	66.5
	3.00	18.8	19.7	66.1	66.7	4.7	5.2	15.6	15.5	32.9	33.2	-	-	-	-	26.1	32.0	65.5	65.2	66.4	66.2
6	4.50	23.5	24.7	64.9	64.9	2.3	2.9	18.1	18.5	23.9	37.7	61.0	60.3	-	-	66.9	66.7	66.6	66.8	65.9	66.0
	3.00	27.6	28.3	64.9	64.8	2.8	3.4	19.1	20.4	27.4	38.5	64.7	63.6	-	-	66.8	66.4	66.2	66.2	65.6	65.5
7	4.50	17.0	16.9	67.0	66.7	4.9	4.8	14.1	11.0	32.8	21.0	-	-	-	-	67.5	67.4	67.1	66.5	59.3	53.0
	3.00	16.8	16.3	66.8	66.1	4.9	4.4	13.5	10.4	32.5	20.7	-	-	-	-	67.1	67.1	66.7	66.6	56.1	48.3
8	4.50	26.7	26.7	65.0	64.4	3.3	2.8	18.2	18.4	42.0	37.4	-	-	-	-	66.9	66.9	66.2	66.4	-	-
	3.00	25.6	26.2	64.2	63.5	3.1	2.7	15.7	16.7	37.4	38.2	-	-	-	-	66.6	66.7	66.4	65.7	-	-
9	4.50	8.0	7.8	22.4	22.4	0	0	17.8	17.7	29.4	29.6	-	-	-	-	-	-	-	-	-	-
	3.00	7.5	7.4	18.6	18.8	0	0	14.9	15.0	24.5	26.4	-	-	-	-	-	-	-	-	-	-
12	4.50	12.6	11.7	37.6	36.9	0	0	9.5	12.3	21.7	31.3	-	-	-	-	-	-	-	-	-	-
	3.00	10.5	9.8	33.6	31.6	0	0	7.9	10.4	21.3	26.8	-	-	-	-	-	-	-	-	-	-
13	4.50	11.6	12.1	53.1	53.8	0.1	0.1	11.3	10.8	29.8	33.2	-	-	-	-	0.1	0	0.3	0.1	0.2	0.2
	3.00	10.8	11.5	53.0	53.6	0.2	0.1	10.0	9.8	30.1	32.1	-	-	-	-	0.1	0	0.3	0.1	0.2	0.2
15	4.50	0.9	0.9	1.2	1.3	0	0	0.1	0.1	0.1	0.2	53.3	53.5	-	-	-	-	-	-	-	-
	3.00	1.0	0.9	1.2	1.3	0	0	0.1	0.1	0.1	0.2	55.1	54.7	-	-	-	-	-	-	-	-
16	4.50	5.1	5.2	32.7	32.6	0	0	11.8	12.5	35.8	38.0	62.4	67.7	-	-	42.0	37.0	-	-	-	-
	3.00	4.9	5.0	32.1	32.2	0	0	10.9	11.7	36.0	38.6	63.0	68.5	-	-	39.6	34.9	-	-	-	-
17	4.50	13.2	13.5	53.8	55.1	0	0.1	14.8	25.7	25.9	40.6	-	-	-	-	-	-	-	-	-	-
	3.00	12.8	13.2	53.8	55.2	0	0.1	14.5	24.9	25.1	38.7	-	-	-	-	-	-	-	-	-	-
21	4.50	0.1	0.1	0.5	0.6	0	0	0	0	0.1	0.1	-	-	-	-	53.6	56.9	-	-	-	-
	3.00	0.1	0.1	0.5	0.6	0	0	0	0	0.1	0.1	-	-	-	-	52.4	56.2	-	-	-	-
22	4.50	14.4	15.3	58.9	60.0	0.9	1.0	0.3	0.3	0.4	0.5	-	-	-	-	-	-	-	-	-	-
	3.00	14.6	15.5	59.6	60.3	0.9	1.1	0.3	0.3	0.7	0.9	-	-	-	-	-	-	-	-	-	-

Table 6.11: Dose coverage to the primary tumor and affected lymph nodes (for the patients with an ICTVu consisting of multiple volumes). The coverage is compared to the clinical goal of critical importance, marking values lower than 95% with red color. There are two sets of IMPT plans, optimized with both 4.5% and 3% density uncertainty. Results from both sets are included here. For both VMAT and IMPT plans, the initial results come from optimization based on the planning CT (CT 1). Those results are compared to the recalculation of the dose distribution on the control CT (CT 2).

Patient	Primary Tumor (T) / Node (N)	VMAT		Density uncertainty [%]	IMPT	
		ICTVu $D_{98\%}$ [% of 66Gy]			ICTVu $D_{98\%}$ [% of 66Gy]	
		critical: $D_{98\%} > 95\%$ of 66 Gy			critical: $D_{98\%} > 95\%$ of 66 Gy	
		CT1	CT2		CT1	CT2
1	T	97,4	99,1	4,50	97,5	95,7
				3,00	98,1	94,4
	N1	97,6	99,6	4,50	97,9	97,6
				3,00	98,3	97,8
	N2	97,8	99,3	4,50	97,6	92,7
				3,00	97,9	92,8
	N3	97,0	99,0	4,50	97,9	97,3
				3,00	98,0	97,0
	N4	97,6	99,6	4,50	98,2	96,5
				3,00	98,1	96,9
	N5	98,0	99,9	4,50	98,0	97,1
				3,00	98,4	96,5
3	T	98,4	99,2	4,50	97,4	95,7
				3,00	97,8	96,6
	N1	98,6	97,1	4,50	97,4	94,0
				3,00	97,7	96,1
	N2	98,8	100,2	4,50	97,8	96,1
				3,00	98,5	97,5
5	T	98,1	97,8	4,50	97,1	96,2
				3,00	97,9	95,8
	N1	98,3	99,3	4,50	97,9	97,5
				3,00	98,1	97,9
6	T	97,8	92,3	4,50	97,5	70,6
				3,00	97,7	70,7
	N1	98,7	95,7	4,50	97,5	88,0

Continued on next page

Table 6.11: Dose coverage to the primary tumor and affected lymph nodes (for the patients with an ICTVu consisting of multiple volumes). The coverage is compared to the clinical goal of critical importance, marking values lower than 95% with red color. There are two sets of IMPT plans, optimized with both 4.5% and 3% density uncertainty. Results from both sets are included here. For both VMAT and IMPT plans, the initial results come from optimization based on the planning CT (CT 1). Those results are compared to the recalculation of the dose distribution on the control CT (CT 2). (Continued)

				3,00	98,3	85,2
	N2	99,3	92,4	4,50	97,6	83,8
				3,00	98,4	85,8
	N3	96,2	92,6	4,50	97,7	93,8
				3,00	98,4	95,1
	N4	98,5	93,7	4,50	97,6	90,3
				3,00	98,2	91,5
	N5	99,1	97,9	4,50	97,9	97,6
				3,00	98,3	98,3
8	T	99,2	100,4	4,50	98,0	97,2
				3,00	98,2	97,2
	N1	98,9	100,6	4,50	97,9	97,9
				3,00	98,6	97,4
9	T	98,6	99,9	4,50	97,9	95,0
				3,00	98,3	95,8
	N1	98,7	101,7	4,50	98,2	96,9
				3,00	98,6	96,9
17	T	97,6	97,3	4,50	98,1	98,0
				3,00	98,2	97,9
	N1	98,4	96,2	4,50	98,5	98,3
				3,00	98,5	97,6
22	T	98,2	98,0	4,50	97,5	96,7
				3,00	97,6	96,8
	N1	98,9	99,0	4,50	97,9	97,1
				3,00	98,3	97,3

Bibliography

[1] Editor Ugo Amaldi. 'A Facility for Tumour Therapy and Biomedical Research in South-Eastern Europe'. In: *CERN Yellow Reports: Monographs* CERN-2019-002.https://doi.org/10.23731/CYRM-2019-002 (2019).

[2] F. H. Attix. *Introduction to radiological physics and radiation dosimetry*. Wiley-VCH Verlag GmbH & Co. KGaA, 2004, pp. 124–159, 160. ISBN: 0-471-01146-0.

[3] Maria Moksnes Bjaanæs et al. 'Improved adaptive radiotherapy to adjust for anatomical alterations during curative treatment for locally advanced lung cancer'. In: *Physics and Imaging in Radiation Oncology* 18 (2021), pp. 51–54.

[4] Peter Bruce, Andrew Bruce and Peter Gedeck. *Practical Statistics for Data Scientists, 2nd Edition*. O'Reilly Media, Inc., 2020, p. 162. ISBN: 978-1-492-07294-2.

[5] Jerrold T. Bushberg et al. *The Essential Physics of Medical Imaging*. Fourth Edition. Wolters Kluwer, 2021, pp. 45, 63, 65–66. ISBN: 978-1975-1-0322-4.

[6] Micol De Simoni et al. 'FRED: a fast Monte Carlo code on GPU for quality control in Particle Therapy'. In: *Journal of Physics: Conference Series* 1548 (May 2020), p. 012020. DOI: 10.1088/1742-6596/1548/1/012020.

[7] Loïc Feuvret et al. 'Conformity index: A review'. In: *International Journal of Radiation Oncology*Biology*Physics* 64.2 (2006), pp. 333–342. ISSN: 0360-3016. DOI: https://doi.org/10.1016/j.ijrobp.2005.09.028. URL: https://www.sciencedirect.com/science/article/pii/S0360301605027197.

[8] Eric J. Hall and Amato J. Giaccia. *Radiobiology for the Radiologist*. Eighth Edition. Wolters Kluwer, 2019, pp. 353, 364–368, 448. ISBN: 9781496335418.

[9] Edward C. Halperin et al. *Perez and Brady's Principles and Practice of Radiation Oncology*. Sixth Edition. Lippincott Williams & Wilkins, 2013, p. 972. ISBN: 978-1-4511-1648-9.

[10] Lone Hoffmann et al. 'Adaptation is mandatory for intensity modulated proton therapy of advanced lung cancer to ensure target coverage'. In: *Radiotherapy and Oncology: journal of the European Society for Therapeutic Radiology and Oncology* 122.3 (2017), pp. 400–405. DOI: https://doi.org/10.1016/j.radonc.2016.12.018.

[11] ICRU. *ICRU Report 62: Prescribing, Recording, and Reporting Photon Beam Therapy (Supplement to ICRU Report 50)*. https://archive.org/details/icru-62-1. 1999.

[12] Michael C. Joiner and Albert van der Kogel. *Basic Clinical Radiobiology Fourth Edition*. CRC Press, 2009, p. 70. ISBN: 9780340929667.

[13] Faiz M. Khan. *The Physics of Radiation Therapy*. 4th Edition. Lippincott Williams & Wilkins, 2010, p. 199. ISBN: 978-0-7817-8856-4.

[14] Faiz M. Khan and John P. Gibbons. *Khan's The Physics of Radiation Therapy*. Fifth Edition. Lippincott Williams & Wilkins, 2014, pp. 42–48, 439, 538. ISBN: 978-1-4511-8245-3.

[15] John P. Kirkpatrick, Albert J. van der Kogel and Timothy E. Schultheiss. 'Radiation Dose–Volume Effects in the Spinal Cord'. In: *International Journal of Radiation Oncology*Biology*Physics* 76.3, Supplement (2010). Quantitative Analyses of Normal Tissue Effects in the Clinic, S42–S49. ISSN: 0360-3016. DOI: https://doi.org/10.1016/j.ijrobp.2009.04.095. URL: https://www.sciencedirect.com/science/article/pii/S0360301609032969.

[16] Feng-Ming Kong et al. 'Radiation dose effect in locally advanced non-small cell lung cancer'. In: *Journal of Thoracic Disease* 6.4 (2014), pp. 336–347.

[17] Martin Krzywinski and Naomi Altman. 'Visualizing samples with box plots'. In: *Nat Methods* 11 (2014), pp. 119–120. URL: https://doi.org/10.1038/nmeth.2813.

[18] Hans Paul van der Laan et al. 'Organ sparing potential and inter-fraction robustness of adaptive intensity modulated proton therapy for lung cancer'. In: *Acta Oncologica* 58.12 (2019). PMID: 31556764, pp. 1775–1782. DOI: 10.1080/0284186X.2019.1669818. eprint: https://doi.org/10.1080/0284186X.2019.1669818. URL: https://doi.org/10.1080/0284186X.2019.1669818.

[19] Sverre Levernes. *Nomenclature for volumes in radiotherapy. Technical document 14*. Norwegian. Østerås: Norwegian Radiation and Nuclear Safety Authority, 2019. URL: https://dsa.no/publikasjoner/_/attachment/inline/9d2a42a5-241e-4299-86cf-6b02a0abf3b9:2400dff7cb71f4bff583473d690fcb79650dd59e/TekniskDokument14_rev2020.pdf.

[20] Nicoletta J Lomax and Stefan G Scheib. 'Quantifying the degree of conformity in radiosurgery treatment planning'. In: *International Journal of Radiation Oncology*Biology*Physics* 55.5 (2003), pp. 1409–1419. ISSN: 0360-3016. DOI: https://doi.org/10.1016/S0360-3016(02)04599-6. URL: https://www.sciencedirect.com/science/article/pii/S0360301602045996.

[21] Ranald MacKay and Adam Aitkenhead. 'Proton therapy'. In: *External Beam Therapy*. Oxford University Press, June 2019. ISBN: 978–0–19–878675–7. DOI: 10.1093/med/9780198786757.003.0004. URL: https://doi.org/10.1093/med/9780198786757.003.0004.

[22] Shane Mesko and Daniel Gomez. 'Proton Therapy in Non-small Cell Lung Cancer'. In: *Current Treatment Options in Oncology* 19.12 (2018), p. 76.

[23] Cancer Registry of Norway. *Cancer in Norway 2022 - Cancer incidence, mortality, survival and prevalence in Norway*. Oslo: Cancer Registry of Norway, 2023, pp. 3, 60–65.

[24] 'Chapter 15 - Treatment-Planning Optimization'. In: *Proton Therapy Physics (Series in Medical Physics and Biomedical Engineering)*. Ed. by Harald Paganetti. CRC Press Taylor & Francis Group, 2012, pp. 475, 476. ISBN: 978-1-4398-3645-3. DOI: https://doi.org/10.1016/B978-0-323-24098-7.00044-7. URL: https://www-taylorfrancis-com.ezproxy.uio.no/books/edit/10.1201/9780367803551/proton-therapy-physics-harald-paganetti.

[25] E.B. Podgoršak. *Radiation Physics for Medical Physicists*. Second Edition. Springer-Verlag Berlin Heidelberg, 2010, pp. 11, 22, 622, 628, 632–633. ISBN: 978-3-642-00874-0.

[26] *Raystation 12A. A guide to optimization in RayStation*. RaySearch Laboratories AB (publ), 2022, p. 9.

[27] *Raystation 12A. User Manual*. RaySearch Laboratories AB (publ), 2022.

[28] Ana María Acosta Roa and Erlend Peter Skaug Sande. 'Retningslinje. Doseplanlegging av kurativ ca. pulm (ekskl. stereotaksi)'. In: *Kreftklinikken (KRE)/Avd. medisinsk fysikk* (2019). URL: https://ehandbok.ous-hf.no/document/41745.

[29] Henry Wagner and Corey Jay Langer. 'Chapter 44 - Non–Small Cell Lung Cancer'. In: *Clinical Radiation Oncology (Fourth Edition)*. Ed. by Leonard L. Gunderson and Joel E. Tepper. Fourth Edition. Philadelphia: Elsevier, 2016, 809–842.e8. ISBN: 978-0-323-24098-7. DOI: https://doi.org/10.1016/B978-0-323-24098-7.00044-7. URL: https://www.sciencedirect.com/science/article/pii/B9780323240987000447.

[30] Fiona Lim Mei Ying. 'Radiotherapy in Lung Cancer'. In: *Radiotherapy*. Ed. by Cem Onal. Rijeka: IntechOpen, 2017. Chap. 2. DOI: 10.5772/67204. URL: https://doi.org/10.5772/67204.